Universidade de Aveiro
2009
Departamento de Engenharia Mecânica

Ponmozhi Jeyaraj

Desenvolvimento e Caracterização de Nanofluidos

Universidade de Aveiro Departamento de Engenharia Mecânica
2009

Ponmozhi Jeyaraj

WATER BASED NANOFLUIDS DEVELOPMENT AND CHARACTERIZATION

Dissertação apresentada à Universidade de Aveiro para cumprimento dos requisitos necessários à obtenção do grau de Mestre em Engenharia Mecânica, realizada sob a orientação científica da Doutora Mónica Sandra Abrantes de Oliveira Correia, Professora Auxiliar do Departamento de Engenharia Mecânica da Universidade de Aveiro e do Doutor Nelson Amadeu Dias Martins, Professor Auxiliar do Departamento de Engenharia Mecânica da Universidade de Aveiro

The support from *Fundação para a Ciência e a Tecnologia* (FCT), Portugal is kindly appreciated through the funding of the project PTDC/EME-MFE/66482/2006.

Dedicated to my husband and my son.

o júri

presidente

Prof. Doutor José António de Oliveira Simões
Professor Associado c/agregação do Departamento de Engenharia Mecânica da Universidade de Aveiro

Prof. Doutor Abel Gomes Martins Ferreira
Professor Auxiliar do Departamento de Engenharia Química da Faculdade de Engenharia da Universidade de Coimbra

Prof. Doutora Mónica Sandra Abrantes de Oliveira Correia
Professora Auxiliar do Departamento de Engenharia Mecânica da Universidade de Aveiro (orientadora)

Prof. Doutor Nelson Amadeu Dias Martins
Professor Auxiliar do Departamento de Engenharia Mecânica da Universidade de Aveiro (co-orientador)

Aknowledgments

I would like to express a great deal of appreciation for my guide and advisor Prof. Mónica Oliveira, for her ideas, guidance and generous support. Her physical insight guidance and encouragement have been the impetus for me to keep working hard and to succeed. She has proven to be very considerate and patient advisor who serves as a role model for professional excellence and integrity.

I would also like to express gratitude to my co guide Prof. Nelson Martins for his support, constructive reviews and supportive comments.

I would like to express gratitude to Prof. S. Kanagaraj for giving me this opportunity to work in the Project PTDC/EME-MFE/66482/2006.

Appreciation is also extended to the project PTDC/EME-MFE/66482/2006 members (F.A.M.M. Gonçalves, Prof. A.G.M. Ferreira and Prof. I.M.A. Fonseca), from University of Coimbra, who have carried out experiments on viscosity, density and surface tension with the nanofluids prepared in the University of Aveiro.

Palavras-chave

Nanotubos de carbono, Nanofluidos, condutividade térmica, viscosidade, tensão superficial, densidade.

Resumo

É do conhecimento geral que a existência de fluidos com boa performance térmica é fundamental numa panóplia de sectores industriais, incluindo a produção de energia, indústria química, automóvel, entre outras. Contudo, são as limitações térmicas dos fluidos convencionais que comprometem a eficiência energética e, portanto a redução de tamanho, dos próprios permutadores de calor. De modo a melhorar a performance térmica dos fluidos convencionais, equaciona-se a adição de nanotubos de carbono (CNTs). Assim, com o este estudo, pretende-se contribuir para a redução significativa do tamanho, peso e custos envolvidos em sistemas de transferência de calor e, deste modo, contribuir efectivamente para a resolução de um dos maiores entraves actuais à miniaturização de equipamentos desta natureza.

Neste estudo, variáveis como fracção volumétrica dos CNTs e temperatura do fluido são tidas em consideração. O nanofluido propriamente dito é obtido pela adição, a fluidos convencionais (neste caso, água) de nanotubos tratados quimicamente. A dispersão do nanotubo no fluido base, de modo a inferir homogeneidade, será garantida recorrendo a agitação por ultra-sons.

A relação entre variáveis como viscosidade dinâmica, condutividade térmica, densidade e tensão superficial são, pois, objecto de estudo detalhado.

Keywords Carbon nanotubes, Nanofluids, Thermal conductivity, Viscosity, Surface Tension and Density.

Abstract The present proposal addresses the improvement of thermal characteristics of conventional fluids, having into account the great need for economy dematerialization and energy efficiency in industrial processes and systems, to achieve a higher level of environmental control and consequently a more sustainable development. Studying (and understanding) nanofluids, using available and innovative experimental and computational techniques, is the basis of the research towards the development of custom-designed nanofluids with enhanced properties and functions. Possible applications include more efficient cooling and heating in new and critical applications, like environment control, electronics, nuclear and biomedical instrumentation and equipment, transportation and industrial cooling, heat management, therefore promoting the eco design for energy efficiency. The heat transfer characteristics of conventional fluids obstruct their performance enhancement compromising both energy efficiency and compactness of heat exchangers. This work addresses the improvement of thermal characteristics of conventional fluids by the addition of specific nanoparticles (i.e. multiwalled carbon nanotubes, CNTs) in well defined concentrations, in order to obtain enhanced thermal properties of fluids for process intensification and device miniaturization. Thermal conductivity and rheological properties of nanofluids are studied.

Table of Contents

List of Figures

List of Tables

Chapter 1 – Introduction to Nanofluids and its applications

1.1 - Motivation

Carbon nanotubes are molecular-scale tubes of graphitic carbon with outstanding properties. They are among the stiffest and strongest fibers known, and have remarkable electronic properties and many other unique characteristics. For these reasons they have attracted huge academic and industrial interest, with thousands of papers on nanotubes being published every year. Commercial applications have been rather slow to develop, however, primarily because of the high production costs of the best quality nanotubes. The wide range of electronic, thermal, and structural properties of carbon nanotubes vary according to the different diameter, length, and direction of 'twist' of the nanotube. Many applications arise from the surprising and desirable properties they exhibit, some of which are already being used in new and improved products. For example, carbon nanotubes are highly conductive both to electricity and heat - they exhibit an electrical conductivity as high as copper, and thermal conductivity as great as diamond.

Nanotubes can be either metallic or semiconducting, leading to the potential for developing nanowires, nanoscale electrical components and nanoelectromechanical systems (NEMS). They therefore offer amazing possibilities for creating future nanoelectronic devices, circuits and computers. Carbon nanotubes (CNT) also have extraordinary mechanical properties - they are 100 times stronger than steel, while only one sixth of the weight. These mechanical properties offer huge possibilities - for example, in creating nanocomposites for a variety of application scenarios ranging from military to aerospace to medicine.

1.2 - Research objectives

1.) To enhance the thermal characteristics of the conventional fluids by adding chemically functionalized carbon nanotubes.

2.) To study the thermal characteristics of nanofluids by changing the volume fraction of the carbon nanotubes, at different temperatures.

3.) To characterize the nanofluids in what concerns: density, surface tension, dynamic viscosity and thermal conductivity.

1.3- Nanofluids

Cooling is one of the most important technical challenges that many diverse industries are facing including microelectronics, transportation, solid-state lighting, and manufacturing. Technological developments such as microelectronic devices with smaller (sub-100 nm) features and faster (multi-gigahertz) operating speeds, higher-power engines, and brighter optical devices are driving increased thermal loads, requiring advances in cooling. The conventional method for increasing heat dissipation is to increase the area available for exchanging heat with a heat transfer fluid. However, this approach requires an undesirable increase in the thermal management system's size. There is, therefore, an urgent need for new and innovative coolants with improved performance. The novel concept of 'nanofluids' – heat transfer fluids containing suspensions of nanoparticles – has been proposed as a means of meeting these challenges (Lee et al., 2007)

Heating or cooling fluids are of major importance to many industrial sectors including transportation, energy supply and production, electronics, nuclear and biomedical instrumentation and equipment. However, conventional heat transfer fluids have poor heat transfer properties compared to most solids. Despite considerable previous research and development focusing on industrial heat transfer requirement, major improvements in heat transfer capabilities have been lacking. As a result, a clear need exists to develop new strategies for improving the effective heat transfer behaviour of conventional heat transfer fluids.

Usual heat transfer fluids with suspended ultra fine particles of nanometer size are named as nanofluids, which have opened a new dimension in heat transfer processes. Nanofluids, i.e., dilute suspensions of nanoparticles in liquids may exhibit quite different thermal properties than the pure carrier fluids. For example, numerous experiments with nanofluids have shown that nanofluids provide desirable thermal properties, such as elevated effective thermal conductivities and convection heat transfer coefficients when compared to their base liquids without dispersed nanoparticles. These key thermal features

of nanofluids, together with excellent nanoparticles suspension stability, would open the door to a wide range of engineering applications, such as engine cooling; microelectronics cooling; and biomedical applications, such as nanodrug delivery for cancer therapy, etc. Heat transfer technology stands at the cross roads of miniaturization, on one hand and astronomical increase in heat flux, on the other.

The disadvantages of microparticles in basefluids

It is obvious from a survey of thermal properties that all liquid coolants used today as heat transfer fluids exhibit extremely poor thermal conductivity (with the exception of liquid metal, which cannot be used at most of the pertinent useful temperature ranges). For example, water is roughly three orders of magnitude poorer in heat conduction than copper—as is the case with engine coolants, lubricants, and organic coolants. It goes without saying that all of the efforts to increase heat transfer by creating turbulence, increasing area, etc., will be limited by the inherent restriction of the thermal conductivity of the fluids. Thus, it is logical that efforts will be made to increase the thermal conduction behavior of cooling fluids. Using the suspension of solids is an option that came to mind more than a century ago. Maxwell (1904) was a pioneer in this area who presented a theoretical basis for calculating the effective thermal conductivity of suspension. His efforts were followed by numerous theoretical and experimental studies, such as those by Hamilton-Crosser (1962) and Wasp (1977). These models work very well in predicting the thermal conductivity of slurries. However, all of these studies were limited to the suspension of micro- to macro-sized particles, and such suspensions bear the following major disadvantages:

1. **Settling:** The particles settle rapidly, forming a layer on the surface and reducing the heat transfer capacity of the fluids.
2. **Erosion:** If the circulation rate of the fluids is increased, sedimentation is reduced, but the erosion of the heat transfer devices, pipelines, etc., increases rapidly.
3. **Clogging:** The large size of the particles tends to clog the flow channels, particularly if the cooling channels are narrow.
4. **High pressure drop:** The pressure drop in the fluids increases considerably.
5. Finally, conductivity enhancement based on particle concentration is achieved (i.e., the greater the particle volume fraction is, the greater the enhancement—and greater the

problems, as indicated in 1– 4 above). Thus, the route of suspending particles in liquid was a well known but rejected option for heat transfer applications.

However, the emergence of nanofluids helped to stimulate the re-examination of this option. Modern materials technology provided the opportunity to produce nanometer-sized particles, which are quite different from the parent material in mechanical, thermal, electrical, and optical properties. Thus, nanofluid technology coupled with new heat-transfer-related studies on microchannel flow has provided a new option of revisiting suspensions of nanoparticles. The first proposition in this area was from Argonne National Laboratory (ANL) through the seminal work of (Choi et al., 2001) who designated the nanoparticle suspension in a nanofluid. From a purist's point of view, this designation may not be acceptable—every fluid is "nano" because of its molecular chains—but the term has been accepted and became popular in the scientific community. It must be kept in mind that biologists have been using the term nanofluid for different types of particles, such as DNA, RNA, proteins, or fluids contained in nanopores.

The advantages of nanoparticles in Nanofluids:

The attractive features, which made nanoparticles potential candidates for suspension in fluids, are a large surface area, less particle momentum, and high mobility. With respect to conductivity enhancement, starting from copper, one can go up to multi-walled carbon nanotubes (MWCNTs), which at room temperature exhibit 20,000 times greater conductivity than engine oil (Das et al., 2007). When the particles are properly dispersed, these features of nanofluids are expected to give the following benefits:

1. ***Higher heat conduction*** The large surface area of nanoparticles allows for more heat transfer. Particles finer than 20nm carry 20% of their atoms on their surface, making it instantaneously available for thermal interaction. Another advantage is the mobility of the particles, attributable to the tiny size, which may bring about micro-convection of fluid and hence increased heat transfer. The micro-convection and increased heat transfer may also increase dispersion of heat in the fluid at a faster rate. It has already been found that the thermal conductivity of nanofluids increases significantly with a rise in temperature, which may be attributed to the above stated reasons.
2. ***Stability*** Because the particles are small, they weigh less, and the chance of sedimentation becomes smaller. This reduced sedimentation can overcome one of the

major drawbacks of suspensions, the settling of particles, and contribute to nanofluids stability.

3. ***Microchannel cooling without clogging*** Nanofluids will not only be a better medium for heat transfer in general, but they will also be ideal for microchannel applications where high heat loads are encountered. The combination of microchannels and nanofluids will provide both highly conducting fluids and a large heat transfer area. This cannot be attained with meso- or micro-particles because they clog microchannels. Nanoparticles, which are only a few hundreds or thousands of atoms, are orders of magnitude smaller than the microchannels.

4. ***Reduced chances of erosion*** Nanoparticles are very small, and the momentum that may be imparted to a solid wall is much smaller. This reduced momentum reduces the chances of erosion of components, such as heat exchangers, pipelines and pumps.

5. ***Reduction in pumping power*** To increase the heat transfer of conventional fluid by a factor of two, pumping power must usually be increased by a factor of ten. It can be shown that if one can multiply the conductivity by a factor of three, the heat transfer in the same apparatus doubles. The required increase in the pumping power will be very moderate unless there is a sharp increase in fluid viscosity. Thus, a very large savings in pumping power can be achieved if a great thermal conductivity increase can be brought about with a small volume fraction of particles.

Chapter 2 – Literature Review

2.1 – Nanofluids

Various investigations involving nanofluids have been made considering different types of nanoparticles, i.e., metal-oxides, metals and even carbon nanotubes. Experimental work by a growing number of research groups worldwide revealed that nanofluids exhibit thermal properties superior to those of base fluids or conventional solid-fluid suspensions. In recent years, many experimentalists have reported the anomalously enhanced thermal conductivity (K_{eff}) of nanofluids considering different nanoparticle suspensions. Despite the importance of this effect for heat transfer applications, no agreement has emerged about the key mechanisms of this phenomenon, or even about the experimentally observed magnitude of the enhancement.

Some researchers have observed an anomalous increase in effective thermal conductivity of the nanofluids, while some others found that the traditional Hamilton and Crosser model (1962) could describe the nanofluid effective thermal conductivity. Although the authors observed different phenomena in their experiments, most experimentalists have the following conclusions in common: the thermal conductivity of a nanofluid is influenced by various parameters, such as nanoparticle size, shape and volume fractions, fluid temperature, as well as thermal conductivities of the nanoparticle and base fluid. Additional mechanisms include the effect of nanoparticle clustering, the nature of heat transfer inside the particles, the interaction and collision among particles, thermal waves via hyperbolic heat conduction, and nanoparticle dispersion.

2.1.1 - Nonlinear effects of nanoparticle concentration

Many researchers have found out a nonlinear relationship between thermal conductivity and nanoparticle concentration. Choi et al. (2001) measured the effective thermal conductivity of dispersed nanotubes in synthetic poly-oil, and discovered 160% increase in the thermal conductivity of oil at 1% volume fraction of CNTs. A nonlinear relationship between thermal conductivity and nanotube concentration was also observed in their study, which is not expected in conventional fluid suspensions of micrometer size particles at

such low concentrations. Hong et al. (2005) also found a nonlinear relationship between thermal conductivity and nanoparticle concentration in iron (Fe)-ethylene glycol nanofluids. It is interesting to note that the heat transfer enhancement obtained was higher than that of (Eastman et al., 2001) who used with copper (Cu) nanoparticles. Murshed et al., (2005) also discovered a nonlinear behaviour of water-based nanofluids containing spherical and rod shaped titanium oxide (TiO2) nanoparticles. Investigation of thermal conductivity with Al_70Cu_30-ethylene glycol nanofluids produced by also showed a strong nonlinear behaviour (Chon et al., 2005).

Lee et al., (1999) measured the thermal conductivity of nanofluids and found good enhancement with an increase of particle concentration. Wang et al., (1999) investigated the enhanced heat transfer mechanism of nanofluids. They suggested that the size of the particle is important to enhance the thermal conductivity of mixture. Eastman et al., (2001) measured the thermal conductivity of ethylene glycol nanofluids. They found that the effective thermal conductivity of Cu-ethylene glycol nanofluids were much higher than ethylene glycol containing the same volume fraction of dispersed oxide nanoparticles. The effective thermal conductivity of ethylene glycol in their study, increased by up to 40% for Cu-ethylene glycol containing approximately 0.3 vol% of Cu nanoparticles with mean diameter, 10nm.

2.1.2 – Thermal conductivity of nanofluids

Nanofluids have been observed during the measurement of thermal conductivity (K_{eff}) to depend strongly on temperature and particle size. The selection of the base fluid has almost the same significance as the choice of the nanoparticles in what concerns the enhancement of the thermal conductivity. The particle size and the volume fraction (ϕ) of the nanoparticles are important and seem to play an important role when thermal conductivity enhancement is concerned. Even though some researchers believe that the larger thermal conductivities of the nanoparticle suspensions were the main factors for thermal conductivity enhancement that is not always the case. To further access if size, density or shape of the nanoparticles influence the thermal conductivity of nanofluids, it is of utmost importance to conduct more research on the subject.

2.1.3 – Measurement Methodologies

Table. 1 summarizes the measurement of the effective thermal conductivities, where researchers employed different methodologies, i.e., steady-state method, transient hot- wire method, temperature oscillation method, and optical method. The effective thermal conductivities of nanofluids were mostly measured via transient hot-wire method, as this is one of the most accurate ways to determine the thermal conductivities of materials Choi et al. (1995), Lee et al. (1999), Eastman et al. (2001), Xie et al. (2002), Murshed et al. (2006). The latter reported method seems to be more appropriate than the steady state method due to the numerous advantages such as the elimination of natural convection effects and the attainment of faster responses. In this approach, an electrically insulating coated platinum hot wire is suspended symmetrically in a liquid inside a vertical cylindrical container. This hot wire serves as both a heating element, through electrical resistance heating, and as a thermometer, by measuring the temperature-dependent change in the electrical resistance of the platinum wire. Although the transient hot-wire (THW) method has been widely used for measuring effective thermal conductivities of nanofluids, a number of questions have been raised regarding the accuracy of this methodology and whether convective currents or other parameters might impact or affect the measured results. After comparing the transient hot wire method and transient hot strip method, Vadasz et al. (2005) indicated that the extremely high effective thermal conductivities obtained using the transient hot wire method may be due to the thermal wave effects via heat conduction and suggested that the transient strip method provided more accurate experimental results than the hot wire method. Five possible reasons for the anomalously increased effective thermal conductivity were classified -

1. Hyperbolic or dual-phase-lagging thermal wave effects not accounted for in using the transient hot wire data processing combined with extremely high values of the time lag due to the heterogeneous mixture.
2. Thermal resonance due to hyperbolic thermal waves combined with an amplified periodic signal possibly from short-radio-wave or cellular phones.
3. Particle driven or thermally driven, natural convection.
4. Convection induced by electro-phoresis.
5. Hyperbolic thermal natural convection.

Li et al. (2008) compared the transient hot-wire method and steady-state cut-bar method when investigating the Al_2O_3/water nanofluids with a particle diameter of 47 nm at different volume fractions under room temperature. It showed that at room temperature, both the transient hot-wire method and steady-state method results have nearly identical values for the effective thermal conductivity of the nanofluids tested.

More recently, researchers started to measure the nanofluid thermal conductivity by optically based techniques (Venerus et al. (2006); Putnam et al. (2006); Rusconi et al. (2006)). Similar to the THW method or steady method, the optical methods also presented some controversies. Some authors observed thermal conductivity enhancement; however, others argued that the thermal conductivity enhancement can be predicted by the effective medium theory (i.e., Hamilton-Crosser theory), and that the level of thermal conductivity enhancement is independent of temperature. Except for the measurement methodologies, subtle but critical differences among nanofluid samples (i.e., different dispersion techniques and effects) or due to experimental errors may have significant influence on the assessment of the effective thermal conductivity.

Table 1: Summary of Experimental studies on Thermal Conductivities of Different Nanofluids

Researchers	Nano-particles used	Basef fluid	Volume fraction	Methods used	Thermal conductivity Results
Masuda et al. (1993)	Al_2O_3(13nm)	Water	4.3	Transient hot-wire method	33% enhancement
Eastman et al (1997)	Al_2O_3/CuO/Cu	Water,HE-200 oil	5	Transient hot-wire method	60% enhancement in CuO Nanofluid
Lee et al. (1999)	Al_2O_3/CuO	Water, EG	4.3	Transient hot-wire method	15% enhancement for Al_2O_3/water 20% enhancement for CuO/EG
Wang et al. (1999)	Al_2O_3/CuO	Water, EG, Poly-Oil	3	Steady state parallel plates	12% enhancement on Al_2O_3 nanofluid
Xuan & Li (2000)	Cu	Water, EG	1-5%	Transient hot-wire method	Volume fraction and particle size influence were studied.
Eastman et al. (2001)	Cu	EG	0.3	Transient hot-wire method	40% enhancement
Choi et al. (2001)	CNTs	Poly-Oil	1.0	Transient hot-wire method	160% enhancement
Xie et al. (2002)	Al_2O_3	water	5	Transient hot-wire method	20% enhancement
Das et al. (2003)	Al_2O_3/CuO	water	1-4	Temperature oscillation	2-4 fold increase with temperature from 21-52ºC
Patel et al. (2003)	Au/Ag	Water, toluene	0.011/0.00026	Transient hot-wire method	5%-21% and 7%-14% enhancement with temperature from 21-71ºC

Table 1: Summary of Experimental studies on Thermal Conductivities of Different Nanofluids (continuation)

Researchers	Nano-particles used	Basef fluid	Volume fraction	Methods used	Thermal conductivity Results
Putra et al. (2003)	Al_2O_3/CuO	Water	1%/4%	Steady state parallel plates with convection	From 21-51ºC CuO(1%)8%-30% enhancement; CuO(4%)15%-35% enhancement; Al_2O_3(1%)3%-10%enhancement;Al_2O_3(4%)10%-22% enhancement
Wen & Ding (2004)	Al_2O_3	Water	0.5-2%	Transient hot-wire method	3%-10% enhancement at 22ºC
Assael et al. (2005)	CNTs	Water	0.6	Transient hot-wire method	38% enhancement
Chon et al. (2005)	Al_2O_3	Water	1	Transient hot-wire method	7%, 10%, 14% increase with temperature from 21-71ºC
Rusconi et al. (2006)	Colloidal	Water	1-15%	Optical thermal lensing method	No anomalous enhancements are measured.
Zhang et al. (2006)	Al_2O_3, ZrO_2, TiO_2, CuO	Water	1-14%	Transient short hot-wire method	No anomalous enhancements are measured, traditional Hamilton-Crosser model is valid
Lee & Peterson. (2006)	Al_2O_3/CuO	Water	2, 4, 6, 10%	Steady state parallel plates, traditionally referred to 'cut-bar appartus' was used.	52% enhancement for 6% CuO nanofluids and 30% enhancement for Al_2O_3 are observed at T=34ºC.
Putnam et al. (2006)	C60-C70/Au	Toluene/ethanol	1-0.6% & 0.35%	Optical beam deflection	No anomalous enhancement
Venerus et al. (2006)	Au/Al_2O_3	Water/petroleum oil	0.002, 2.5	Optical (Forced Rayleigh scattering)	No temperature influence on enhancement

Table 1: Summary of Experimental studies on Thermal Conductivities of Different Nanofluids (continuation)

Researchers	Nano-particles used	Basef fluid	Volume fraction	Methods used	Results
Shaikh et al. (2007)	CNTs/EXG (exfoliated graphite)/HTT (heat treated nanofibers)	PAO oil	0.1~1.0%	Optical (modern light flash technique)	CNT based suspension enhanced more than others, 161% enhancement observed for CNT suspensions
Timofeeva et al. (2007)	Al_2O_3	Water	0-10%	Thermal property analyzer based by Transient hot-wire method	No anomalous enhancement
Murshed et al. (2006)	TiO_2, Al_2O_3, Al	Water, EG	0.6	Transient hot-wire method	Temperature influence, 15% increase for TiO_2, 45% increase for Ai/EG nanofluid
Chen et al. (2008)	SiO_2	Water	16%	Transient hot-wire method and small angle X-ray scattering to help dispersion	Thermal conductivity shows a linear increase with the increase of nanoparticles size
Li et al. (2008)	Al_2O_3	Water	0.5%, 2%, 4%, 6%	Optical thermal lensing method and steady state cut-bar method	Enhancements are observed, measured valued shows good agreement of both methods at room temperature

2.2 –Nanofluids – Thermophysical Properties

2.2.1 – Thermal conductivity for CNT nanofluids

Choi et al. (2003) have produced nanotube-in-oil suspensions and measured their effective thermal conductivity. The measured thermal conductivity is anomalously greater than the theoretical predictions for 1.0 vol% CNTs in oil (i.e 160%) and is nonlinear with nanotube loadings. The anomalous phenomena show the fundamental limits of conventional heat conduction models for solid/liquid suspensions. Jiang et al. (2008) measured the thermal conductivities of four kinds of CNT-R113 nanorefrigerants and at 1.0 vol% observed an increase of thermal conductivity to be 82%, 104%, 43%, and 50% respectively. They have also studied the influence of diameter and aspect ratio of CNT on nanorefrigerants and (Chen et al., 2008) measured thermal conductivity and observed it to increase for CNT concentration in Distilled Water (DW) and Ethylene glycol (EG) and found out that temperature variation has no obvious effects on thermal conductivity enhancement. At low volume fractions (<0.4 CNT vol %), nanofluids have lower viscosity than the corresponding base fluid due to the lubricative effect of nanoparticles. Liu et al. (2005) investigated CNT with EG and synthetic engine oil and demonstrated the thermal conductivity enhancement to be 12.4% for 1 vol %, for CNT-EG, and 30% for 2 vol % for CNT-synthetic oil nanofluid. Xie et al. (2003) have treated CNTs with nitric acid to make it hydrophilic and measured the thermal conductivity enhancement for the DW, EG and decene. Xie et al. (2009) prepared the nanofluids, indicated that the straightness ratio, aspect ratio, and aggregation have a collective influence on the thermal conductivity of CNT nanofluids. Assael et al. (2005) added carbon multi-walled nanotubes (C-MWNTs) and alternatively carbon double walled nanotubes (C-DWNTs) in water in order to enhance the thermal conductivity of this traditional heat transfer fluid. Hexadecyltrimethyl ammonium bromide (CTAB) and Nanosperse AQ were employed as dispersants. The transient hot-wire technique was used for the measurement of the thermal conductivity with an instrument built for this purpose. The absolute uncertainty is reported to be better than 2%. The maximum thermal conductivity enhancement obtained was 34% for a 0.6% volume C-MWNT suspension in water with CTAB.

2.2.2 - Viscosity of nanofluids

Compared with the experimental studies on thermal conductivity of nanofluids, there are limited rheological studies reported in the literature. Li et al. (2002) measured the viscosity of water with copper oxide (CuO) nanoparticle suspensions using a capillary viscometer. The results showed that the apparent viscosity of nanofluids decreased with increasing temperature. However, as they pointed out, the capillary tube diameter may influence the apparent viscosity for higher nanoparticle mass fractions, especially at lower temperatures.

Wang et al. (1999) also measured the relative viscosity of Aluminium oxide (Al_2O_3)-water and Al_2O_3-ethylene glycol nanofluids. The results show an increase of relative viscosity with increased solid volume fraction for the two nanofluids highlighting that the desirable heat transfer increase may be offset by the undesirable increase in pressure drop. Das et al. (2003) also measured the viscosity of Al_2O_3 –water nanofluids against shear rate. Their results showed an increase of viscosity with increased particle concentrations. There is strong possibility that nanofluid may be non-Newtonian; even viscoelastic in some cases. Further experimental studies are needed to define the viscosity models of nanofluids to enable its modeling in numerical in simulation studies. The viscosity of CNT–water nanofluids as a function of shear rate was measured by (Ding et al., 2006). The author observed that the viscosity of nanofluids increased with increasing CNT concentration and decreasing temperature. Also, the shear thinning behaviour was reported by the author. The latter, meaning that the nanofluids can provide better fluid flow performance due to higher shear rate, at the wall.

He et al. (2007) show that the viscosity of nanofluids increases with increasing particle volume fraction and particle size. Furthermore, the results also show that the measured viscosity of nanofluids is significantly larger than that of the predicted value by the Einstein equation.

2.2.3 – Surface tension of nanofluids

Das et al. (2003) used Al_2O_3 nanoparticle concentration in water and studied the surface tension for 1, 2 and 4% particle volume concentration. Murshed et al. (2008) studied the temperature dependence of surface tension, interfacial tension and viscosity of a nanofluid and investigated its applicability in droplet-based microfluidics. Experimental results show

that nanofluids having TiO_2 nanoparticles of 15 nm diameter in deionized water exhibit substantially smaller surface tension and interfacial tension than those of the base fluid (i.e. deionized water). These surface and interfacial tensions of this nanofluid were found to decrease almost linearly with increasing temperature. Surface tension remains practically unaffected by the presence of nanoparticles in the basefluid without any kind of dispersant. It must be noted, however, that the surface tension of the suspension are affected by the stabilizing agents (mostly surfactants) usually employed during nanofluid preparation.

2.2.4 – Density of nanofluids

As density is an important property of nanofluids that directly affects the Reynolds number, friction factor, pressure loss, and Nusselt number, there is a need to focus on accurately determining the density of several nanofluids. Vajjha et al. (2009) measured the density of different nanofluids over a temperature range of 0ºC to 50ºC for several particle volume concentrations. The results obtained were compared with a widely used theoretical equation and good agreement between the theoretical equation and measurements were obtained for Al_2O_3 and antimony pentoxide (Sb_2O_5): stannic oxide (SnO_2) nanofluids. However, a deviation was observed for zinc oxide (ZnO) nanofluid where density is seen to increase with particle volume concentration.

2.3 – Nanofluids – modeling thermophysical properties

2.3.1 – Thermal conductivity of nanofluids

Most of the thermal properties of nanofluids measured greatly exceed the values predicted by classical macroscopic models. For example, the classical conductivity theories of solid-fluid suspensions used for large-size particle suspensions (Maxwell, 1873; Hamilton and Crosser, 1962; among others) cannot explain why low concentrations of nanoparticles can enhance the thermal conductivity of base fluids notably more than the model predications.

In the conventional models, the particle volume fraction, shape, orientation and the thermal conductivity of the particle and the base fluid, are considered to be the most important factors controlling the thermal conductivity of the conventional suspensions. As a result, continuum models developed for suspensions of millimeter or micrometer

particles can no longer describe the enhanced thermal conductivities of nanofluids observed with most thermal conductivity measurement. In addition to the big gap between the experimental data and model predictions, the strongly temperature and size dependent nanofluid thermal conductivities have produced a great requirement to understand the thermal transport mechanisms in nanofluids. It is expected that energy transport mechanisms at the nanoscale would differ from macroscale mechanisms. Wang et al. (1999) first proposed new mechanisms behind enhanced thermal transport in nanofluids, such as particle motion, surface action, and electrokinetic effects. They have suggested that nanoparticle size is important in enhancing the thermal conductivity of nanofluids.

Xuan et al. (2000) recommended several possible mechanisms for enhanced thermal conductivity of nanofluids, such as the increased surface area of nanoparticles, particle–particle collisions, and the dispersion of nanoparticles. Keblinski et al. (2002) proposed four possible microscopic mechanisms for the anomalous increase in the thermal conductivity of nanofluids, which include Brownian motion of the particles (which was discussed as being negligible), molecular-level layering of the liquid at the liquid–particle interface, the ballistic rather than diffusive nature of heat conduction in the nanoparticles, and the effects of nanoparticle clustering. In order to model the thermal conductivities of nanofluids, researchers usually extend existing models or develop new ones.

2.3.2 – Models for Thermal conductivity of carbon nanofluids

In the last few years, attempts have been made to model the enhancement in thermal conductivity of CNT nanofluids by various assumptions like liquid layering, fractal theory etc. Xue et al. (2005) modelled the thermal conductivity of CNT nanofluids using field factor approach, with a depolarization factor and an effective dielectric constant. The model is found to be working fairly well in predicting the thermal conductivities of CNT suspensions. Nan et al. (2003) presented a simple formula for thermal conductivity enhancement in CNT composites, which is derived from the (Maxwell-Garnett., 1904) model by the effective-medium approach. The model over-predicts the enhancement in the thermal conductivity of CNT suspensions when calculated with typical values of CNT thermal conductivities. Nan et al. (2004) also developed a new model by incorporating interface thermal resistance with an effective-medium approach. However, the model requires the thermal resistance value at the surface of CNTs, which is difficult to get for different types of CNTs and their combinations with different solvents. Recently, (Lei Gao

et al., 2006) presented another model, based on differential effective medium theory, derived from the Maxwell– Garnett (1904) model. The model suggests a non-linear dependence of thermal conductivity of CNT nanofluids over volume concentration of the nanotubes, with slow increase at low concentrations and rapid at high concentrations.

There are some other models for the prediction of thermal conductivity of CNT nanofluids, but lack of conformity or validation with experimental observations.

2.3.3 – Models for viscosity of nanofluids

Einstein. (1956) was the first to calculate the effective viscosity of a suspension of spherical solids using the phenomenological hydrodynamic equations. By assuming that the disturbance of the flow pattern of the matrix base fluid caused by a given particle does not overlap with the disturbance of flow caused by the presence of a second suspended particle. Even since Einstein's initial work, researchers have made progress in extending the Einstein theory in two major areas.

1.) To extend the Einstein equation to higher particle volume concentrations by including particle-particle interactions. The theoretical equation can be expressed as: $\mu_{eff}=(1+c_1\phi_p+c_2\phi_p^2+c_3\phi_p^3+\ldots..)\mu_b$
2.) To take into account the fact that the effective viscosity of a mixture becomes infinite at the maximum particle volume concentration ϕ_{pmax}

To include the effect of non-spherical particle concentrations efforts have been made. Experimental data for the effective viscosity of nanofluids are limited to certain nanofluids. The ranges of the parameters (the particle volume concentration, temperature, etc.) are also limited. Still, the experimental data show the trend that the effective viscosities of nanofluids are higher than the existing theoretical predictions. In an attempt to rectify this situation, researchers proposed equations for specific applications, e.g., Al_2O_3 in water (Maiga et al., 2004), Al_2O_3 in ethylene glycol (Maiga et al., 2004), TiO_2 in water (Tseng et al., 2003), and CuO in water with temperature change (Kulkarni et al., 2006). The problem with these equations is that they do not reduce to the Einstein equation at very low particle volume concentrations and, hence, lack a sound physical basis.

Chapter 3 – Preparation of CNT-Water Nanofluids

3.1 Introduction

Nanofluids does not simply mean a liquid-particle mixture. Nanofluids are engineering fluids containing nano-particles in base fluids. Carbon nanotubes (CNTs) are an interesting new molecular form of carbon in the fullerene family, discovered by (Iijima, 1991). Due to unique electronic and mechanical properties of CNTs (Chen et al., 2005) and also their resistance to acid/basic media (Serp et al., 2003) they have attracted a special attention. However, the hydrophobic and inert nature of the surface of as-prepared nanotubes is unfavourable for practical applications. In order to improve the interaction of CNTs and foreign molecules, it is necessary to modify the surface of nanotube oxygen-containing groups, which are interesting to improve the interaction of CNTs with the solvent matrix are formed on the surface of nanotubes either by chemical treatment such as nitric acid or dry treatment like dielectric barrier discharge (DBD) plasma in the oxygen-based atmosphere. Purification process like thermal oxidation and acid washing produce oxygenated functional groups. Due to its strong oxidation feature and its lengthy process, functionalization using nitric acid could be more destructive in comparison with the plasma treatment. However, plasma treatment creates less functional groups than that of acid treatment. In other words, plasma treatment mainly functionalizes the surface of the material, whereas, as far as chemical treatment is concerned, beside affected surface, some changes in the bulk of the material might occur (Vesali et al., 2009). Functionalization causes opening up of tube ends (Tsang et al., 1994) and generation of defects on the sidewall of nanotubes (Banerjee et al., 2005), therefore access into the cavity of the nanotubes can be achieved.

In order to increase the dispersibility of multi-walled carbon nanotubes (MWNTs) in water without any additives, various acid treatments were used. Generally, acid treatment is used to remove or purify carbon nanotubes. MWNTs treated with a mixture of nitric and sulphuric acids showed high dispersion stability by means of UV-visible spectrophotometry and higher crystallinity than other samples. In addition, it was clearly

shown that acid treatment efficiently removed the impurities of MWNTs, which was proven by thermo gravimetric analysis. In particular, one of functional groups, cyano (C-N) bonding characterized by Fourier transform-infrared after acid treatment were formed on the surface of MWNTs (Kim et al., 2008).

With the present work it is intended to prepare water based nanofluids with different volume percentages of carbon nanotubes. With following sections of this chapter it is intended to describe the methods and materials used to accomplish the task.

.

3.2 Raw materials specifications

Multiwalled CNTs were purchased from Cheap Tubes Inc, USA, with the specifications listed in Table 2.

Table 2: Specification of multi-wall carbon nano tubes

Properties of MWCNTs	Specification
Outer diameter	50 – 80nm
Inner diameter	5 – 10 nm
Ash content	1.5 wt%
Purity	95 wt%
Length	10 – 20 µm
Specific surface area	60 m^2/g
Electrical conductivity	>10 S/cm

Transmission electron microscopy (TEM) study revealed that the raw CNTs were not only aggregated, but also entangled as it can be seen in from Fig. 1. It is evident that raw CNTs are not ready to form stable suspensions (Vesali et al., 2009). The length of CNTs varies from 10-20 µm and has the possibility to entangle with other nanotubes when mixed with water.

Fig. 1. Transmission electron microscopy image of raw- CNTs (Cheaptubes, USA)

3.3 Chemical treatment of CNTs

In order to disentangle the CNTs aggregates and introduce hydrophilic functional groups on the surface of the nanotubes by acid treatment, sulphuric acid and nitric acid are used to modify their surfaces. Xie et al. (2003) used a treatment process that is similar to the present work. In their study, one gram of raw CNT and 40 ml of the acid mixture (3:1 of H_2SO_4 and HNO_3) were boiled and refluxed for 1 hour. Then, the sample was diluted with distilled water, filtered till the washings show no acidity. The cleaned CNTs were collected and dried at 150ºC for 12 hours to remove the water adhering to them. From the image (Fig. 2) no aggregates or entanglements of raw CNTs were found after the chemical treatment.

The treated CNTs have the hydrophilic group, i.e., the carboxyl group, the TEM study reveals that the diameters of MWCNTs were reduced by this acid-treatment, which would suggest that the sidewall of CNTs was etched and, therefore, the carboxyl group would be also induced at the sidewall of CNTs partially as well as the ends. The nanotubes consisting of large aggregates, as manufactured, can be easily dispersed to individual fibers by treatment with nitric acid or a mixture of nitric and sulphuric acids (Esumi et al., 1995).

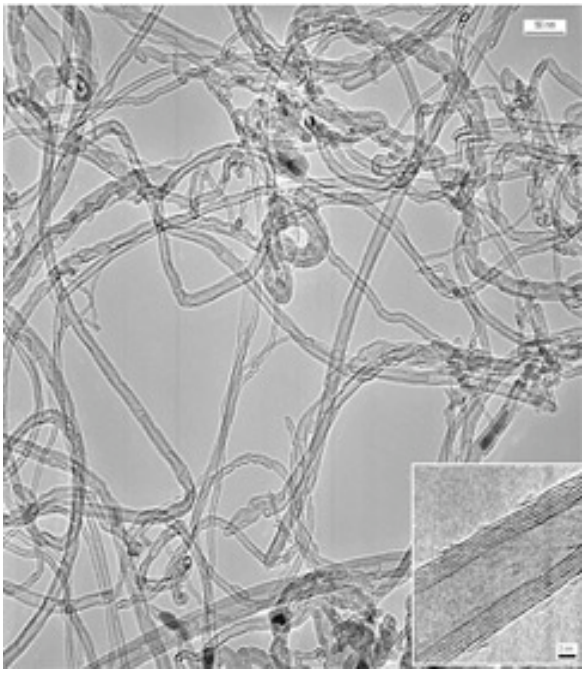

Fig. 2. TEM image of chemically treated CNTs

The chemical treatment method for the raw CNTs in the present work is as follows:

1.) The raw CNTs are mixed with the acid mixture (3:1 of H_2SO_4 and HNO_3).

2.) The Mixture is boiled for 30 mins in a container mounted on the hot plate magnetic stirrer, which is maintained at a temperature of 413.15K.

3.) The mixture is allowed to cool and diluted with ample distilled water.

4.) The sample is washed and filtered continuously till the washings show no acidity.

5.) It is washed till the pH of the final sample becomes 7.

6.) The cleaned CNTs are collected and dried at 373.15K in an oven till there are no traces of water attached.

7.) Then the dried pellets are grinded in A11 basic analytical mill shown in Fig. 3

The A11 basic analytical mill also called as batch mill and can be used for impact grinding of hard, brittle or non-elastic materials by means of the high grade stainless steel beater, for samples with Mohs hardness of up to 6.

Fig. 3. Photograph of the mill used for grinding dry CNT pellets used in this study

The mill has a circumferential speed of 53m/s. When the hard CNT pellets are grinded in the mill, a very fine powder of CNTs is obtained that can be well dispersed in basefluids. But, if it is grinded in a porcelain bowl with pestles manually, one do not get the CNTs as fine powder as obtained using the mill. The CNTs when mixed with the basefluid and sonicated settles rapidly without giving a stable mixture for long period of time.

There are actually many-tailored made CNT dispersions for example

1.) High viscosity carbon nanotube dispersion

2.) Low viscosity carbon nanotube dispersions

3.) Water based carbon nanotube dispersions

4.) Solvent based carbon nanotubes dispersion

5.) Customer matrix based carbon nanotubes dispersion

The present work is in need of the water based carbon nanotube dispersions therefore, chemical modification of the CNT surface and good dispersion of carbon nanotubes are required for industrial applications of the CNTs. Surface treatment of the CNTs may roughly be classified into two categories, one is generation of the nanotube-bound carboxylic acid and the other is direct attachment of functional groups to the graphitic surface. Chemical oxidation and amine treatment are included in the first category. The CNTs that are opened at the end and the terminal carbons are converted to carboxylic acids by oxidation in concentrated sulphuric and nitric acids.

3.4 Preparation of CNT-water nanofluids

Preparation of stable nanofluids is quite an involving task, after chemical treatment. Treated carbon nanotube (TCNT) powders must be added into a base fluid in a mixing container. The TCNT/fluid mixture must be subjected to intensive sonication to make well-dispersed and homogeneous suspension. Xie et al. (2003) refer to the preparation of Stable CNT nanofluids for DW and EG without the need of surfactant.

In the work here reported the TCNTs were used for preparing nanofluids for different volume fractions considering a density of the CNTs to be 2.16g/cc. The different volume fractions employed for the thermophysical properties study are 0.25, 0.5, 0.75, 1.0, 1.5, 2.0, 2.5, 3.0, 4.0, 5.0 vol %. For measuring thermal conductivity at temperatures 10 and 20ºC, volume fraction up to 5% is prepared and for other temperatures 30, 40, 50, 60ºC CNT-water nanofluid up to 2.5 vol % is utilized. For the viscosity measurements volume fraction up to 4% is prepared.

Water based fluids with different CNT volume fractions were prepared according to the following methodology:

1.) The required amount of TCNTs according to the volume percentage used for each sample is measured in a precision weight balance with readability up to 1mg.
2.) Mix CNTs with the base fluid i.e. with distilled water.
3.) Sonicate the mixture with the help of the Ultrasonicator (Fig. 4). for an hour or more till a homogenous mixture is obtained.

The sonicator was purchased from Frontline electronics Ltd, India. The technical specification of the sonicator used for the sonication of the samples in the present work has the operating voltage of 230V and mean operating frequency of 20±3 KHz. The sonicator rod, which is made of stainless steel, is 115 mm in length and 12mm tip diameter. The power output is 600 watts.

Fig. 4. Ultrasonicator used for sonication of nanofluids used in this study (Frontline electronics, india)

Comparing Fig. 1 and Fig. 2 one could find that the CNTs are not much disentangled in Fig. 2 than in Fig. 1 after the chemical treatment process. This reveals that a good treatment process has been carried out in this study. In order to visually inspect whether the mixture is homogenous, the prepared CNT nanofluids are transferred to another beaker and checked for any deposits at the bottom surface. No such settling is found. A photograph of the stable CNT-Water nanofluids arranged in a row of increasing volume fraction is shown in Fig. 5. The maximum volume capacity of nanofluids that can used for sonication in the Ultranicator is 150 ml. Hence, 150 ml of nanofluids at different volume fraction are prepared each time for the measuring the thermophysical properties.

Fig. 5. Photograph of the prepared CNT-Water nanofluids at different volume fractions

Chapter 4 – Study of colloidal stability of nanofluids using UV-spectrophotometer

4.1 – Introduction

The long-term colloidal stability of dispersion will be of great importance in a number of industries such as pharmaceutical, ceramic, paints and pigments. The term "stability" can have different connotations to different applications. When applied to colloids, a stable colloidal system is one in which the particles resist flocculation or aggregation and exhibits a long shelf life. This will depend upon the balance of the repulsive and attractive forces that exist between particles, as they approach one another. If all the particles have a mutual repulsion then the dispersion will remain stable. However, if the particles have little or no repulsive force then some instability mechanism will eventually take place e.g. flocculation, aggregation etc.

In certain circumstances, the particles in a colloidal dispersion may adhere to one another and form aggregates of successively increasing size that may settle out under the influence of gravity. An initially formed aggregate is called a floc and the process of its formation flocculation. The floc may or may not separate out. If the aggregate changes to a much denser form, it is said to undergo coagulation. An aggregate usually separates out either by sedimentation (if it is more dense than the medium) or by creaming (if it less dense than the medium). The term's flocculation and coagulation have often been used interchangeably. Usually coagulation is irreversible whereas flocculation can be reversed by the process of deflocculation. The Fig. 6 schematically represents some of these processes.

Although the stability of nanofluid is very important for its application, there is a little study on estimating the stability of suspensions. UV–vis spectrophotometric measurements have been used to quantitatively characterize colloidal stability of the dispersions. Jiang et al. (2003). is the first report to quantitatively characterize colloidal stability of the dispersions by UV–vis spectrophometric measurements. When the sediment time reaches 500 h, the supernatant CNT concentration drops as much as 50% for the bare CNT suspension, compared to 15% with the addition of sodium dodecyl sulphate (SDS).

Furthermore, after 150 hours, no precipitation is found for CNT/SDS dispersions, exhibiting an extreme stability.

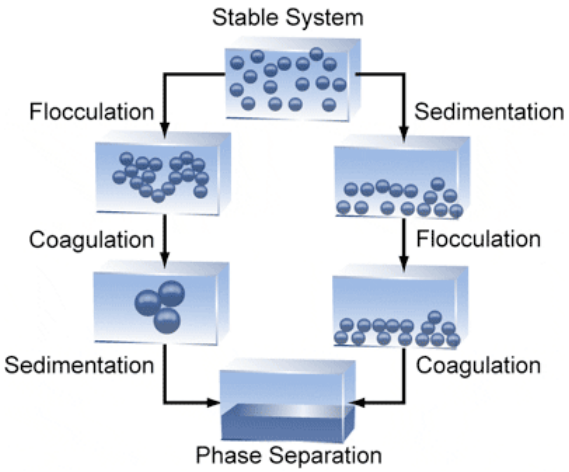

Fig. 6. Schematic representation of the colloidal solution. (Source: http://www.malvern.com/LabEng/industry/colloids/Stabilized_colloid_system.gif)

Hwang et al. (2007) have also used UV-vis spectrophotometer to estimate the suspension concentration with increasing sediment. Kanagaraj et al. (2008) used the UV spectrophotometric technique to quantitatively characterize colloidal stability of CNTs where a good stability of nanofluid over time was observed.

4.2 – Experimental set up and Methodology

The UV Spectrophotometer (Fig. 7) uses two light sources, a deuterium lamp for ultraviolet light and a 20W tungsten halogen (long-life 2000 hour) lamp for visible light. The light beam passes through a slit and hits a diffraction grating. The grating can be rotated allowing for a specific wavelength to be selected. At any specific orientation of the grating, only monochromatic (single wavelength) successfully passes through a slit. A filter is used to remove unwanted higher orders of diffraction. One of the beams is allowed to pass through a cuvette (which contains the solvent) and the intensity of the light beam is measured. The other light passes through the cuvette that contains the sample (nanofluid). The intensities of the light beams are then measured at the end.

The technical specification of this UV-vis spectrophotometer are 190 ~ 1100nm with a spectral band width (resolution) of 5nm. The wavelength display, setting, accuracy and

repeatability are 0.1nm, 0.1nm, ± 1.0nm, ± 0.3nm. The wavelength scanning speed is approximately 24 ~ 1400nm/min, with the recording range for the absorbance -0.3 ~ 3.0Abs and transmittance of -399 ~ 399%. The baseline correction can be done automatically with the computer memory. The standard peak pick function allows for clear and accurate detection of the most sensitive wavelengths. The standard RS-232C connector is used to connect an optional printer or a computer equipped with a standard RS-232C interface.

Fig. 7. UV-vis Spectrophotometer (Shimadzu corporation, Germany)

The methodology used for finding the absorbance of all the samples are

1.) Samples with different concentration from 0.0324, 0.05184, 0.0648, 0.0842, 0,0972, 0.10368gm/litre are prepared for the spectral scan.

2.) Perform a baseline correction without any sample in the sample compartment to set the background to zero over the currently selected wavelength range. This ensures a good reference point before collecting data.

3.) A data collection method will be created using a wavelength range of 600 to 200nm.

4.) Mediums scan speed and a sampling interval of 1.0nm is set as the parameters for measuring. The wider the data sampling interval is, the less the obtained data point becomes, which substantially makes the scan speed faster.

5.) The measuring mode is set to absorbance in the instrument parameters.

6.) The supernatant of each sample is taken in a 10mm rectangular cuvette and mounted on the cell holder that is in the sample compartment and the spectral scan is performed.

7.) In the overlay mode the overlaygraph sets the X-axis to the wavelength range in the method that is set previously in point 3 and the Y-axis is manually set to properly display the data.

8.) The peak pick is displayed in the operation pane and is used to display all of the peaks and valleys in a data set, as well as the wavelength and absorbance of the data set at each peak and valley.

9.) The wavelength corresponding to the maximum value of absorbance is used for the calibration plot. All the samples have more or less the same wavelength corresponding to its peak absorbance.

4.3 – Results and Discussion

The absorption of nanofluid is observed at 263nm.With increasing sediment time, the absorbance of CNTs in the nanofluid was diminished at 263nm, which is used to determine the CNT concentration in nanofluid by fitting the calibration curve. A UV–vis spectrophotometer was used to calculate quantitatively the CNT concentration with increasing sediment time. A linear calibration curve was drawn at a wavelength of 263nm for CNT dispersion in water that varies from 32.4 to 103.68 mg/l. Fig. 8 shows a linear relation between CNT concentration and the absorbance of suspended nanotubes in nanofluids.

Fig. 9a shows the calibration curve (Kanagaraj et al., 2008) that is similar to the presen study but with different concentration of CNTs in each sample. Fig. 9b shows the supernatant solution versus the sedimentation time and it is observed that the average concentration of CNT was maintained at 9.35mg/l after 200 hours. It is more consistent

with the concentration of CNTs prepared for the experimental study. The stability of nanofluids is improved in an aqueous solution because the hydrophobic surfaces of CNTs are modified hydrophilically and the repulsion forces amoung the suspended nanotubes increase due to decrease of pH values, which is the surface change of CNTs in water.

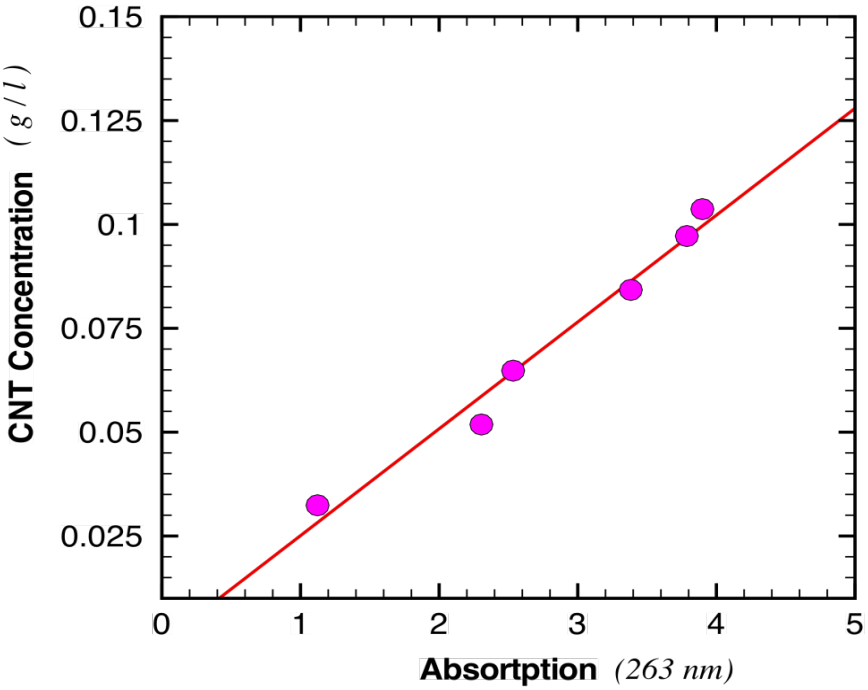

Fig. 8. Calibration curve of CNTs in Distilled water

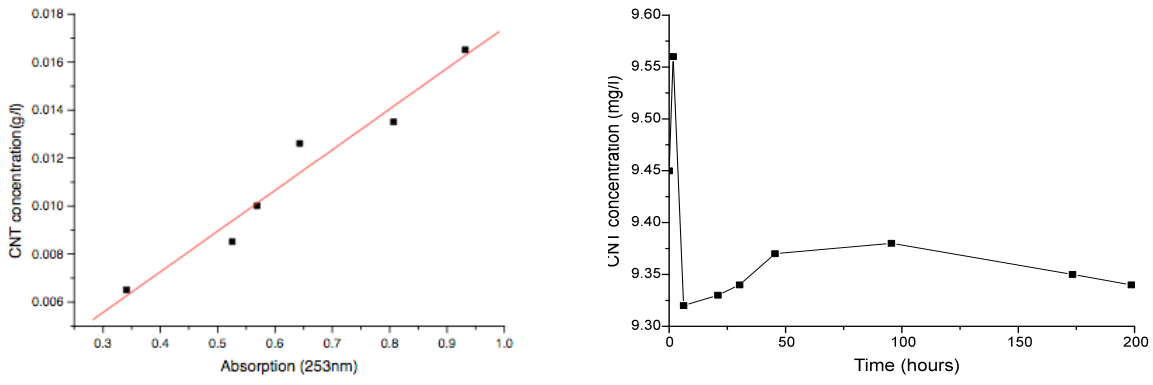

(a) (b)

Fig. 9 (a) Calibration curve for CNTs in Distilled water (b) Concentration of CNT in nanofluids (Kanagaraj et al., 2008)

In order to assess the colloidal stability, the samples prepared were submitted to the spectral scan, plots from Fig. 10 to Fig. 15 are obtained from the overlay graph showing all the peaks and valleys obtained while finding the peak absorbance. The table showing all the peak and valleys are also provided to get an insight in the values obtained (from Table. 3 – Table. 8)

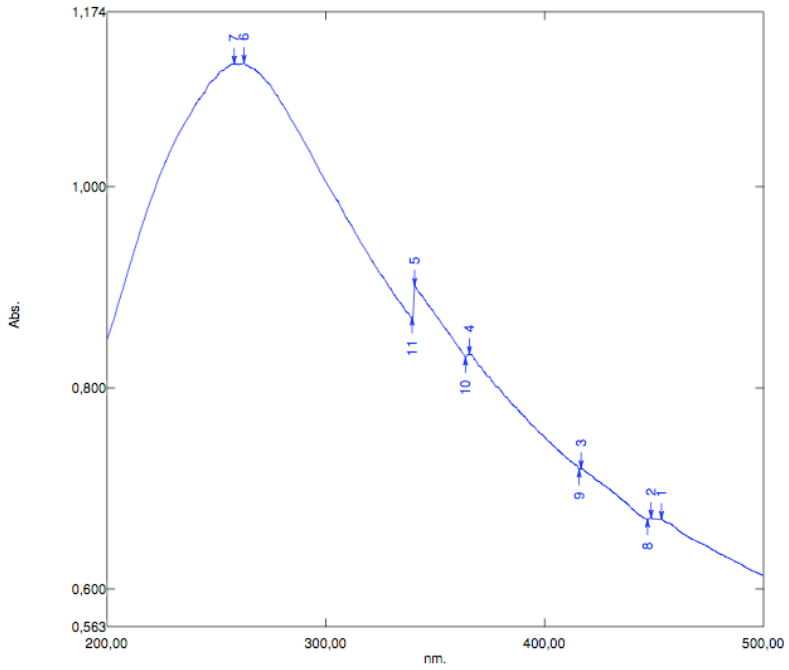

Fig. 10. Absorbance curve for 0.0324 gm

Fig. 10 shows the wavelength versus the absorbance curve, corresponding to the values in Table. 3, for 0.0324 grams of CNTs dispersed in a litre of distilled water. Carrying out the scanning of the prepared sample in the peak pick spectrum module gives the different scanning results of absorbance attaining the peak and valley at diiferent wavelengths. Corresponding to the higher peak absorbance value the wavelength is taken as the final value, after which the absorbance diminishes. In Table 3, the maximum absorbance is at 1.123 corresponding to the wavelength of 262.60nm.

Fig. 11 shows only one peak value at 263nm wavelength with the absorbance value as 2.305 as shown in Table. 4. The curve attained is very smooth and there are no visible peaks other than the highest peak, like wise we have got the same kind of trend for Fig. 12 where 0.0648 gm is mixed in a litre of distilled water.

Table 3 : Absorbance table for 0.0324 gm

No.	P / V	Wavelength	Abs.
1	P	453,40	0,669
2	P	448,60	0,671
3	P	416,60	0,720
4	P	365,60	0,834
5	P	340,60	0,901
6	P	262,60	1,123
7	P	258,20	1,122
8	V	447,00	0,669
9	V	415,80	,719
10	V	363,80	0,830
11	V	339,40	0,870

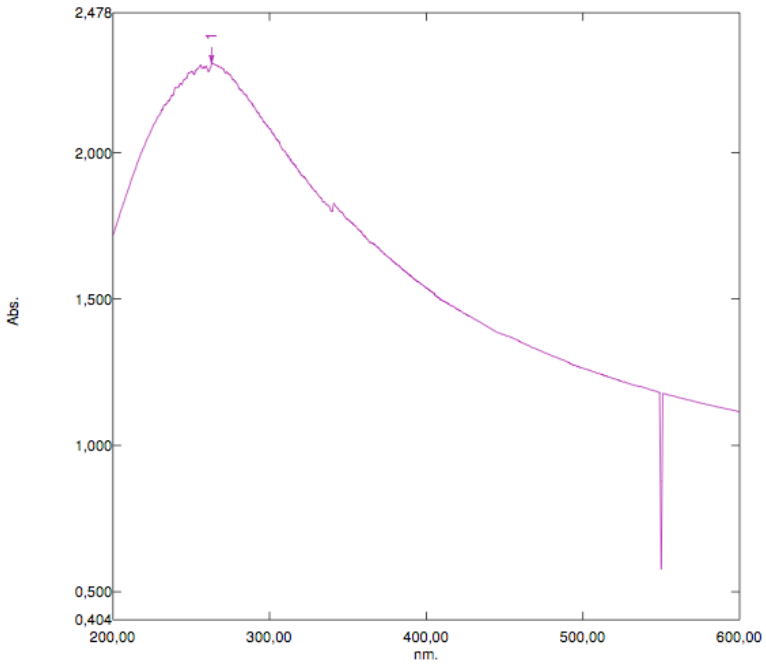

Fig. 11. Absorbance curve for 0.05184 gm

This plot (Fig. 11) shows the wavelength versus the absorbance for 0.05184 grams of CNTs dispersed in a litre of distilled water. As shown in Table 5 the maximum absorbance is 2.534 for the 259.50nm wavelength, here too there are no valleys or other peaks obtained during the process of scanning. Where as for the further sample measurement where the particles added is little higher as greater than 0.08424 gms up to 0.10368 gms per litre, the absorbance curve is not smooth but staggered as seen in Figs. 13 – 15. The staggererdness can be explained as due to more amount

CNTs added for the scanning, the particles make the solution more opaque and dense. So when scanning through the range of wavelengths while recording the absorbance readings at each wavelength in the scanned range is more difficult to pass through the particles which are added little more than the previous samples.

Table 4 : Absorbance table for 0.05184 gm

No.	P	Wavelength	Abs.
1	P	**263,00**	**2,305**

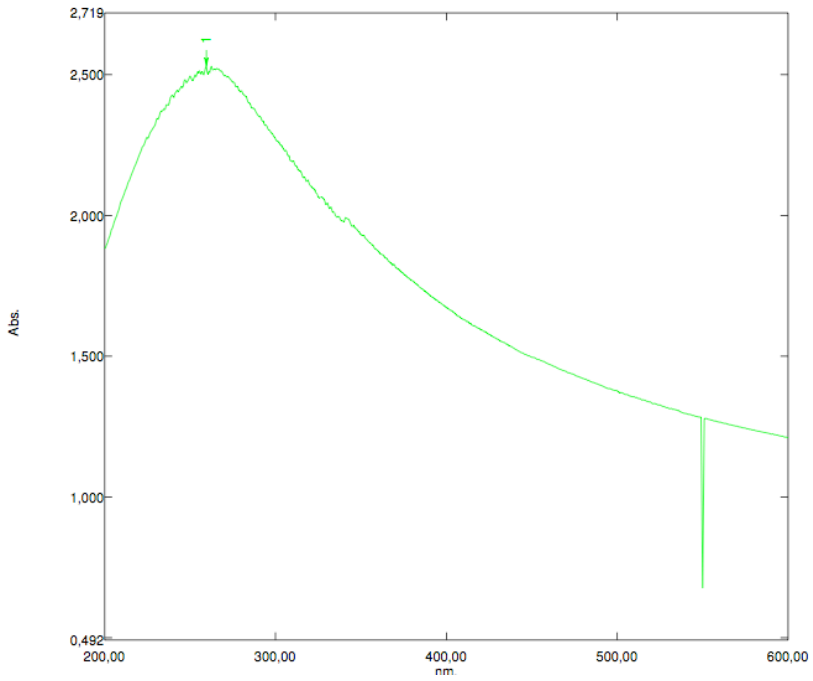

Fig. 12. Absorbance plot for 0.0648 gm

Table 5 : Absorbance table for 0.0648 gm

No.	**P**	**Wavelength**	**Abs.**
1	P	259,50	2,534

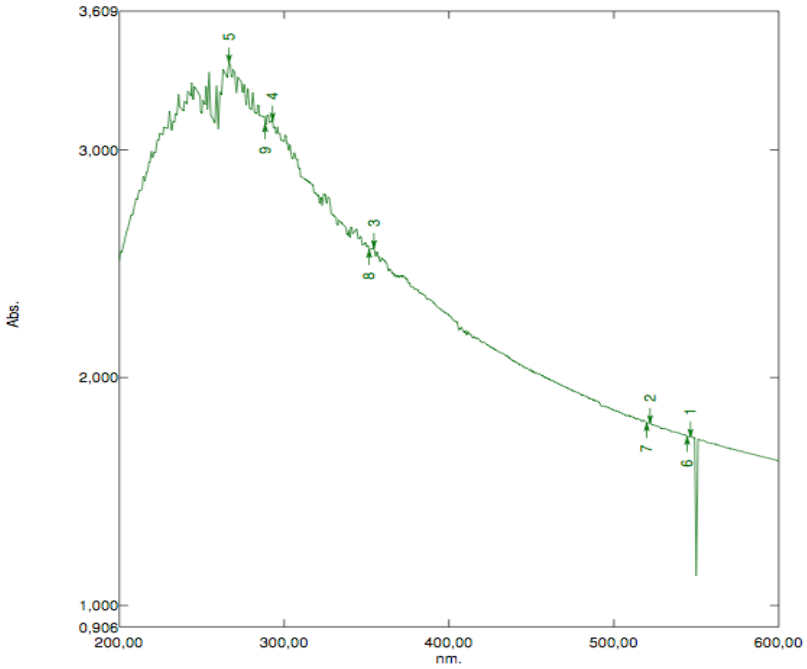

Fig. 13. Absorbance plot for 0.08424 gm

Table 6 : Absorbance table for 0.08424 gm

No.	P	Wavelength nm.	Abs.
1	P	546,50	1,741
2	P	522,00	1,801
3	P	354,50	2,569
4	P	293,00	3,128
5	P	266,50	3,383
6	V	544,50	1,740
7	V	520,00	,800
8	V	351,50	2,561
9	V	288,50	3,113

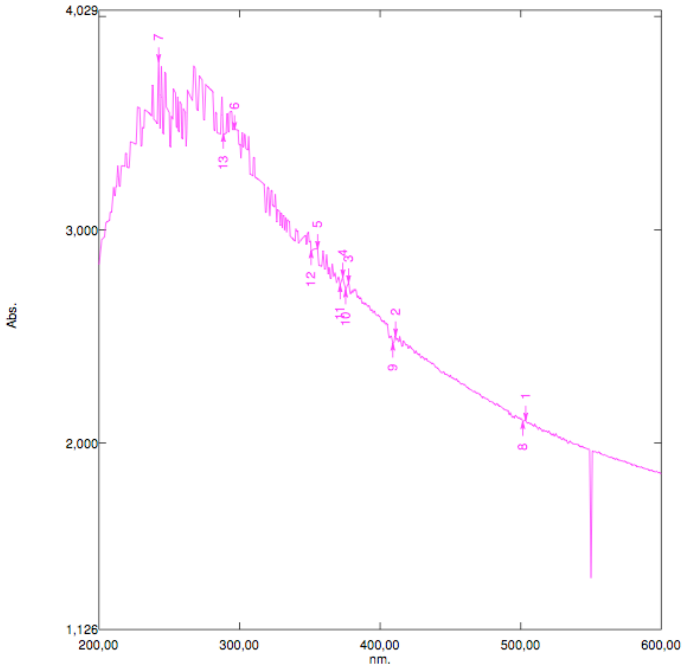

Fig. 14. Absorbance plot for 0.0972 gm

Table 7 : Absorbance table for 0.0972 gm

No.	P/V	Wavelength nm.	Abs.
1	P	503,50	2,107
2	P	411,00	2,502
3	P	377,50	2,751
4	P	373,50	2,777
5	P	355,50	2,912
6	P	296,50	3,470
7	P	242,50	3,787
8	V	501,50	2,102
9	V	409,00	2,468
10	V	375,50	2,718
11	V	371,50	2,742
12	V	351,00	2,901
13	V	288,50	3,448

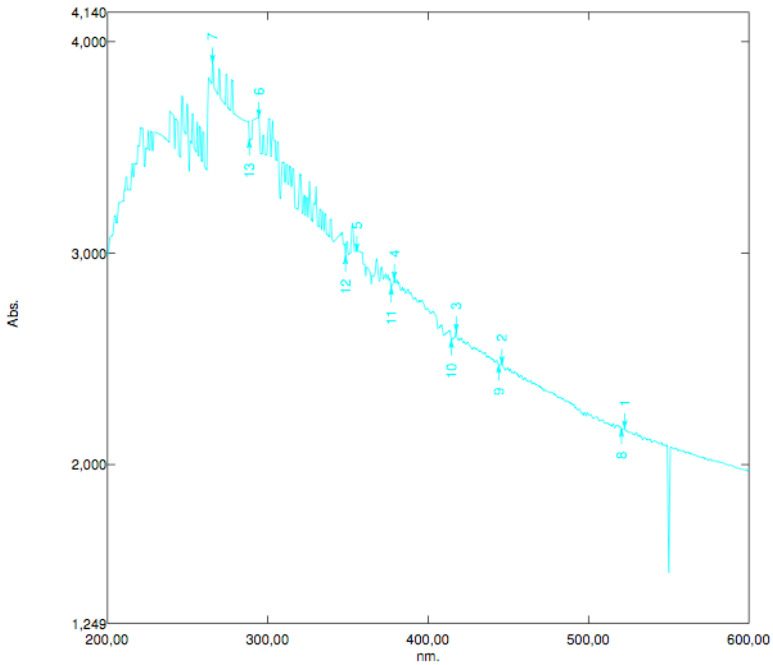

Fig. 15. Absorbance plot for 0.10368 gm

Table 8 : Absorbance table for 0.10368 gm

No.	P/V	Wavelength nm.	Abs.
1	P	522,50	2,169
2	P	446,00	2,473
3	P	417,50	2,628
4	P	379,00	2,874
5	P	355,50	3,009
6	P	294,50	3,643
7	P	265,50	3,899
8	V	520,50	2,168
9	V	444,00	2,471
10	V	414,50	2,590
11	V	377,00	2,840
12	V	348,50	2,985
13	V	288,50	3,536

Chapter 5 – Measurement of Thermal conductivity

5.1 – Thermal conductivity

The idea of increasing thermal conductivity of fluids with conducting particles suspended is not new. Ahuja et al., (1975) carried out the studies on practical implication of hydrodynamics and heat transfer of slurries. However the usual slurries with suspended particles of the order of micro to millimeters suffer from a number of drawbacks. The abrasive action of the particles causes erosion of components, clogging becomes a major problem in a small flow passage and the requirement of momentum transfer increases the pressure drop considerably.

In addition to these the tendency of micro / millimeter size particles to settle under gravity brings fouling and related problems. Thus even though the slurries have higher conductivities, are hardly useable as heat transfer fluids from other technological considerations. The above bottleneck of slurries with micron or greater size particles can be removed by using particles of nanometer dimensions. The concept was first materialized by a series of research works at the Argonne National Laboratory and probably (Choi, 1995) was the first to call the fluids with suspended particles of nanometer size, as 'nanofluids', which gained popularity.

The work presented in this chapter focus the study undertaken on the assessments of the thermal conductivity of water based nanofluids at various temperatures, below 373K. The literature is scarce in what concerns thermal conductivity of CNT based nanofluids at temperatures different from ambient. So the temperature range is studied from 283.15K to 333.15K in steps of 10. The results obtained will be discussed in the following sections.

5.2 – Experimental set up and Methodology

The experimental setup shown in Fig. 16, is used to measure the thermal conductivity of the prepared CNT-nanofluid samples. It consists of a constant temperature water bath, a KD2 Pro thermal property analyzer, a Styrofoam box to house and support a double jacketed bottle. The Thermal conductivity for all the samples is measured with a KD2 Pro

thermal property analyzer (Decagon devices) which was also used for the studies reported by (Ding et al. 2006) and (Timofeeva et al. 2007). The KD2 Pro uses the same principle as the transient hot wire technique for measuring the thermal conductivity, as mentioned earlier.

Fig. 16. Experimental setup for measuring the thermal conductivity

The nanofluid sample for the analysis is placed in a 20ml volume container (double jacketed) and the temperature of the sample is maintained by a constant temperature water bath. The constant temperature water bath was purchased from VWR International with a heating capacity of 2.2 kW. The temperature range for the bath is from -25 to +150ºC, so the nanofluid sample can be maintained thermally stable within this operating range. To save the power the cooling capacity of the bath varies with temperature, as for 20, 0, -10ºC the cooling capacity is 581, 423, 216 Watts respectively. The flow rate pressure and suction are 22 and 15 L/min, respectively. The bath fluid used is Kryo 30, which allows for highly accurate thermostating, even at extreme temperatures. The fluid (Kryo 30 solution) is forced to flow in and out of a double jacket bottle with the help of a silicon pipe, which can support extreme temperature changes. The KS-1 sensor of the KD2 Pro which has

operating environment temperature range of -50 to 150ºC is then inserted into the bottle, for the needle to approximate the medium with the least disturbances to the sample, to guaranty accurate measurements. To minimize forced convection, the sensor is well supported in the liquid on a firm bench to prevent shaking during the measurements. The orientation of the sensor must be vertical for better results. The double jacket bottle is kept inside a Styrofoam, which is carved exactly to the shape of the bottle to ensure a thermally stable sample.

The following method is used for all thermal conductivity measurements undertaken

1.) A small portion (20 ml) is taken from the main prepared sample and maintained at a particular temperature.

2.) The KS-1 sensor is used to measure thermal conductivity, and the readings are taken at a 15 mins time interval.

3.) The measurement is carried out for the particular temperature until the same reading is observed for, at least, four times.

4.) To obtain the thermal conductivity for all remaining temperatures under study, the sample is replaced. A new sample is always used for different temperatures measurements.

5.3 – Results and Discussion

5.3.1 –Measurement of thermal conductivity of CNT-water based nanofluids at various temperatures and particle volume fractions.

Thermal conductivity of CNT-water based nanofluids has been measured at various temperatures and volumes fractions. The results of the measurements undertaken are presented and discussed ahead. In this thesis K_p stands for the thermal conductivity of the particle and K_i is the thermal conductivity of the basefluid and, whereas K_{eff} is the effective thermal conductivity of nanofluids.

Measurement of thermal conductivity of CNT-water based nanofluids at various temperatures for particle volume fraction, ϕ= 0.25%

Thermal conductivity is therefore measured for nanofluid samples prepared with 0.25, 0.5, 0.75, 1.0, 1.5, 2.0 and 2.5% CNT volume fractions for temperatures from 283.15K to 333.15K. Three more samples of 3.0, 4.0, 5.0 vol% are added to the studies for temperature studies for 283.15 and 293.15K. The latter are carried out to assess the relative dependency of thermal conductivity on temperature.

In order to assess the repeatability of the results, and therefore the usefulness of the study, the thermal conductivity was measured at constant time intervals for a period of 90 mins. The same study was carried out at all temperatures and volume fractions. Figs 17 - 22 summarize the results obtained for the samples prepared with 0.25% volume fraction from 283.15 to 333.15K. The remaining study summarizing thermal conductivity versus time from temperature, 283.15 to 333.15K for the other tested volume fraction, (0.5%, 0.75%, 1.0%, 1.5%, 2.0%, 2.5%) is presented in Appendix from Figs. 51 - 74.

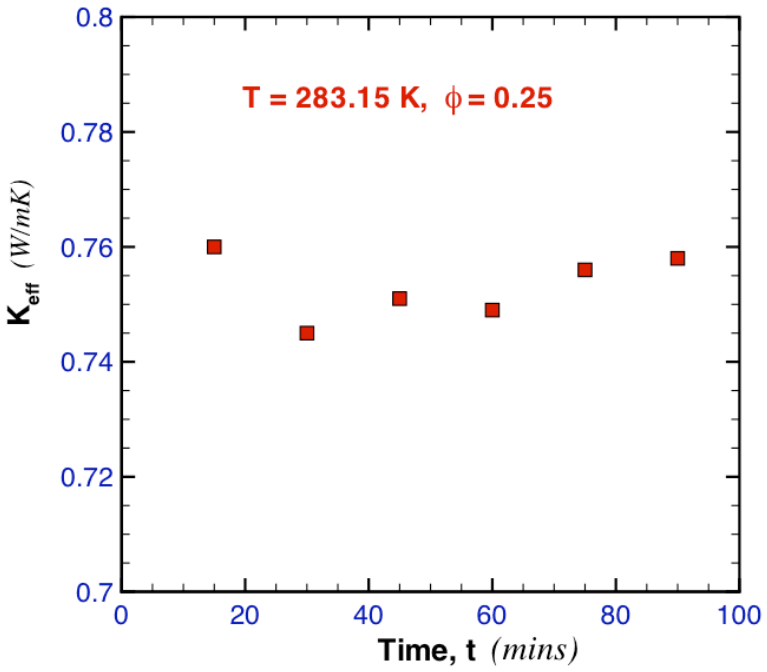

Fig. 17. Thermal conductivity versus time (t = 90 min, T = 283.15K, ϕ = 0.25)

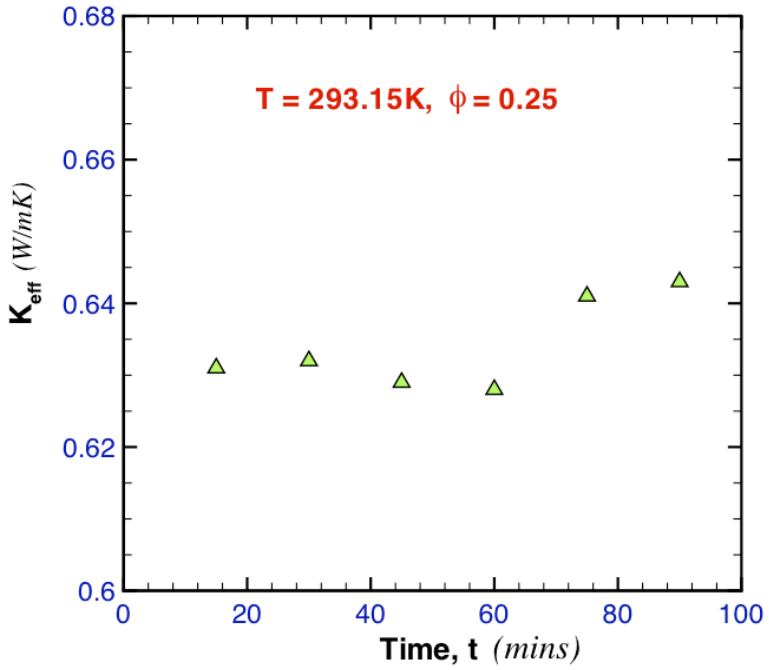

Fig. 18. Thermal conductivity versus time (t = 90 min, T = 293.15K, ϕ = 0.25)

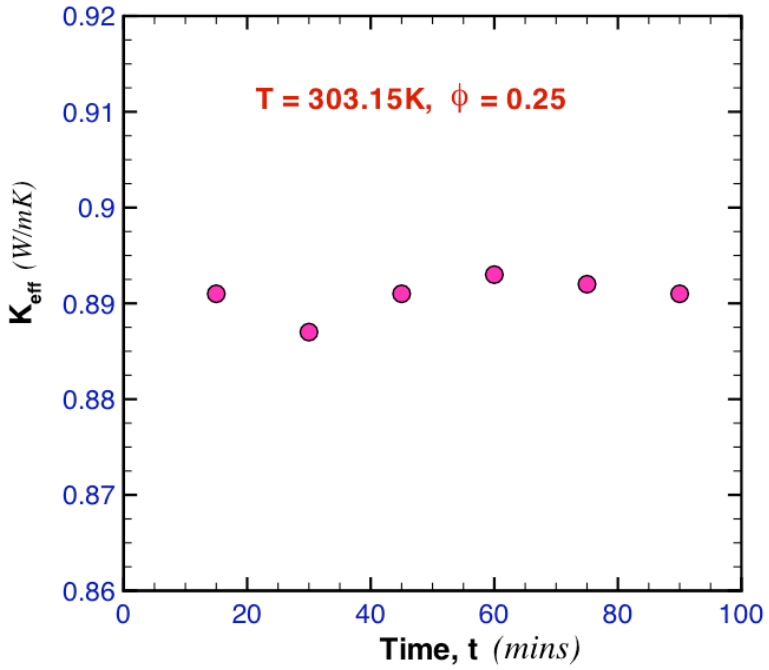

Fig. 19. Thermal conductivity versus time (t = 90 min, T = 303.15K, ϕ = 0.25)

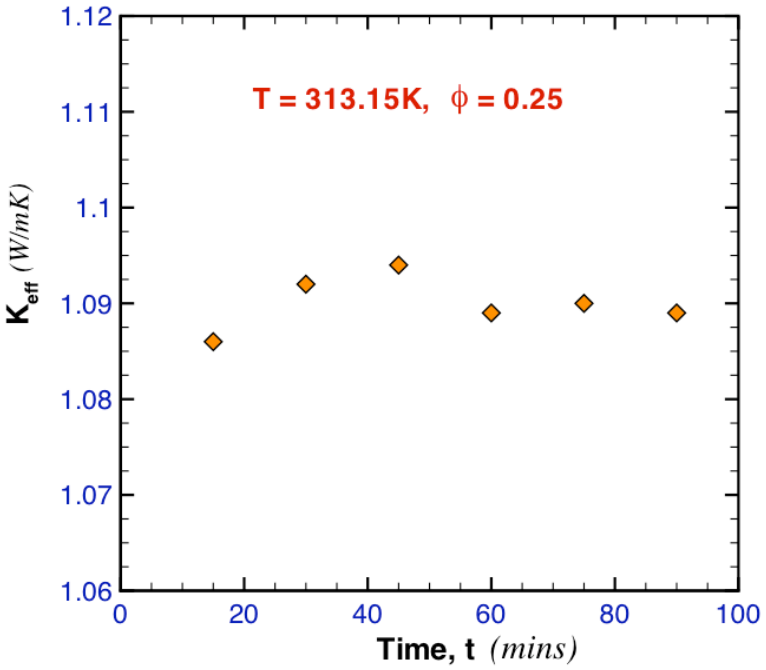

Fig. 20. Thermal conductivity versus time (t = 90 min, T = 313.15K, ϕ = 0.25)

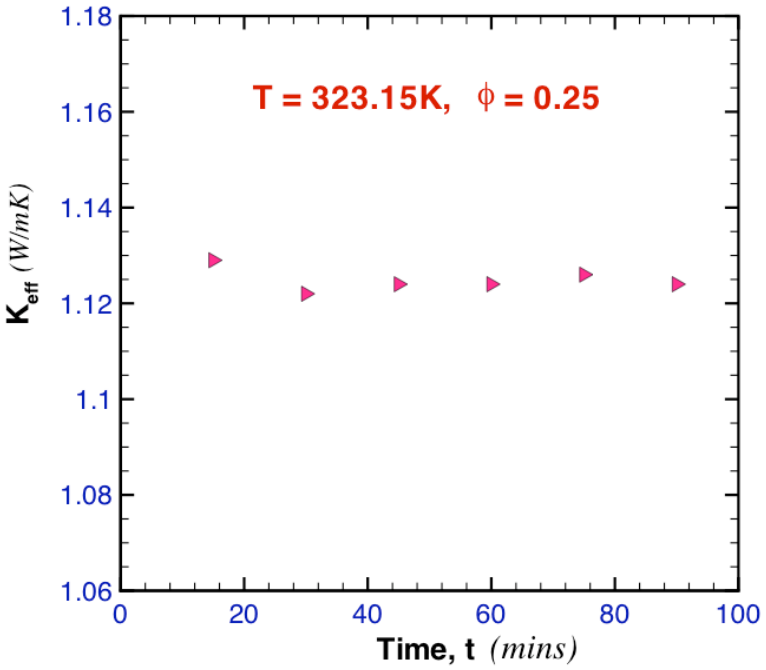

Fig. 21. Thermal conductivity versus time (t = 90 min, T = 323.15K, ϕ = 0.25)

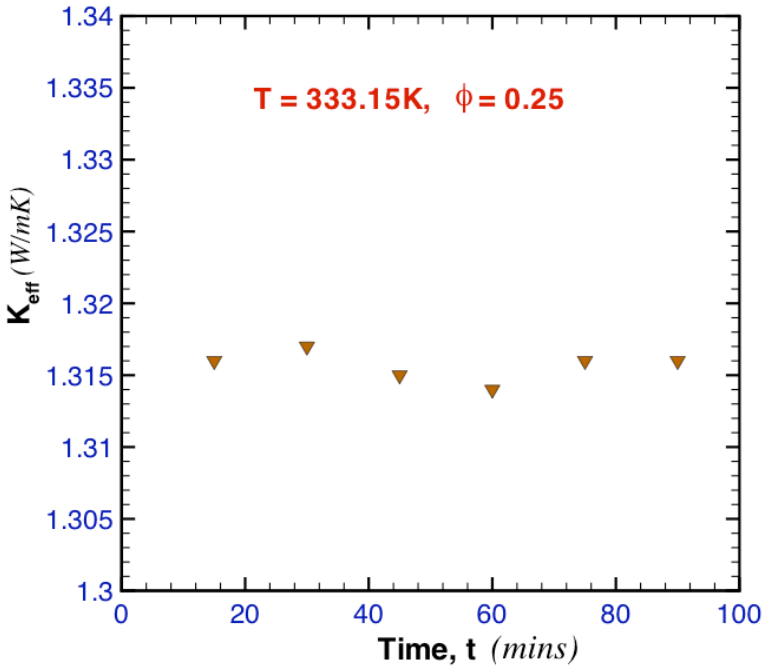

Fig. 22. Thermal conductivity versus time (t = 90 min, T = 333.15K, ϕ = 0.25)

The CNT-water based nanofluid at 278.15K is observed to freeze. Whereas at 283.15K has been observed to be completely in a liquid state. There is therefore a requirement to establish new latent heat for these particular fluids. In general the thermal conductivity increase has been observed with temperature rise for the same volume fraction. Fig. 23 presents the thermal conductivity versus temperature for 0.25 vol %. It can be observed that there is no linear increase in thermal conductivity, instead thermal conductivity decreases for 293.15K and again there is a sharp increase till it reaches 313.15K. The thermal conductivity is less for 293.15K than for 283.15K, for all volume fractions tested. The thermal conductivity of ice i.e; water at 273.15K is 2.23 W/mK but when the temperature is increased it decreases to 0.588W/mK for 283.15K, 0.605W/mK for 293.15K presenting a linear trend till it reaches its maximum at 333.15K 0.654W/mK. In the present study two trends are observed. The first one within the temperature range (283.15-293.15K), where thermal conductivity clearly decreases as temperature rises. The other, within 293.15-333.15K, where thermal conductivity can be seen to increase as the temperature of the nanofluids rises. The same is valid for all CNT concentrations studied, as presented in the Appendix (Fig. 54, Fig. 58, Fig. 62, Fig. 66, Fig. 70, Fig. 74)

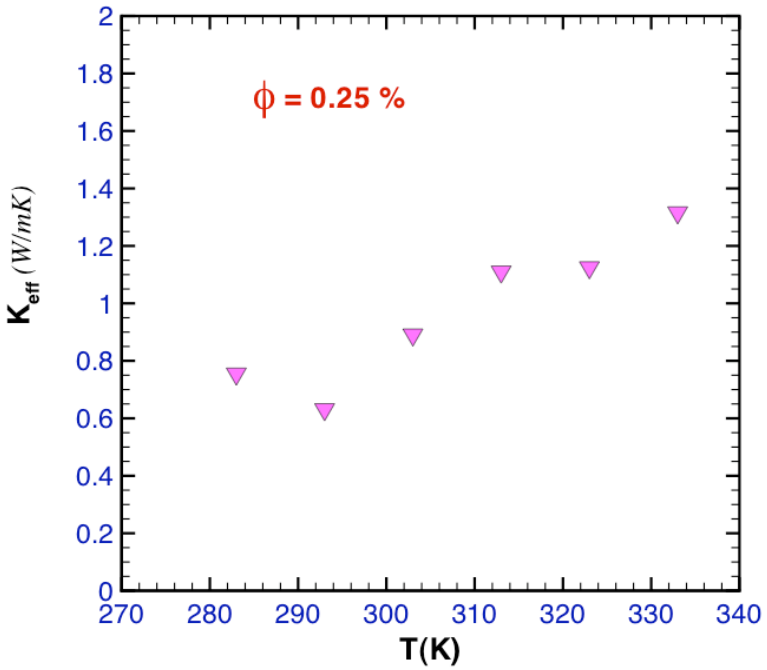

Fig. 23. Variation of thermal conductivity with increase in temperature from 283.15K to 333.15K for ϕ = 0.25%

5.3.2 Comparision of thermal conductivity versus temperature at all volume fractions (ϕ) studied

The datas presented in Table. 9 are plotted in the Fig. 24 establishing a comparision of thermal conductivity versus temperature for all the volume fractions. Like the present results, Patel et al. (2003), has also reported that thermal conductivity enhancement ratios of Cu nanofluids are enlarged considerably when the temperature increases, however (Chen et al., 2008) showed a different results as for CNT nanofluids, the thermal conductivity enhancement behaviours for very low volume fraction of 0.01, 0.006 and 0.002 almost keep constant when the tested temperatures vary. Brownian motion differences in these nanofluid systems may contribute to the observed differences. The Brownian motions of the suspended Cu nanoparticles are prone to take place and will become more intensive when the temperature rises. The micro convention caused by the Brownian motions would help to enhance the thermal conductivity of the suspensions, whereas for the CNT suspensions used with EG and cylindrical nanotubes with large aspect ratios, the effect of Brownian motion is not so obvious.

In the present study there is a decrease in thermal conductivity at 293.15K for all volume fractions tested, which deserves special attention . As the particle volume fraction is increased in the base fluid the thermal conductivity also increases. But there is a slight variation for ϕ = 1.5%, as the thermal conductivity decreases further for 303.15K instead of increasing like all other samples tested. For ϕ = 2.5%, the thermal conductivity at 323.15 and 333.15K are relatively lower than the other sample's thermal conductivity. One possible reason for this, may be that the thermal conductivity is highly dependent on other important factors such as the structure of the CNTs, clustering and even experimental accuracy.

Table 9: Thermal Conductivity for water and CNT-water nanofluid at different volume percentage and temperature

	CNT volume fraction (%)										
Temp (K)	0.25	0.5	0.75	1.0	1.5	2	2.5	3.0	4.0	5.0	Water
283.15	0.755	0.815	0.822	0.856	0.871	0.874	0.890	0.897	0.917	0.959	0.588
293.15	0.631	0.595	0.570	0.582	0.589	0.676	0.680	0.688	0.688	0.758	0.605
303.15	0.891	0.887	0.887	0.891	0.894	0.894	0.921				0.619
313.15	1.110	1.093	1.120	1.213	1.283	1.311	1.384				0.632
323.15	1.125	1.453	1.476	1.499	1.520	1.540	1.582				0.644
333.15	1.316	1.572	1.591	1.592	1.624	1.680	1.700				0.654

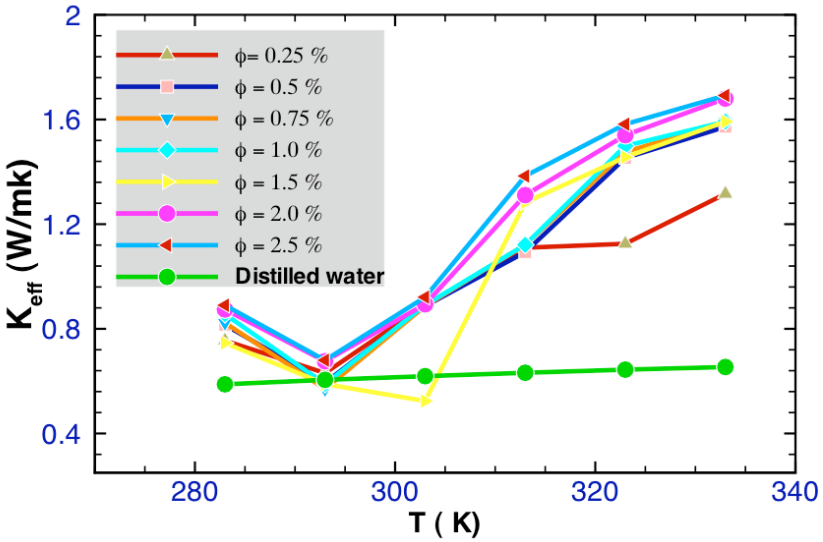

Fig. 24. Variation of thermal conductivity with temperature at different volume fraction

The variation of thermal conductivity with temperature at different volume fractions is presented in Figs. 25 – 30. It is clear that the thermal conductivity increases with ϕ but it cannot be said to a linear increase. Thermal conductivity gradually increases as ϕ increases at 283.15K, moreover at 293.15K, 303.15K and 313.15K, the thermal conductivity decreases for ϕ = 0.5, 0.75 and 1.0 vol % when it reaches 323.15K and then 303.15K, a steep shoot-up in thermal conductivity can be observed within the range of 0.5 % to 2.5 %. There is no sufficient literature reference to justify or compare the present study for the different temperature, and volume fraction, studied of the experimentalist, have carried work for volume fraction up to 1 vol% and at ambient temperature. An exception made to the work of Das et al. (2003) examined the effect of temperature on thermal conductivity enhancement for nanofluids containing AL_2O_3 and CuO. They have attempted for the range of temperature within 294.15K to 325.25K and observed a 2 to 4-fold increase in thermal conductivity. Li and Peterson (2006) have again investigated thermal conductivity enhancement for AL_2O_3 and CuO nanofluid, from 300.15K to 308.15K. Patel et al., (2003) studied gold (Au) and silver (Ag) nanoparticles based nanofluids for a temperature range of 303.15 to 333.15K.

.

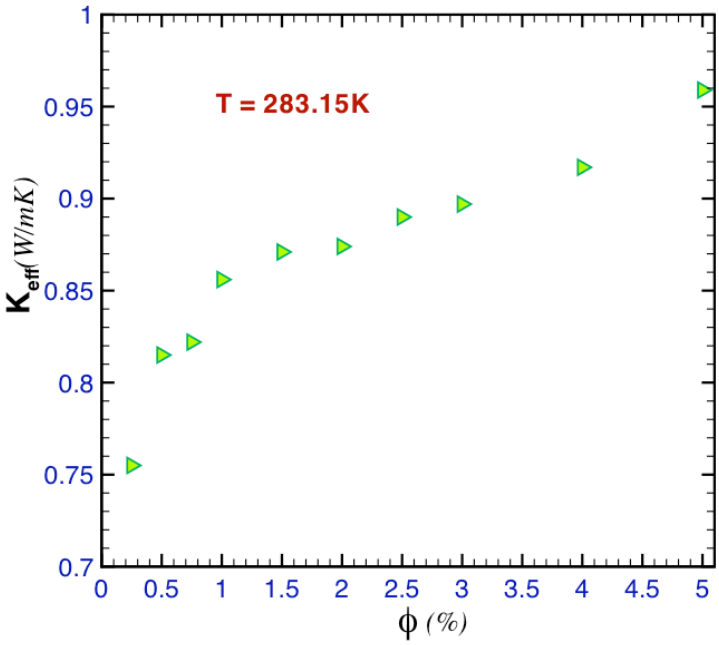

Fig. 25. Thermal conductivity of CNT – water nanofluids as a function of ϕ at T = 283.15K

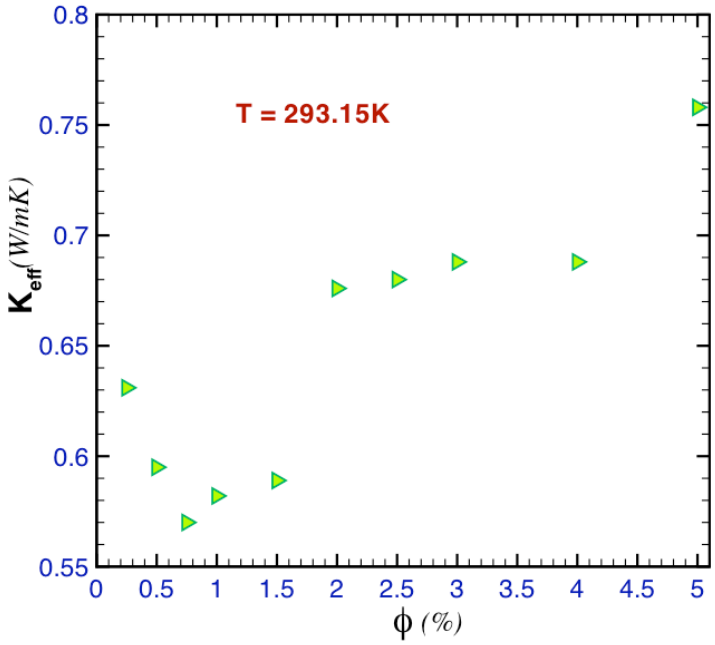

Fig. 26. Thermal conductivity of CNT – water nanofluids as a function of ϕ at T = 293.15K

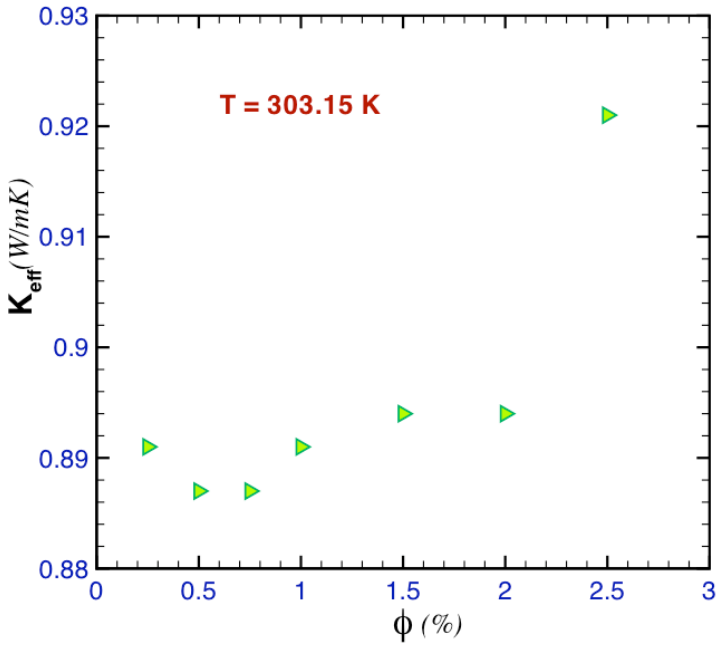

Fig. 27. Thermal conductivity of CNT – water nanofluids as a function of ϕ at T = 303.15K

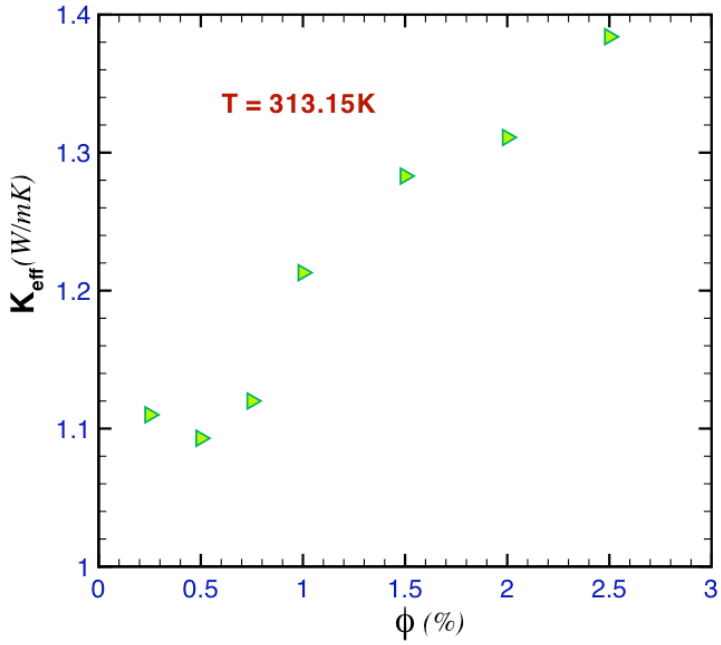

Fig. 28. Thermal conductivity of CNT – water nanofluids as a function of ϕ at T = 313.15K

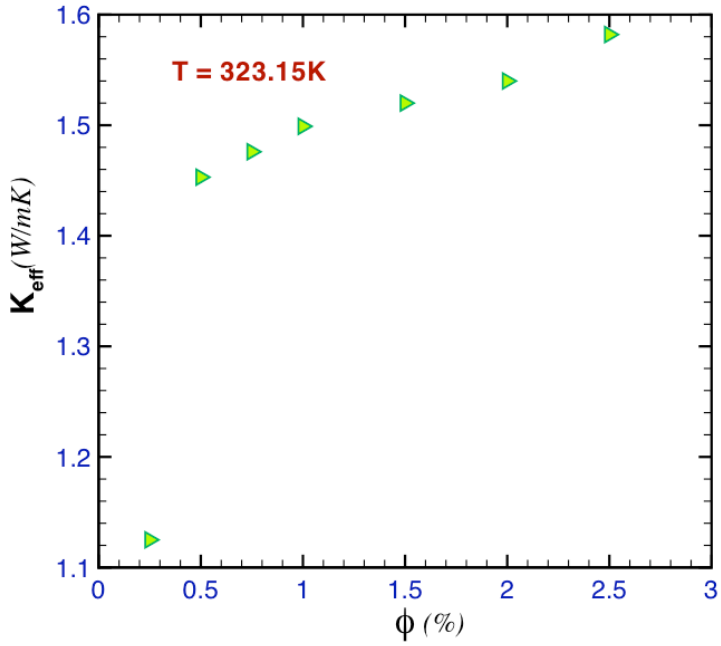

Fig. 29. Thermal conductivity of CNT – water nanofluids as a function of ϕ at T = 323.15K

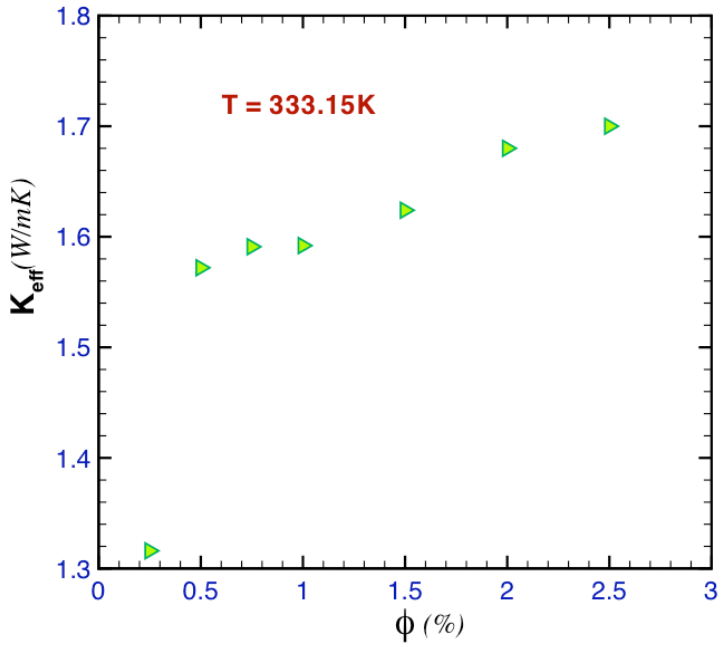

Fig. 30. Thermal conductivity of CNT – water nanofluids as a function of ϕ at T = 333.15K

5.3.3 Comparision of CNT-water nanofluid K/K_i Vs ϕ for temperatures from 283.15K to 333.15K

Anomalous increase in thermal conductivity was reported by Choi et al. (2001) when measuring the effective thermal conductivity CNT-EG nanofluid. Results displayed that the measured thermal conductivity was anomalously greater than the theoretical predictions and was nonlinear with nanotube loading. The present study results also show an anomalous increase in thermal conductivity. Table. 10 presents the values of K_{eff}/K_i up to 333.15K. At 323.15K and 333.15K for all the samples tested, the percentage increase in thermal conductivity can be seen to be more than 100. There is a gradual increase in thermal conductivity percentage for the rise in particle volume fraction at 283.15K, 293.15K, 303.15K, whereas from 313.15K to 333.15K there is a higher percentage increase when ϕ rises. As it can clearly be depicted from Fig. 31.

Table 10: Experimental datas for K_{eff}/K_i for as a function of Carbon Nanoparticle volume percentage

CNT volume fraction (%)										
Temp(K)	0.25	0.5	0.75	1.0	1.5	2.0	2.5	3.0	4.0	5.0
283.15	1.284	1.386	1.3989	1.455	1.48	1.486	1.513	1.525	1.559	1.6309
293.15	1.0429	0.9834	0.9421	0.9619	0.9735	1.1173	1.1239	1.372	1.1372	1.2528
303.15	1.4391	1.4329	1.4329	1.4394	1.4442	1.4442	1.4879	-	-	-
313.15	1.7563	1.7294	1.7721	1.9193	2.0300	2.074	2.1898	-	-	-
323.15	1.7466	2.256	2.291	2.3276	2.360	2.391	2.456	-	-	-
333.15	2.0122	2.403	2.432	2.434	2.483	2.568	2.599	-	-	-

The highlighted cells show the thermal conductivity percentage increase of more than 100%. The latter can be supported with the published results, which have been included and reported (Table. 1, Section 2.1.3)

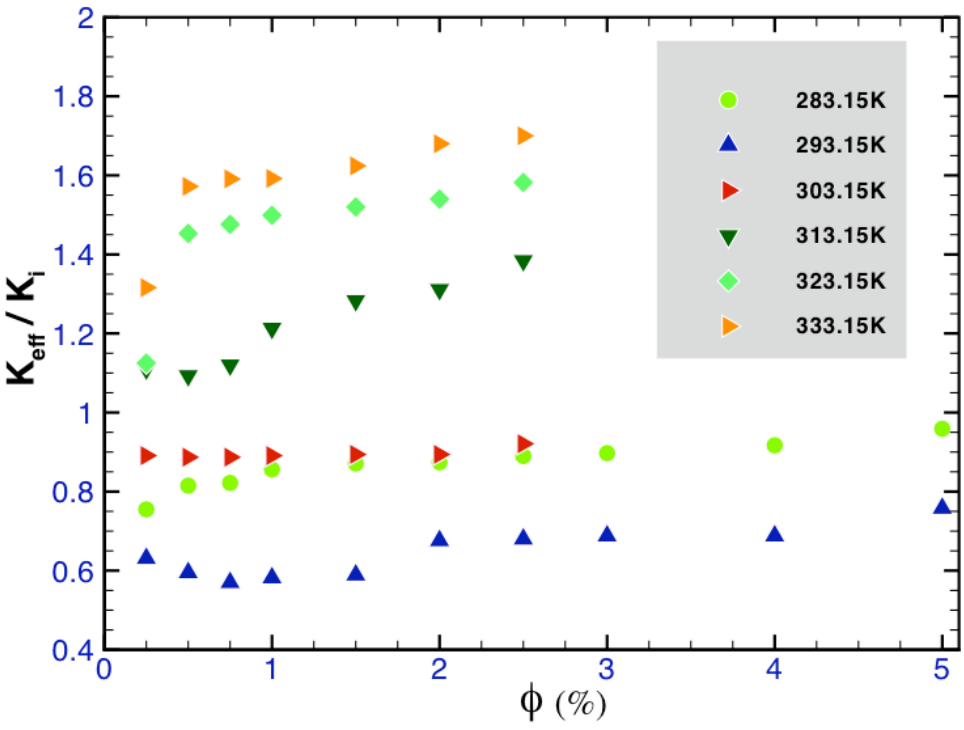

Fig. 31. Ratio of thermal conductivity of nanofluid and base fluid at different temperatures and volume fractions.

5.3.4 Comparision of the present results with the literature

Table. 11 presents the experimental work from different authors and Fig. 32 is the comparision of percentage increase in thermal conductivity of CNT-water nanofluids with the previously published results of CNT-water nanofluids from Ding et al. (2006), Xie et al. (2003), Chen et al. (2008). Looking at these figures it can be said that the percentage increase in thermal conductivity rises with particle concentration. For example, the percentage increase in thermal conductivity at ϕ = 0.5 % is 43.29% whereas it increases to a slightly higher value of 43.94 for ϕ =1.0%. Unlike the results of Ding et al. (2006) whose value, increased from 35% to 79% from 0.5 to 1.0 vol%, in the present study the percentage increase in thermal conductivity is almost negligible while ϕ increases from 0.5% to 1.0%. The present results lie well within the published results of Ding et al (2006) and Chen et al. (2008) and are in good agreement with the results of Chen who also found almost constant values of thermal conductivity while ϕ increased from 0.5 to 1.0. The discrepancy among the different groups should rely on the properties of CNTs used, the aspect ratio, the inclusion of dispersants, and the experimental errors involved. Of course the authors have not done experiments on varied temperature, so ambient temperature is taken into consideration. For the analysis further systematic research is necessary to obtain a whole map for the thermal conductivities of CNTs.

Table 11: Comparision study of experimental results with the literature

ϕ	Present study	Ding et al (2006)	Xie et al (2003)	Chen et al (2008)
0.50	43.29	35.0	-	6.5
0.75	43.29	52.0	-	-
1.00	43.94	79.0	7.0	12.0

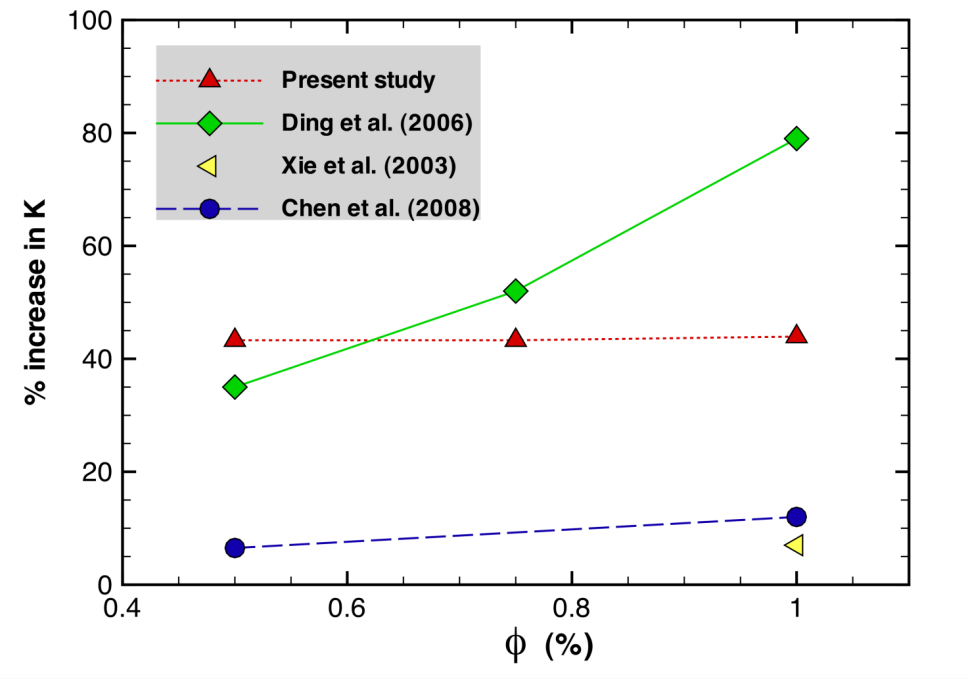

Fig. 32. Comparison of the present experimental data for the percentage increase in thermal conductivity of CNT-Water nanofluids.

5.3.5 –Comparison of results with the theoretical model

The need for explaining the results observed can be fulfilled by theorizing it or fitting it to the existing theories. The classical theory of thermal conductivity of fluid with suspended solid particles is from Maxwell (1881) more than a century back, which assumes the shape of particles to be spherical. This theory was subsequently modified for non-spherical particles by Hamilton and Crossser (1962) for solid to liquid thermal conductivity ratio of more than 100. Lee et al., (1999) confirmed that even though the model of Hamilton and Crosser agrees well with Al_2O_3-water or ethylene glycol nanofluid, it fails in the case of nanofluids containing CuO nanoparticles. Thus, it can be said that simple model using the concept of suspensions of millimeters to micrometer dimensions are doubtful for application to nanofluids. All the investigations mentioned above-present thermal conductivity at room temperature and hence failed to have an insight to probable the enhancement mechanism. Here in this section K_{eff} is the effective thermal conductivity (can also be said as thermal conductivity) of nanofluid and K_b is the thermal conductivity of the basefluid, K_p is the thermal conductivity of the nanoparticle. The models that are being employed here for comparing with the present results are given in Table 12.

Table 12: Theoretical models employed for comparision with the present experimental study

Investigators	Effective Thermal conductivity	Remarks
Hamilton and Crosser [1962]	$\frac{k_p + (n-1)k_b - (n-1)(k_b - k_p)\phi}{k_p + (n-1)k_b + (k_b - k_p)\phi}$	For non-sperical particles, $K_p/K_b > 100$, n is an empirical shape factor (n=3/ψ, ψ is the spericity)
Xue [2005]	$\frac{1-\phi+2\phi\frac{k_p}{k_p-k_b}\ln\frac{k_p+k_b}{2k_b}}{1-\phi+2\phi\frac{k_b}{k_p-k_b}\ln\frac{k_p+k_b}{2k_b}}$	For CNT based nanofluids and including the axial ratio and the space distribution.
Patel et al [2008]	$1+\frac{k_p\phi r_b}{k_p(1-\phi)r_p}$	For CNT based nanofluids . r_b = radius of basefluid molecular size (0.2 nm) r_p = average ratio of the suspended CNTs

Fig. 33 presents the experimental study here reported with the above mentioned theoretical models at 293.15K only for Carbon nanotubes as the nanoparticles, and distilled water as the basefluid. The present results are qualitatively in good agreement with Hamilton and Crosser model and patel model. The linear fit line is exactly parallel with the lines of the other models. The results of the present study are well below the values of other model, may be because the ambient is here considered to be 293.15K.

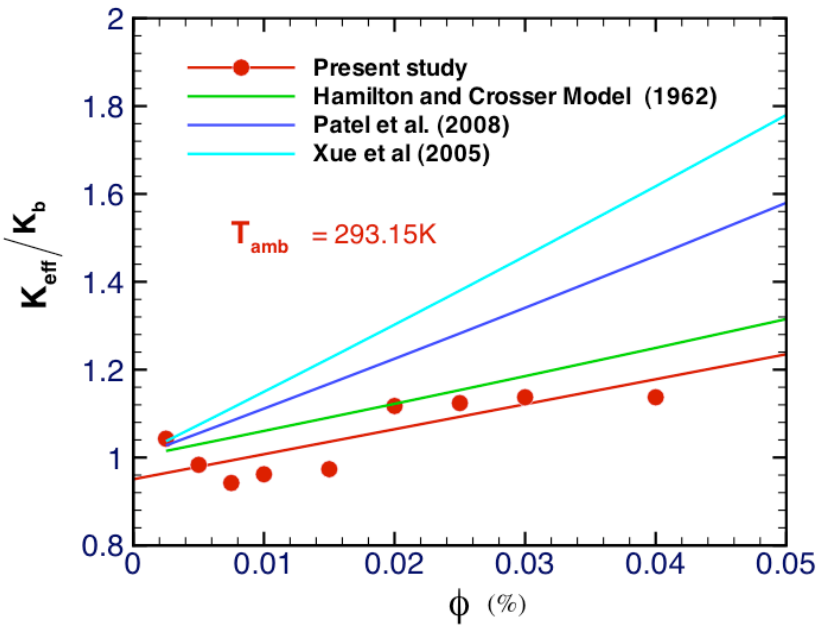

Fig. 33. Theoretical model comparisons with the present study for 293.15K

Fig. 34 represent the results compared at 303.15K as the ambient temperature varies for different countries. Here the present study results are well above all theoretical predictions and there is a slight percentage increase for increasing particle concentrations. There is clearly no linear increase in the thermal conductivity percentage increase but a very gradual rise, the latter may be sufficient to conclude that there is an optimum value of volume fraction after which there is not much increase in thermal conductivity, establishing the limits of the investment in nanoparticles and therefore nanofluids preparation, but further insight on the subject is definitely required.

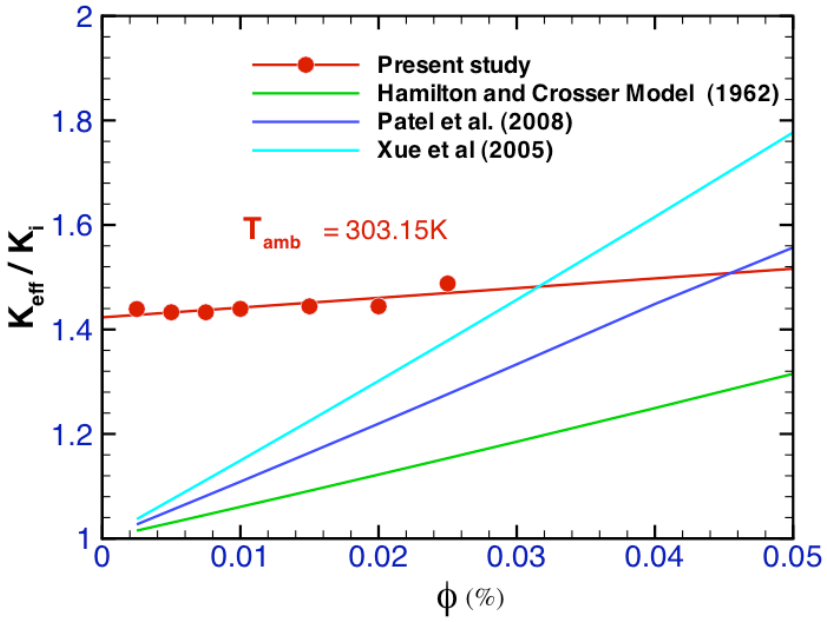

Fig. 34. Theoretical model comparisons with the present study for 303.15K

Chapter 6 – Measurement of viscosity

6.1 – Introduction

Lee et al. (2008) investigated the effective viscosities and thermal conductivity of aluminium oxide (Al_2O_3) nanoparticles with volume fraction of 0.01–0.3 vol.% dispersed in water. An oscillation viscometer (VM-10A, CBC Co., Ltd) was used to measure the viscosity of the nanofluids. All data were collected for temperatures ranging between 20ºC and 40ºC. The results have shown that viscosity of nanofluids significantly decreases with increasing temperature. Moreover, the authors found out that the measured viscosities of nanofluids exhibit a nonlinear relation with the particle concentration and increase with increasing particle concentrations.

The viscosity measurements for the CNT-water based nanofluid of particle volume fraction from 0.25 vol% up to 4 vol% within the temperature range 298.15K – 328.15K, are described and discussed in the following sections.

6.2 – Experimental set up

The viscosity was measured using a controlled stress rheometer, Haake, Model RS1 (Fig. 35). The rheological tests were carried out with a sensor system Z34 DIN that comprises one rotor and one beaker, with a connected thermocontroller. The spindle used was 20.00 mm (radius) at a clearance to bottom equal to 7.2 mm. The accuracy of the data was assessed via a Brookfield viscosity standard (4.30 mPa.s) from Engineering Laboratories, Inc., Stoughton, U.S.A.

The measurements were performed in the shear rate range from 0 to 600 sec^{-1} for temperatures from 298.15 to 318.15K. For all the nanofluids CNT-water, tested at least three measurements were made, to evaluate the accuracy of the results, including 250 or 125 data points, depending on the range of shear rate. The maximum precision was ±0.01 and ±0.17mPas, the minimum for the range of shear rate from 50 to 150 sec^{-1}.

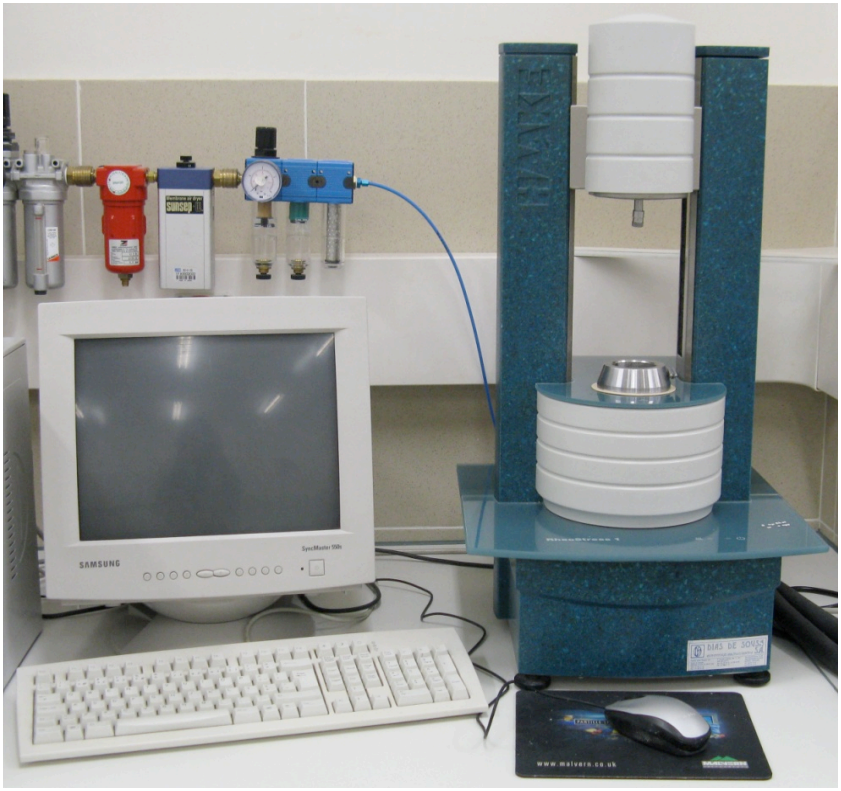

Fig. 35. The experimental setup of the controlled stress rheometer, model RS1, Haake

At low shear rates, in the range of 20-100 s^{-1} (slightly less than 100 s^{-1}), the CNT-water nanofluids show a pseudo-plastic behavior, where for shear rates exceeding 100 s^{-1} a dilatant behavior can be observed. Both present non-Newtonian behaviors, since the viscosity varies with the shear rate, it remains constant. The pseudo-plastic behavior is commonly known as "shear-thinning fluid" and occurs when the increased shear rate results in a reduction in the sample viscosity. A dilatant behavior, "shear thickening" is characterized by rise in the viscosity with increasing shear rate.

6.3 – Results and Discussion

6.3.1 – Viscosity Measurements at different temperatures and volume fractions

By analyzing the charts presented in Fig. 36 it appears that with a temperature increase from 298.15 to 328.15K there is a clear decrease in viscosity. The results obtained at all temperatures and for all samples studied, seem to present similar trends. For the sample with 0.50 vol% there is, as expected, the same behavior: pseudo-plastic at low shear rates and dilatant at higher shear rates. Without exception, at 1.5 vol% the viscosity decreases

with temperature and from 100-120 sec^{-1} increases with shear rate. Also, the shear stress decreases slightly with increasing temperature.

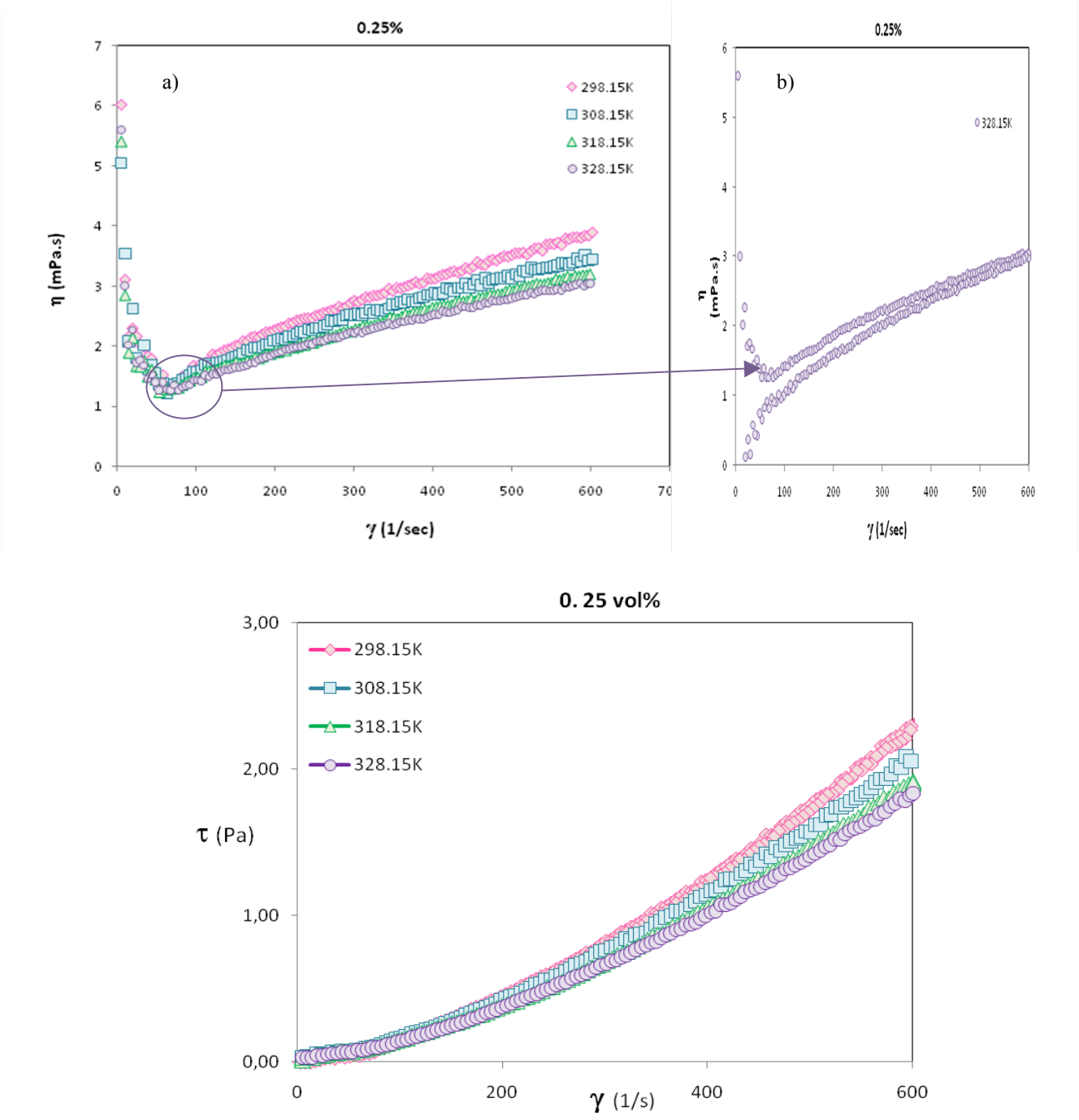

Fig. 36. Viscosity and shear stress for 0.25% at 298.15K, 308.15K, 318.15K,328.15K

The CNT-water nanofluid with 1.0 vol% in Fig. 37 is the only one in which there has been a visible difference between the various temperatures studied. Moreover, at the temperature of 328.15K, the viscosity at 300 sec^{-1} is higher than for the temperatures of 308.15 and 318.15 K. However, as the shear rate increases, at the temperature of 328.15K the viscosity decreases, below 318.15K but more than at 308.15K.

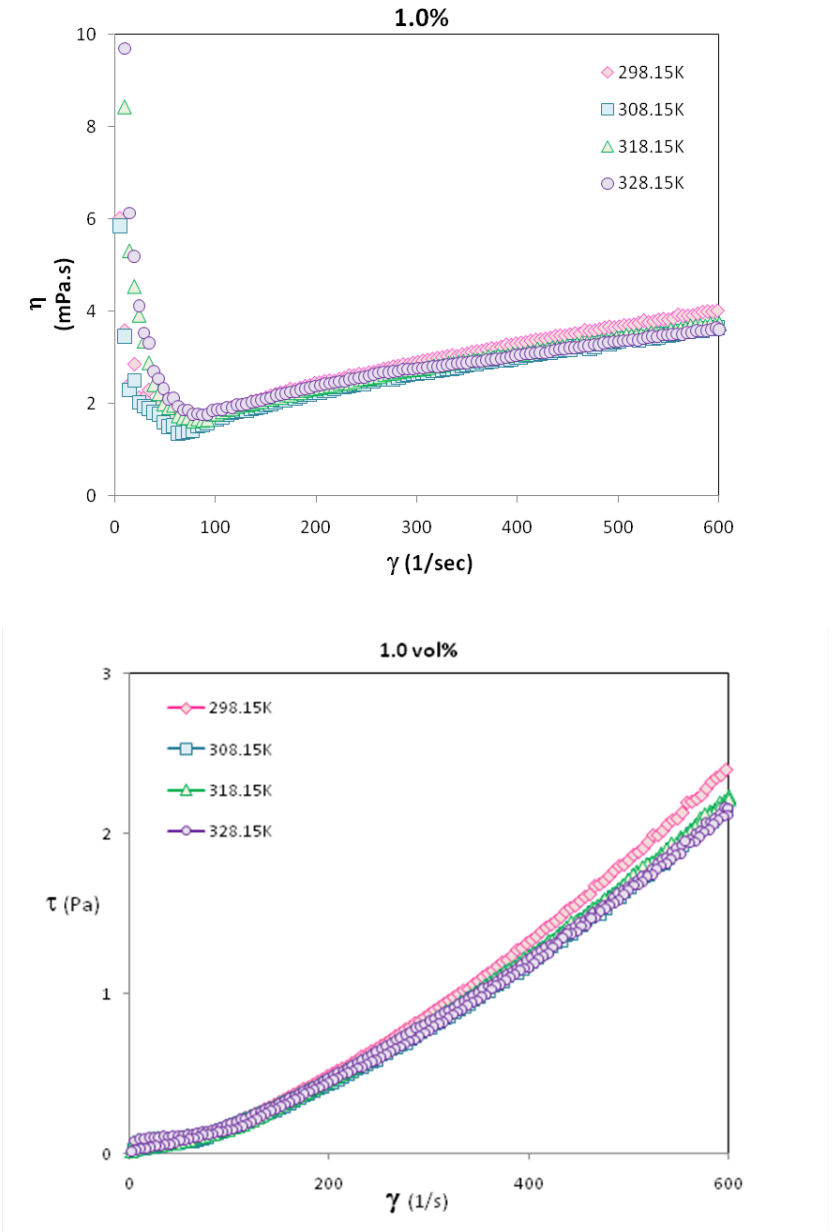

Fig. 37. Viscosity and shear stress for 1.0% at 298.15, 308.15, 318.15,328.15 K

While presenting these little differences in temperatures, it should be referred that the viscosity depends heavily on the preparation of the samples and even the collection for analysis (at least three tests are conducted for the same sample).

Physical and chemical effects usually cause the characteristics of non-Newtonian suspensions. The main physical parameters to consider are:

- Concentration of the particles;
- Size of the particles;
- Particle size distribution;
- Shape of particles.

Effect of particle concentration: when solid particles are added to a pure liquid and the resulting mixture is caused to flow, the effect of the presence of the particles is to distort the streamlines such that they curve around the particles instead of remaining parallel as they would do in a uniform shear field. This distortion results in an increase in viscosity, as more work is required for streamline distortion. In dilute suspensions of non-interacting particles, this is the sole effect responsible for viscosity increase, but as the particle concentration is raised, the distortion of streamlines around one-particle influences the degree of streamline distortion around a neighbouring particle. Particles are now interacting inasmuch as there now exists a mutual influence on the hydrodynamic forces generated in the fluid separating the particles. In addition, temporary, or sometimes more permanent, doublets or triplets are formed between particles that have the effect of immobilizing liquid between them. The result is that the occluded liquid is not now available in which remaining particles may be dispersed. The overall volume fraction of particles has, therefore, been increased effectively above that calculated purely from consideration of the volume of suspension occupied by solid particles only. It is possible for permanent immobilization of liquid between particles to occur if there exists sufficient distortion of the flow field in the suspension.

The precise cause of shear-thinning behaviour is unknown, but one may postulate that: if collision between particles at high concentrations is one of the main factors determining suspension viscosity, then as shear rate in the suspension is increased, the collision frequency, which determines momentum transfer between particles and therefore

energy dissipation, may not keep pace with the rising shear rate; the overall effect would be a reduction in viscosity.

The behaviour dilatant, on the other hand, is probably caused by the various mechanical interactions between particles: one of the main factors would be the substantial frictional forces generated at particle surfaces in addition to momentum transfer. Owing to the increasing contribution from mechanical interactions between particles as particle concentration is raised, it seems highly unlikely that any suspension will retain Newtonian properties, except at very low rates of shear.

Particle size: If all the forces acting in a suspension arise from hydrodynamic interactions only then suspension viscosity is independent of shear rate. If a viscometer is used so that its surface producing shear in a suspension is large compared with the particle size, partial concentration is low or medium, but not high approaching an unsaturated state, and the viscosity values are independent of viscometer size, then the viscosity would not depend on particle size either.

Particle size distribution: The viscosity can be minimized through a selection appropriate distribution of size, maintaining the total concentration density of particles in or on the other hand, it is possible to maximize the concentration of particles using an optimal distribution of particles, not however exceeding the allowable levels of viscosity.

Form of particle-effects of the irregularity in the form of particles in the viscosity of the suspension: Many experimental studies have indicated that, for a given overall solid volume fraction present in suspension, the greater the anisometry, the larger is the viscosity. Thus lowest viscosities are found for spherical particles systems whereas fiber suspensions of very high aspect ratio are highly viscous at comparatively low solids concentrations.

According to Clarke (1967), as the particles become more asymmetrical, the suspensions become more dilatant. Clarke (1967) investigated a number of factors which influence suspension viscosity, including the shear rate, particle size, particle density and particle size distribution, but concluded that the shape of the particles for a given concentration exerts a greater influence on the viscosity than any of the other factors mentioned above. The rotation of non-spherical particles under the action of a velocity gradient causes an increase in the frequency of contacts and, hence, an increase in effective

concentration. At the lower concentrations where the influence of the solids is mainly hydrodynamic, differences in the viscosity between the various suspensions are small.

For a given solids volume concentration, irregularly shaped particles give higher viscosity than spherical ones for the same mean particle size. The magnitude of the increase in viscosity, rises as either the anisometry of the irregularly shaped particles becomes more marked or the aspect ratio of axially symmetrical particles is increased. There is some evidence which suggests that the effect of particle size distribution on the viscosity of concentrated, irregularly-shaped particle suspension is less important than for a spherical particle system.

Analyzing the graph in the Fig. 38 for the viscosity (η) vs shear rate (γ) and shear stress (τ) vs shear rate (γ) under temperature of 308.15K, the viscosity rises with increasing concentration of nanoparticles and decreases with temperature. Both the dilatant and pseudo-plastic behaviour exist. As for shear stress depending on the shear rate, in this case, the sample volume of 4.0%, record levels of shear stress higher than the other samples that is, as in other samples there is only a slight increase in shear stress, for 4.0 vol% the value increases away from the rest, mainly from 200 s^{-1}.

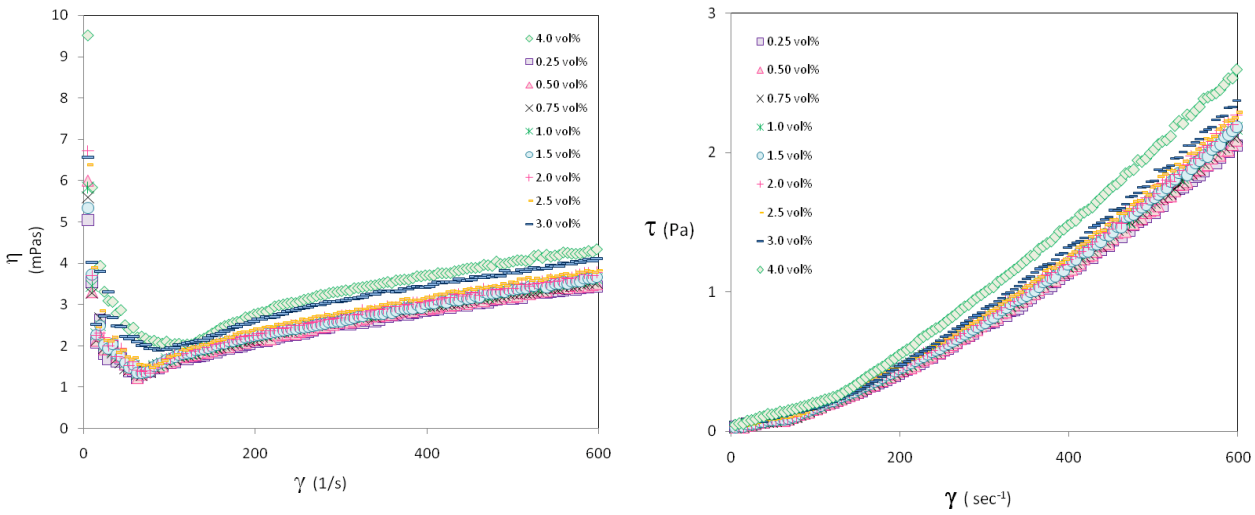

Fig. 38. Viscosity vs shear rate for all volume fractions at 308.15K, and shear stress *vs* shear rate for different volume fractions at 308.15K.

In general for the entire sample, viscosity rises with increasing volume fraction and decreases with temperature. When the applied shear rate is low, like 60 s^{-1}. Shear thinning behaviour is seen for the nanofluids at 60 s^{-1}. But when high shear rate was applied shear thickening behaviour is seen for the nanofluids at 350 s^{-1}. The other graphs for shear stress

and viscosity for different volume fractions and temperatures are included in the appendix section from Figs. 75 – 81.

6.3.2 - Viscosity Vs Volume fraction for different temperatures

The viscosities for the various temperatures were studied at three chosen cutting speed, 10, 50 and 100 s^{-1}, including the characteristics of pseudo-plastic behaviour as shown from Fig. 39 and Fig. 40. With an increasing cutting speed of 100 s^{1}, the viscosity decreases and, with increasing of CNTs volume fraction the viscosity rises. Regardless of temperature, viscosity is always higher for lower cutting speeds and slows the growth of this. These plots are consistent with the pseudo-plastic behaviour, in which the viscosity decreases with increasing speed of cutting. From 200 s^{-1}, the viscosity for all the samples increases with the speed of cut (up to 600 s^{-1}).

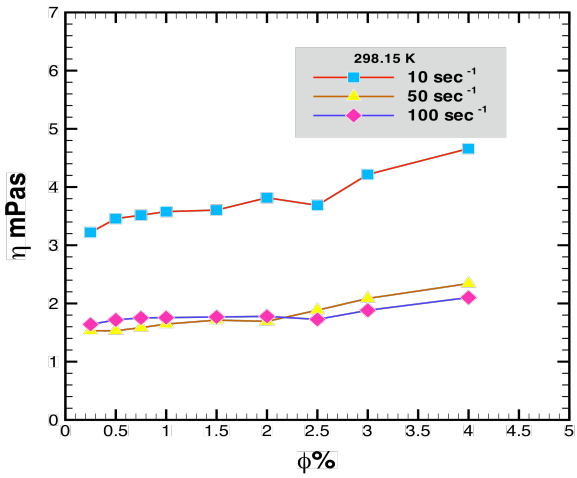

Fig. 39. Viscosity of the CNT-Water nanofluids at 10, 50 and 100 s^{-1}, at 298.15K

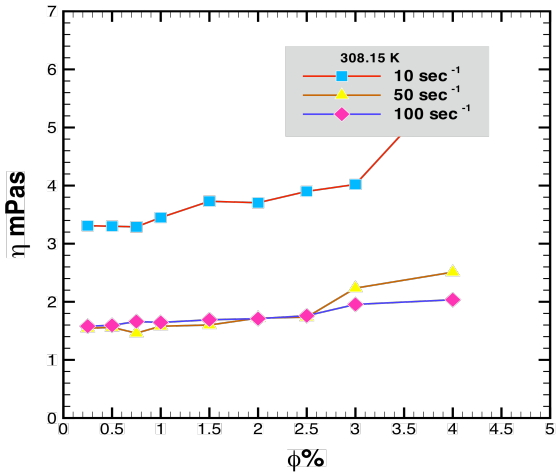

Fig. 40. Viscosity of the CNT-Water nanofluids at 10, 50 and 100 s^{-1}, at 308.15K

The thixotropic behavior is frequently observed in materials such as greases, heavy printing inks and paints. When subjected to varying rates of shear, a thixotropic fluid reacts in the manner shown in Fig. 41 cut-off speed is raised to a certain point, after that immediately decreases to the point of departure. It should be noted that the curves of "rise" and "descent" do not coincide. This hysteresis curve is caused by the decrease in viscosity of the fluid with the increase in the cut-off time. These effects may or may not be reversible, some thixotropic fluids when stable for some time, recover its initial viscosity, while for others it never happens.

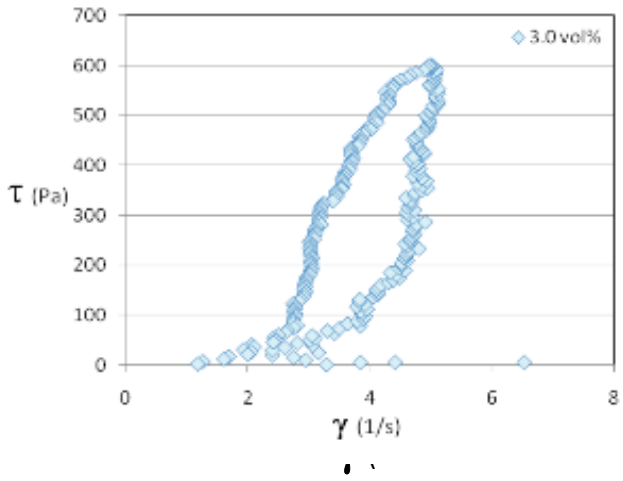

Fig. 41. Thixotropic behaviour exibited by high volume percentage sample

6.3.3 Theoretical models comparing with the present viscosity measurement

Einstein (1956) was the first to calculate the effective viscosity of a suspension of spherical solids using the phenomenological hydrodynamic equations. By assuming that the disturbance of the flow pattern of the matrix base fluid caused by a given particle does not overlap with the disturbance of flow caused by the presence of a second suspended particle, he derived the equation presented in Table.13.

Experimental data for the effective viscosity of nanofluids are limited to certain nanofluids. The ranges of the parameters (the particle volume concentration, temperature, etc.) are also limited. Still, the experimental data show the trend that the effective viscosities of nanofluids are higher than the existing theoretical predictions. In an attempt to rectify this situation, researchers proposed equations applied to specific applications, e.g., Al_2O_3 in water (Maiga et al., 2004a), Al_2O_3 in ethylene glycol (Maiga et al., 2004a), titanium dioxide (TiO_2) in water (Tseng and Lin, 2003), and CuO in water with temperature change (Kulkarni et al., 2006). The problem with these equations is that they do not reduce to the Einstein equation at very low particle volume concentrations and, hence, lack a sound physical basis. In Table. 13 the theoretical models are presented and the first three models Einstein (1906), Batchelor (1977), Maiga et al., (2004) are used for comparing the viscosity results at ambient temperature under analysis Kulkarni et al., (2006) present temperature as one of the parameter, so it is here used for comparing the results obtained during the present study at different temperatures.

The three models from the literature are used to compare the present viscosity results and it is clearly evident that the results are well above all the predictions and a slight deviation from the main trend should be noted when observing the results for 2.5 vol % as shown in Fig. 42. The Einstein model is far away from the present result whereas the Maiga et al seem to represent better the current situation. Furthermore all theoretical models lack in the inclusion of particle size, temperature, clearly showing the need for further research into the subject.

Table 13: Effective viscosity models for comparing with the present viscosity results

Investigator	Theoretical Model
Einstein (1906)	$\mu_{eff} = (1 + 2.5\phi_p)\mu_b$
Batchelor (1977)	$\mu_{eff} = (1 + 2.5\phi_p + 6.2\phi_p^2)\mu_b$
Maiga et al. (2004)	$\mu_{eff} = (1 + 7.3\phi_p + 123\phi_p^2)\mu_b$
Kulkarni et al. (2006)	$\ln \mu_{eff} = -(2.8751 + 53.548\phi_p - 107.12\phi_p^2) + (1078.3 + 15857\phi_p + 20587\phi_p^2)(1/T)$

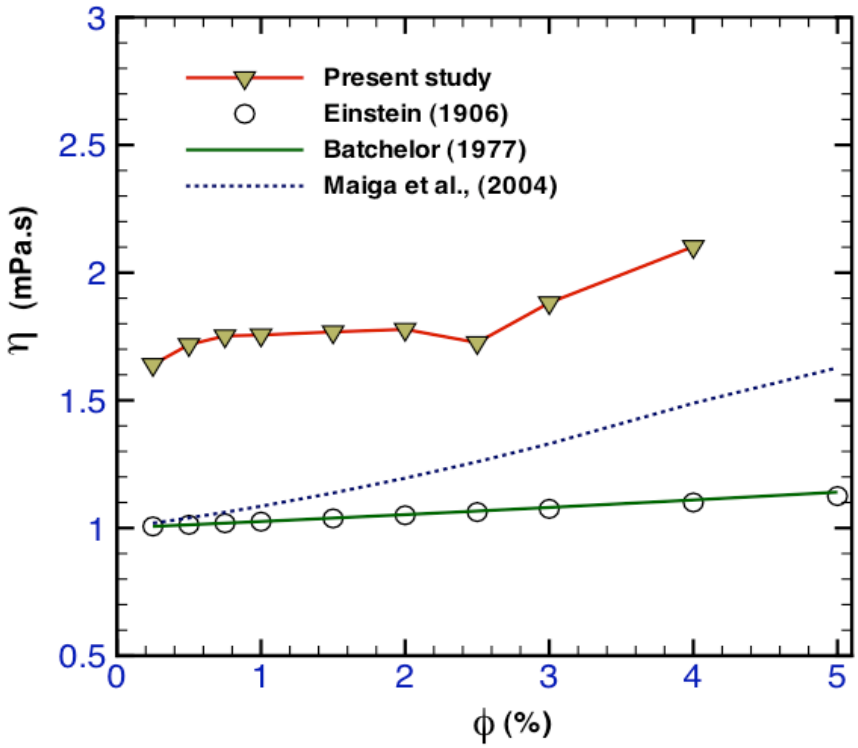

Fig. 42. Comparision for the viscosity results with the theoretical models at ambient temperature

The data presented in Fig. 43 establishes the comparision between the present viscosity results with those of Kulkarni model for 298.15K, 308.15K, 318.15K, 328.15K. At the temperature of 298.15K and 308.15K the model seems to over predict the present results. Moreover for 318.15K and 328.15K the model underpredicts the present results above. For 328.15K there is a very increase from 0.25 vol% to 2.5 vol%, but for 318.15K there is great variation from 1.5 vol %.

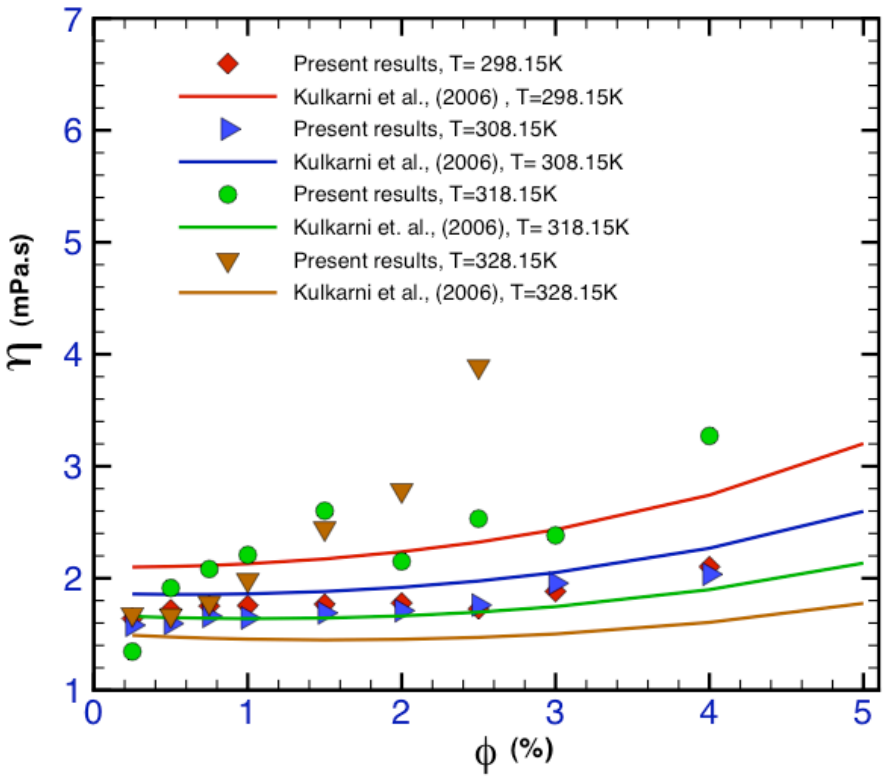

Fig. 43. Comparision of viscosity with Kulkarni et al., (2006) at different temperatures.

Chapter 7 – Measurement of surface tension and density

7.1 – Introduction

The surface tension study assumes a relative importance. Since it may cause some effects in flows when nanofluids is used as heat transfer fluid, due to gravity the fluid drops become spherical when separated. One example of a positive application of surface tension is the use of sprayers to paint a surface. Surface tension causes paint to form very small droplets that cover a surface uniformly without forming drips and runs. Water at 20°C has a surface tension of 72.8 dynes/cm compared to 22.3 for ethyl alcohol and 465 for mercury.

Understanding surface tension better could lead to new materials processing techniques that either reduce surface tension's influence or take advantage of it. Because a microgravity environment greatly reduces buoyancy-driven fluid flows and sedimentation, surface tension flows become very important. The importance of surface tension research in microgravity is that surface tension-driven flows can interfere with experiments involving fluids. As nanofluids have high heat transfer characteristics than the conventional base fluids, it can replace the latter and the surface tension properties becomes very important for further proceedings in the research. Surface tension in an important parameter in pool boiling. There are not much density measurements from the literature and density measurements at different temperatures for all nanofluids.

In this chapter surface tension and density measurements on CNT-water nanofluids are described and discussed. The results obtained are also compared with those found in the literature.

7.2 – Experimental set up and Methodology

The surface tension was determined by method of Du Nouy (method of the ring). Surface and equilibrium liquid-liquid interfacial tensions were measured using a PC controlled KSV Sigma 70 tension balance which employs the Du Noüy ring-detachment method. The“pendant drop” method is adopted for surface tension measurements (KSV® CAM

200), by M.N. Pantzali et al 'Measuring transport properties of nanofluids. Fig. 44 shows the experimental setup for the measuring with PC controlled KSV Sigma 70 tension balance, which is used for measuring the surface tension at different temperatures.

Fig. 44. Experimental set up of surface tension measuring with PC controlled KSV Sigma 70 tension balance, KSV Instruments LTD

The platinum ring in the tension balance was thoroughly cleaned by immersion in a concentrated solution of nitric acid during several hours. Then it was rinsed with acetone, carefully flamed in a Bunsen burner, washed again with acetone and dried. The measurements were automatically corrected to the actual values by means of the Huh and Mason compensation for interface distortion. The temperature inside the surface tension measurement vessel was maintained and controlled at 298.15±0.10 K using a UltraTerm bath. For the surface tension each experimental point results from a set of about 3 measurements for each nanofluid (0.25%-4%).

Fig. 45 shows the density meter Experimental densities were measured using an Anton Paar DMA 60 digital vibrating tube densimeter, with a DMA 512P measuring cell in the temperature of 298.1 K and pressure range (0.10 to 25.00) MPa. The temperature in the

vibrating tube cell was measured with a platinum resistance probe which has a temperature uncertainty of ±0.01 K coupled with a GW Instek Dual Display Digital Multimeter GDM-845. A Julabo P-5 thermostatic bath with silicone oil as circulating fluid was used in the thermostat circuit of the measuring cell which was held constant to ±0.01K.

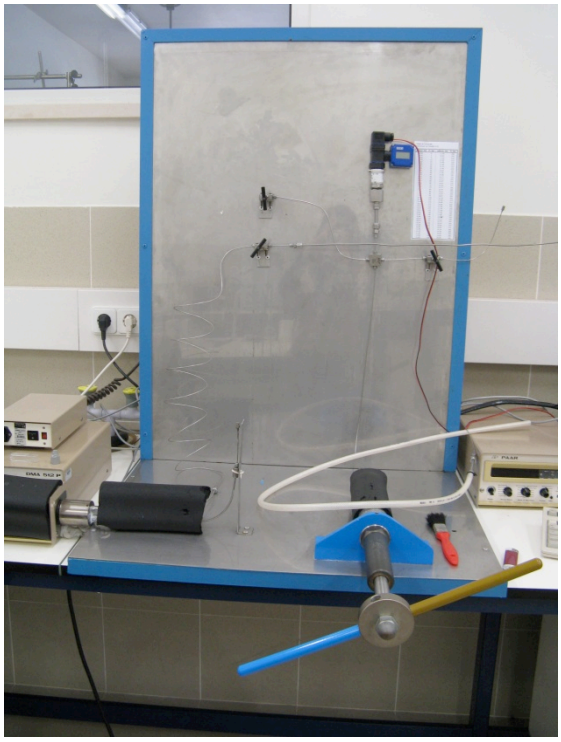

Fig. 45. Anton Paar DMA 60 digital vibrating tube densimeter Range: 300-400 bar

The required pressure was generated and controlled with a Pressure Generator Model 50-6-15, High Pressure Equipment Co., using acetone as the hydraulic fluid. The diameter of metallic tube is 1.59×10-3 m and the buffer is more than 1 m in length which guarantees the inexistence of diffusion of the hydraulic liquid in the liquid contained in the cell of densimeter. Pressures were measured with a pressure transducer (Wika Transmitter S-10, WIKA Alexander Wiegand GmbH & Co.) with a maximum uncertainty of ± 0.03 MPa. An NI PCI-6220 data acquisition board (DAQ) from National Instruments (NI) was used for the real time registration of values of period, temperature and pressure. For this task a Labview application was developed. Modules of temperature (NI SCC-FT01) and pressure (NI SCC-CI20) was installed into a NI SC-2345 carrier and connected to the DAQ board.

Density determination by pycnometer is a very precise method. It uses a working liquid with well-known density, such as distilled water. The pycnometer (Fig. 46) is a glass flask with a close-fitting ground glass stopper with a capillary hole through it. This fine hole releases a spare liquid after closing a top-filled pycnometer and allows for obtaining a given volume of measured and/or working liquid with a high accuracy.

Method:

1.) To measure the mass of the dry pycnometer and then the mass of the distilled water (m_{DW}) and mass of the nanofluids (m_{nf}) samples with the help of mass balance.

2.) Then with equation 1 and 2 the density of nanofluid (ρ_{nf}) can be found. ρ_{DW} is the density of the distilled water.

$$V_{nf} = V_{DW} \quad \text{..... Equation 1}$$

$$\rho_{nf} = \frac{m_{nf}}{m_{DW}} \rho_{DW} \quad \text{..... Equation 2}$$

Fig. 46. pycnometer used for measuring the density of the samples

7.3 – Results and Discussion

Surface tension

As the temperature increases the surface tension decreases and as the volume fraction increases there is a very slow and gradual increase in the surface tension of the CNT-water nanofluids observed. Table. 14 presents the surface tension values of water used to compare the surface tension of CNT-water nanofluid at 25ºC.

Table 14: Surface tension values for water from 10ºC to 100ºC

	Surface Tension (±0.10)						
T (ºC)	*10*	*15*	*20*	***25***	*30*	*35*	*40*
γ (mN/m)	74.36	73.62	72.88	**72.14**	71.40	70.66	69.92
	Surface Tension (±0.10)						
T (ºC)	*45*	*50*	*60*	*70*	*80*	*90*	*100*
γ (mN/m)	69.18	68.45	66.97	65.49	64.01	62.54	61.06

Table.15 presents the surface tension values at 298.15K for 0.25 vol % which are obtained from the surface tension balance meter whereas for the remaining volume fractions studied, the results can be seen from table19 to Table 26 in the Appendix.

Table 15: Surface tension of CNT-water nanofluid for 0.25 vol% at 298.15

Sl.No	**Time**			**ST (mN/m)**			**T (ºC)**		
1	49	49	48	65.61	67.58	69.61	25	25.1	25.2
2	69	71	70	65.38	67.48	69.55	25	25.2	25.2
3	90	93	91	65.32	67.45	69.53	25	25.2	25.2
4	114	114	113	65.29	67.43	69.51	25	25.2	25.2
5	136	137	135	65.25	67.42	69.51	25	25.2	25.2
6	159	160	157	65.23	67.41	69.49	25	25.2	25.2
7	182	180	180	65.22	67.39	69.49	25.1	25.2	25.2
8	206	203	201	65.21	67.37	69.47	25.1	25.2	25.2
9	229	226	224	65.21	67.36	69.46	25.1	25.2	25.2
10	252	249	245	65.20	67.35	69.44	25.1	25.2	25.2
Total		_		65.29	67.42	69.51		_	
				67.41					

As seen in Table. 14 the surface tension decreases as the temperature increases for water. In the present study, since the samples are tested for just one temperature but for

different volume fraction up to 4%, the surface tension is found to increase as the volume fraction rises. This is shown in Table. 6 and the values are plotted in Fig. 47. The values for 0.75 vol % and 1.5 vol % deviate and the curve is not linear. The deviation may be caused by the preparation method uncertainity and the experimental error.

Table 16 : Surface tension values (ST) at different volume fractions at 298.15K

ϕ %	ST mN/m
0.25	67.41
0.50	71.84
0.75	69.63
1.0	72.22
1.5	68.62
2.0	71.89
3.0	70.60
4.0	72.09

The values obtained for surface tension at 298.15K resembles more or less with those of water at 298K for all the volume fractions. It seems that in order to further discuss this issue, more results may be obtained mainly in what concerns temperature variation.

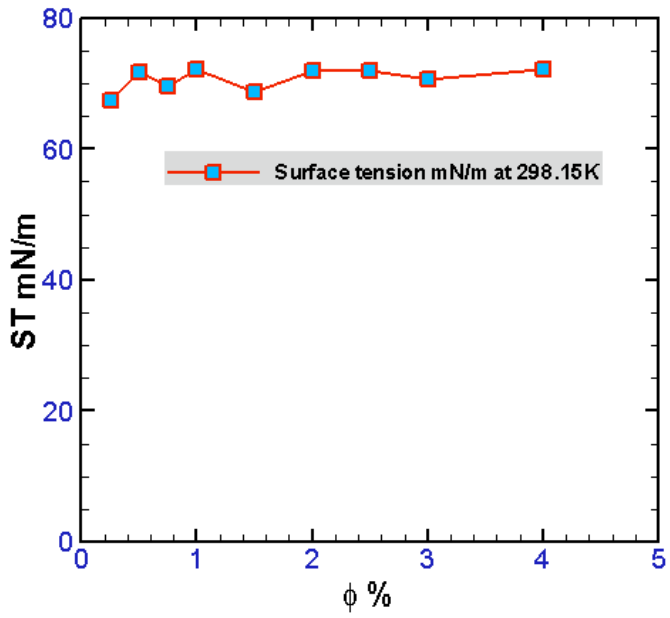

Fig. 47. Surface tension for different ϕ % at 298.15K

Density

The density of CNT-water nanofluids was measured with the aid of a pycnometer as well as a densimeter since it was intended to determine the surface tension of the samples. The results are presented in Table. 17. Analyzing the values in Table 17 one could find that the nanofluids have densities similar to water and in some cases higher. The densimeter is used to determine the densities of only two samples, namely 0.25 and 0.75%. The values are comparatively similar between the two methods used.

Table 17: Results for CNT-water nanofluid obtained by densimeter and pycnometer

ϕ % CNT+Water	**ρ(g/cm^3) Pycnometer**	**ρ(g/cm^3) Densimeter**
0.25	0.9973	1.0002
0.50	0.9981	--
0.75	1.0014	1.0054
1.0	0.9012	--
1.5	0.9515	
2.0	1.0028	--
2.5	1.0037	--
3.0	0.9962	--
4.0	0.9555	--

Looking at densities as a function of the concentration of carbon nanotubes in the Fig. 48, it appears that no major difference in density occurs, except for the sample of 1.0 vol% which has much lower density values compared to other samples.

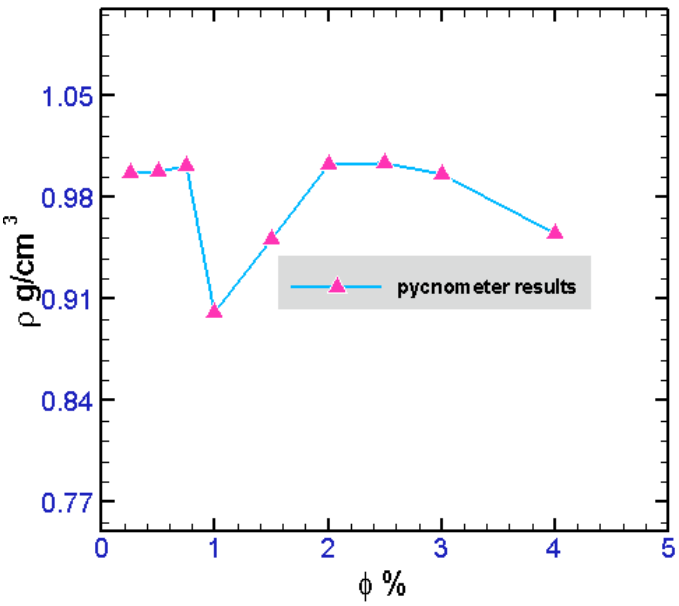

Fig. 48. Density as a function of volume fraction with the results obtained from pycnometer

Fig. 49 presents the densities of the two samples measured at 298.15K using a densimeter. For both the samples, one could find a slight increase in density while the pressure is increased from 1 to 250 bar. The densities of the sample at 0.25 vol% are slightly lower than those at 0.75 vol%.

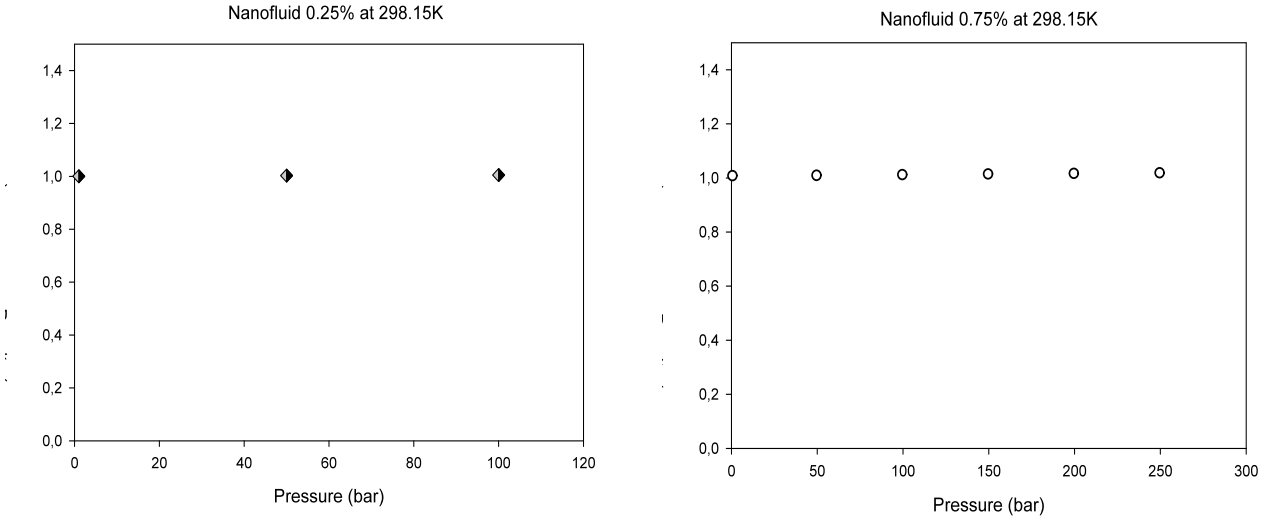

Fig. 49. Density *vs* pressure plot for the nanofluids of 0.25 and 0.75 vol% at 298.15K, measured using a densimeter.

To have a better insight, the results are also compared with analytical models from the literature (Buongiorno, 2006).

$$\rho_{nf} = \phi\rho_p + (1-\phi)\rho_{bf} \quad \text{..... Equation 3}$$

Where ρ_{nf}, ρ_p, ρ_{bf} are densities of nanofluids, particle and basefluid respectively. The compiled results are presented in Table 18.

Table 18 : Table with density using Buongiorno's model for all volume fractions

ϕ%	ρ_{nf}(g/cm^3)
0.25	1.0029
0.50	1.0058
0.75	1.0087
1.0	1.0116
1.5	1.0174
2.0	1.0232
2.5	1.0290
3.0	1.0348
4.0	1.0463

In Fig. 50, density of the nanofluids measured with the aid of both the pycnometer and the densimeter are presented. The measured values are in excellent agreement with those of Buongiorno (2006) for volume fractions in the range $0.25 \leq \Phi \leq 0.75$. For $\Phi > 0.75$, the measured values deviate from those results.

When observing the comparision plot of the results obtained by pycnometer, the densimeter and the literature, the densimeter results are well between the two lines and there is no much difference in values in each method. In general as the volume percentage of CNTs increases the density of the nanofluid increases, and the latter is well in agreement with that seen from Buongiorno model results. The experimental values have slight variations that can be due to many reasons, but mainly due to experimental errors. In

general the density decreases with temperature and increases with particle volume concentration.

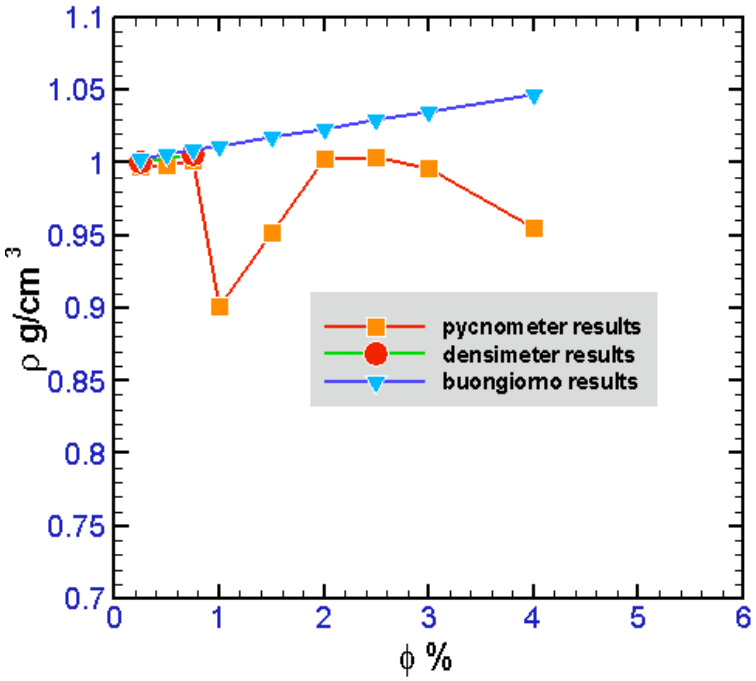

Fig. 50. Density of CNT-Water nanofluid by two different method at 298.15K and compared to Buongiorno

Conclusions of the present work:

A surfactant free CNT-water nanofluid is developed by tailoring the surfaces of the CNTs to be hydrophilic through acid treatment and the dispersibility of the CNTs was dramatically enhanced by sonication. The results of the study can be summarised as follows:

1.) The stability of the nanofluid is estimated by UV-vis spectrophotometric analysis. pH value of nanofluid increases with an increase of CNT concentration and they are well dispersed in water by ultrasonication and maintained over 97% of initial solution even after 200 hours. Thus, it is concluded that CNTs are well dispersed by ultrasonication which supply external mechanical energy to help the nanotubes to overcome the vanderwalls forces.

2.) A thermal conductivity enhancement is consistent with the increase in nanotube loading, but is reduced with thermal conductivity increase of the base fluid. Thermal conductivity measurements have revealed that the thermal conductivity enhancement ratio reaches more than 100% at 333.15K for all volume fractions studied (from 0.25 to 2.5%).

3.) Shear stress is directly proportional to the shear rate at all temperatures. Shear stress decrease with an increase of CNT concentration and decreases with temperature. Viscosity of nanofluids decreases with an increase of temperature and its effect is nullified at higher shear rates. The viscosity of nanofluids increases significantly for a small increase of CNT concentration which is more prominent at 328.15K.

4.) The Surface tension and density of the CNT-water nanofluid increase with nanoparticle increase in base fluid.

5.) The existing models for predicting thermal conductivities of CNT nanofluids and models for predicting viscosity of nanofluids underpredict the present study results.

The promising features of without surfactant, good fluidity, long term stability, and high thermal conductivity would enable the CNT-water nanofluids to be used as advanced coolants in thermal engineering.

Works Cited

Ahuja, A.S. "Augmentation of heat transport in laminar flow of polystyrene suspension: Experiments and results." *Journal of Applied physics* 46, no. 8 (1975), 3408-3416.

Assael, M.J., Metaxa, I.N., Arvanitidis, J., Christofilos, D., Lioutas, C. "Thermal Conductivity Enhancement in Aqueous Suspensions of Carbon Multi-Walled and Double-Walled Nanotubes in the Presence of Two Different Dispersants." *International Journal of Thermophysics* 26, no. 3 (2005): 647-664.

Batchelor, G. "The effect of Brownian motion on the bulk stress in a suspension of spherical particles." *Journal of Fluid Mechanics,* 83 (1977), 97-117.

Buongiorno. J. "Convective transport in nanofluids." *Journal of Heat and Mass Transfer* 128 (2006), 240-250.

Chen, S., She, W., Wu, G., Chen, D. and Jiang, M. "A new approach to the functionalization of single-walled carbon nanotubes with both alkyl and carboxyl groups". Chemical Physics Letters, vol. 402, pp. 312–317 (2005).

Choi, E. S., Brooks, J. S., Eaton, D. L., Al-Haik, M. S., Hussaini, M. Y., Garmestani, H., Li, D., Dahmen, K. "Enhancement of thermal and electrical properties of carbon nanotube polymer composites by magnetic field processing." *Journal of Applied Physics* 94, no. 9 (2003), 6034-6039. .

Choi, S.U.S., Zhang, Z.G., Yu, W., Lockwood, F.E., Grulke, E.A. "Anomalous thermal conductivity enhancement in nanotube suspensions." *Applied Physics Letters,* 79 (2001), 2252-2254.

Chon, C.H., Kihm, K. D., Lee, S.P., Choi, S.U.S. "Empirical correlation finding the role of temperature and particle size for nanofluid (Al2O3) thermal conductivity enhancement." *Applied Physics Letters* 87 (2005), 153107-1-3.

Chopkar, M., Das, P.K., Manna, I. "Synthesis and characterization of nanofluid for advanced heat transfer applications." *Scripta Materialia* 55 (2006): 549–552.

Das. S.K. Putra. N. Thiesen. P., Roetzel. W. Temperature dependence of thermal conductivity enhancement for nanofluids, *ASME Trans. J. Heat Trasfer* 125 (2003) 567-574.
Das. S.K., Choi. S.U.S., Yu. W. & Pradeep. T. Nanofluids science and technology. *Chennai: Wiley*, 2007.

Das. S.K., Putra. N., Roetzel. W. "Pool boiling characteristics of nano-fluids." *International Journal of Heat and Mass Transfer* 46 (2003): 851–862 .

Ding. Y., Alias. H., Wen. D., Williams. R.A. "Heat transfer of aqueous suspensions of carbon nanotubes (CNT nanofluids)." *International Journal of Heat and Mass Transfer* 49, no. 1-2 (2006): 240-250.

Eastman, J.A., Choi, S.U.S, Li, S., Yu, W, Thompson, L.J. "Anomalously increased effective thermal conductivities of ethylene glycol-based nanofluids containing copper nanoparticles." *Applied Physics Letters,* 78, no. 6 (2001), 718-720.

Einstein. "Eine neue bestimmung der molekuldimensionen." *Annalen der Physik* (Leipzig) 19 (1906), 289–306.

Esumi, K., Ishigami, M., Nakajima, A., Awada. K. S and Honda. H. "Chemical treatment of carbon nanotubes ." *Letters to the Editor*, (1995), 279-281.

Gao, L., Zhou. X.F. "Differential effective medium theory for thermal conductivity in nanofluids." *Physics Letters A* 348 (2006), 355–360 .

Hone, J. "Carbon Nanotubes: Thermal Properties ." *Dekker Encyclopedia of Nanoscience and Nanotechnology*, (2004) 603-610.

Hong, T.-K., Yang, H.-S. and Choi, C.J. "Study of the enhanced thermal conductivity of Fe nanofluids." *Journal of Applied Physics* 97 (2005), 064311 .

Iijima, S. "Helical microtubules of graphitic carbon". *Nature*, vol. 354, pp. 56 (1991).
Information on http://www.malvern.com/LabEng/industry/colloids/Stabilized_colloid_system.gif.

Investigation on theory of Brownian motion. New York: Dover, 1956.

Jiang, L., Gao, L., and Sun. J., "Production of aqueous colloidal dispersions of carbon nanotubes." *Journal of Colloid and Interface Science* 260 (2003), 89–94 .

Kanagaraj. S., Ponmozhi, J., Varanda. F.R., J.A. Lopes da Silva, A.Fonseca, Monica SA Oliveira, José AO Simões. "Rheological Study of Nanofluids at Different Concentration of Carbon Nanotubes." *Heat and Mass Transfer Conference* . JNTU Hyderabad, India: 19th National & 8th ISHMT-ASME, (2008). 1-6.

Keblinski, P., Phillpot. S.R., Choi. S.U.S., Eastman. J.A. "Mechanisms of heat fow in suspensions of nano-sized particles (nanofuids)." *International Journal of Heat and Mass Transfer* 45 (2002): 855-863.

Koo, J. and Kleinstreuer, C. "Laminar nanofluid flow in micro-heat sinks. ." *International Journal of Heat and Mass Transfer* 48, no. 13 (2005), 2652–2661.

Kulkarni, D. P., Das, D. K., and Chukwu, G. "Temperature dependent rheological property of copper oxide nanoparticles suspension (Nanofluid)." *Journal of Nanoscience and Nanotechnology* 6 (2006), 1150-1154.

Lee, J.H., Hwang, K.S., Jang, S.P., Lee, B.H., Kim, J.H., Choi, S.U.S., Choi. C.J., "Effective viscosities and thermal conductivities of aqueous nanofluids containing low volume concentrations of Al2O3 nanoparticles." *International Journal of Heat and Mass Transfer* 51 (2008), 2651-2656.

Lee, K.J., Yoon, S.H., and Jang, J. "Carbon Nanofibers : A Novel Nanofiller for Nanofluid Applications." *Nano Small Micro*, (2007): 1209-1213.

Lee, S., Choi, S.U.S., Li, S., Eastman, J.A. "Measuring thermal conductivity of fluids containing oxide nanoparticles." *Journal of Heat Transfer- Transactions of the ASME, 280-289.* 121, no. 2 (1999), 280-289.

Li, C.H., Williams W., Buongiorno J., Hu L-W., Peterson G.P. "Transient and steady-state experimental comparison study of effective thermal conductivity of Al2O3/water nanofluids." *Journal of Heat Transfer* 130 (2008), 042407-1-7.

Li, J.M., Li, Z.L., Wang. B.X., "Experimental viscosity measurements for copper oxide nanoparticle suspensions." *Tsinghua Sci. Tech* 7, no. 2 (2002), 198-201.

Li. C.H., Peterson. G.P. ' Experimental investigation of temperature and volume fraction variations on the effective thermal conductivity of nanoparticle suspensions (nanofluids), *Journal of Applied Physics* 99 (8) (2006) 084314.
Lifei Chen, Huaqing Xie , Yang Li, Wei Yu. "Nanofluids containing carbon nanotubes treated by mechanochemical reaction ." *Thermochimica Acta* 477 (2008): 21–24.

Liu, K.V. "Measurement of pressure drop and heat transfer in turbulent pipe flows of particulate slurries." ANL, 88-15.

Liu, M.S., Lin, M.C.C., Huang, I-Te., Wanga, C.C. "Enhancement of thermal conductivity with carbon nanotube for nanofluids." *International Communications in Heat and Mass Transfer* 32 (2005): 1202 – 1210.

Maiga, S. E. B., Nguyen, C. T., Galanis, N., and Roy, G. "Heat transfer behaviours of nanofluids in a uniformly heated tube." *Superlattices and Microstructures* 35 (2004): 543-557.

Maxwell, J.C. *A Treatise on Electricity and Magnetism.*

Murshed S.M, Sohel,T.Say-Hwa, Nguyen, N.T. "Temperature dependence of interfacial properties and viscosity of nanofluids for droplet-based microfluidics." *Journal of physics. D, Applied physics,* 41, no. 8 (2008): 085502.1-085502.5.

Murshed, SMS, Leong ,KC, Yang, C. "Enhanced thermal conductivity of TiO2-water based nanofluids." *International Journal of Thermal Science* 44 (2005): 367-373.

Patel- H.E., Anoop. K.B., Sundararajan. T. and Das. S.K. "Model for thermal conductivity of CNT-nanofluids" Vol. 31, No. 3, pp. 387–390, (2008).

Patel, H.E., Das, S. K., Sundararajan.T. "Thermal conductivities of naked and monolayer protected metal nanoparticle based nanofluids: Manifestation of anomalous enhancement and chemical effects." *Applied Physics LettersS* 83, no. 14 (2003), 2931-2933.

Patel. H.E., Das. S.K., Sundararagan. T., Nair. A.S., George. B., Pradeep. T. Thermal conductivity of naked and monolayer protected metal nanoparticle based nanofluids: Manifestation of anomalous enhancement and chemical effects. *Applied Physics Letters* 83 (2003) 2931-2933.

Peterson, Calvin H. Li and G. P. "Experimental investigation of temperature and volume fraction variations on the effective thermal conductivity of nanoparticle suspensions (nanofluids)." *Journal of Applied Physics* 99 (2006): 084314.

Praveen. K.N, Das. D.K., Tanguturi. K.M., Vajjha. R.S. "Numerical study of turbulent flow and heat transfer characteristics of nanofluids considering variable properties." *International Journal of Thermal Sciences* 48 (2009): 290-302.

Putnam, S.A., Cahill, D.G., Braun, P.V., Ge, Z., Shimmin, R.G. "Thermal conductivity of nanoparticle suspensions." *Journal of Applied Physics* 99 (2006): 084308-1- 6.

Rusconi, R., Rodari, E., Piazza, R. "Optical measurement of thermal properties of nanofluids." *Applied Physics Letters* 89 (2006): 261916-1-3.

S.K. Das, N. Putra, W. Roetzel. " Pool boiling characteristics of nano-fluids." *International Journal of Heat and Mass Transfer* 46, no. 5 (2003): 851-862.

Serp, P., Corrias, M., and Kalck, P. "Carbon nanotubes and nanofibers in catalysis". Applied Catalysis A: General, 253, 337–358 (2003).

Timofeeva, E.V., Gavrilov, A.N. McCloskey, J.M., and Tolmachev, Y.V. "Thermal conductivity and particle agglomeration in alumina nanofluids: Experiment and theory ." *Physical Review E* 76 (2007), 061203 1-16.

Vadasz, J., Govender, S., and Vadasz, P. "Heat transfer enhancement in nano-fluids suspensions: Possible mechanisms and explanations." *International Journal of Heat Mass Transfer* 46 (2005): 2673-2683.

Vajjha. R.S., Das. D. K., Mahagaonkar. B. M. "Density Measurement of Different Nanofluids and Their Comparison With Theory ." *Petroleum Science and Technology* 27 (2009): 612-624.

Venerus, D.C., Kabadi, M.S., Lee S., Peres-Luna. "Study of thermal transport in nanoparticle suspensions using forced Rayleigh scattering." *Journal of applied physics* 100 (2006): 094310-1-5.

Wang, X., Xu, X., and Choi, S.U.S. "Thermal conductivity of nanoparticle–fluid mixture." *Journal of Thermophysics Heat Transfer* 13 (1999): 474–480.

Wang. X., Xu. X., Choi. S.U.S. "Thermal conductivity of nanoparticle–fluid mixture." *Journal of Thermophysics and Heat Transfer* 13, no. 4 (1999): 474-480.

Weiting Jiang, Guoliang Ding , Hao Peng. "Measurement and model on thermal conductivities of carbon nanotube nanorefrigerants." *International Journal of Thermal Sciences*, 2008.

Wenjea J. Tseng, Kuang-Chih Lin. "Rheology and colloidal structure of aqueous TiO2 nanoparticle suspensions ." *Materials Science and Engineering* A355 (2003): 186-192.

Xie, H., Chen. L. "Adjustable thermal conductivity in carbon nanotube nanofluids." *Physics Letters A* 373 (2009), 1861–1864.

Xie, H., Lee, H., Youn, W. and Choi. M., "Nanofluids containing multiwalled carbon nanotubes and their enhanced thermal conductivities." *Journal of Applied Physics* 94 (2003), 4967-4971.

Xuan, Y., Li, Q. "Investigation of convective heat transfer and flow features of nanofluids." *Journal of heat transfer* 125 (2003): 151-155.

Xue. Q., Xu. W.M. "A model of thermal conductivity of nanofluids with interfacial shells." *Materials Chemistry and Physics* 90 (2005): 298–301.

Y. He, Y. Jin, H. Chen, Y. Ding, D. Cang, H. Lu. "Heat transfer and flow behavior of aqueous suspensions of TiO2 nanoparticles (nanofluids) flowing upward through a vertical pipe." *International Journal of Heat and Mass Transfer* 50 (2007): 2272-2281.

Y. Hwang, J.K. Lee , C.H. Lee b , Y.M. Jung , S.I. Cheong, C.G. Lee , B.C. Ku , S.P. Jang. "Stability and thermal conductivity characteristics of nanofluids." *Thermochimica Acta* 455 (2007): 70–74 .

Yimin Xuan, Qiang Li. "Heat transfer enhancement of nanofuids." *International Journal of Heat and Fluid Flow* 21 (2000): 58-64.

Appendix

Measurement of thermal conductivity of CNT-water nanofluids at various temperatures for particle volume fraction, ϕ = 0.5%

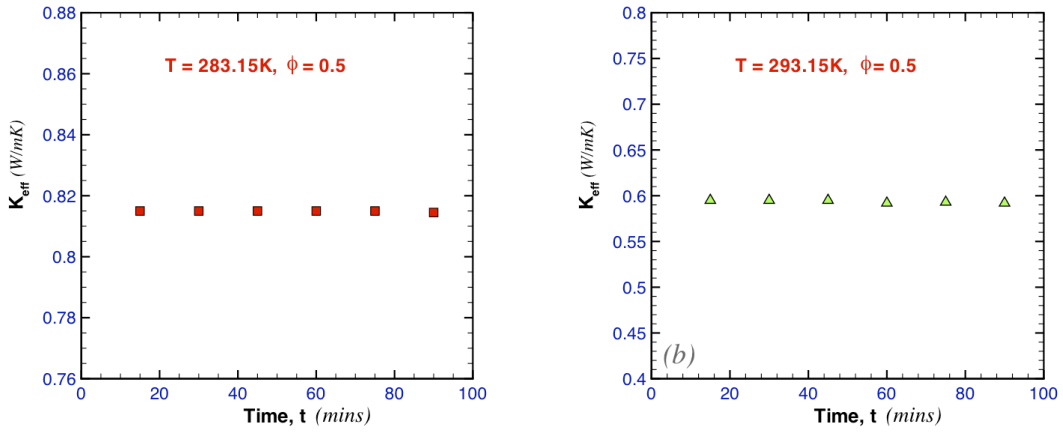

Fig. 51. Thermal conductivity versus time (t = 90 min, ϕ =0.50) at 283.15K & 293.15K

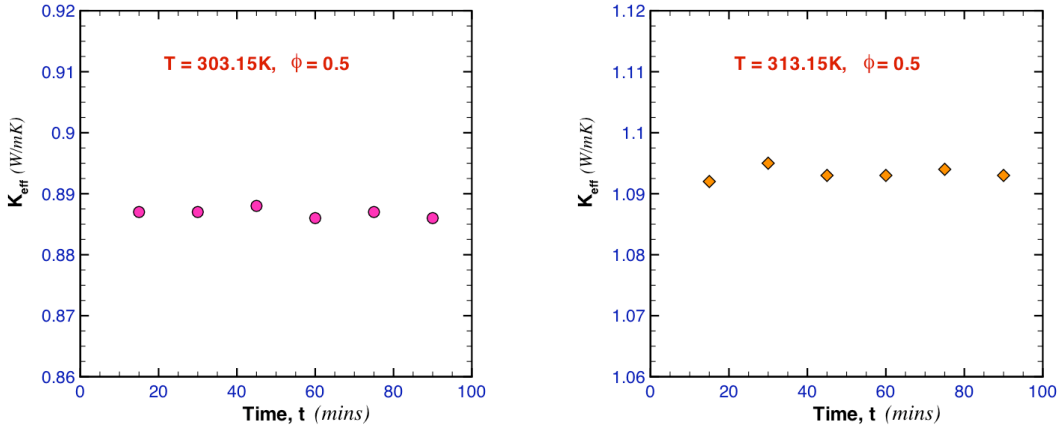

Fig. 52. Thermal conductivity versus time (t = 90 min, ϕ = 0.50) at 303.15K & 313.15K

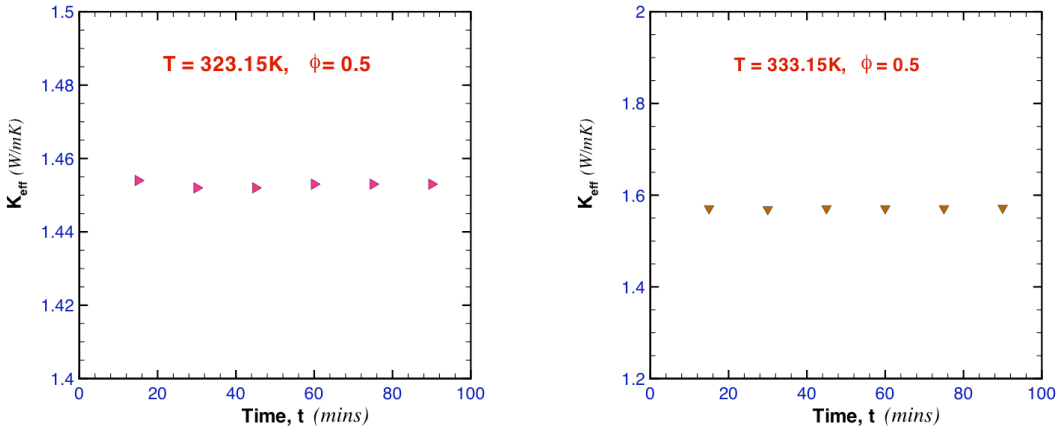

Fig. 53. Thermal conductivity versus time (t = 90 min, ϕ = 0.50) at 323.15K & 333.15K

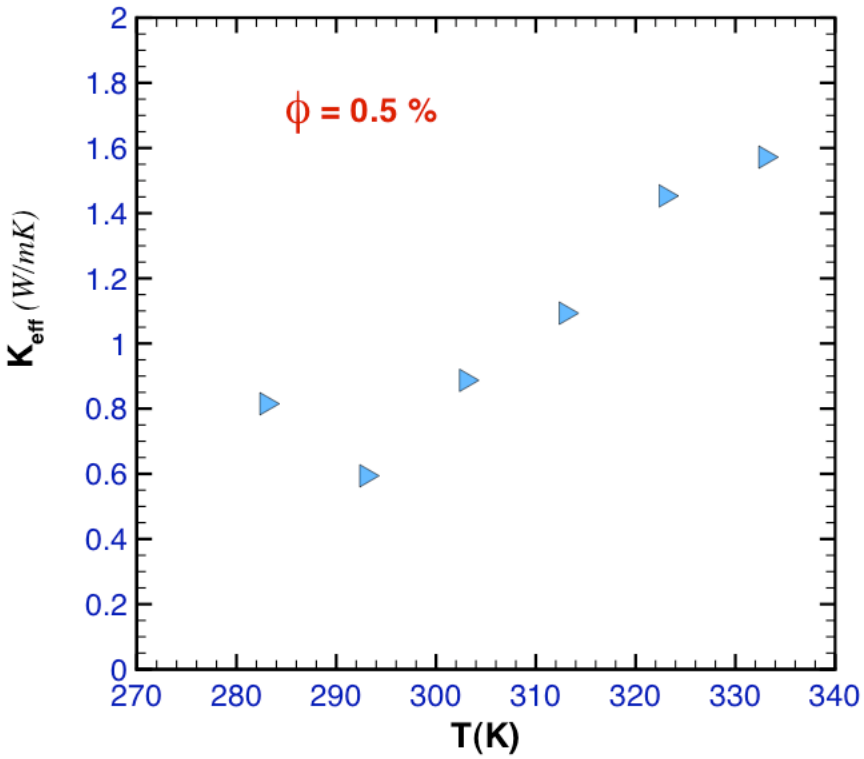

Fig. 54. Variation of thermal conductivity with increase in temperature from 283.15K to 333.15K for ϕ = 0.5%

Measurement of thermal conductivity of CNT-water nanofluids at various temperatures for particle volume fraction, ϕ = 0.75%

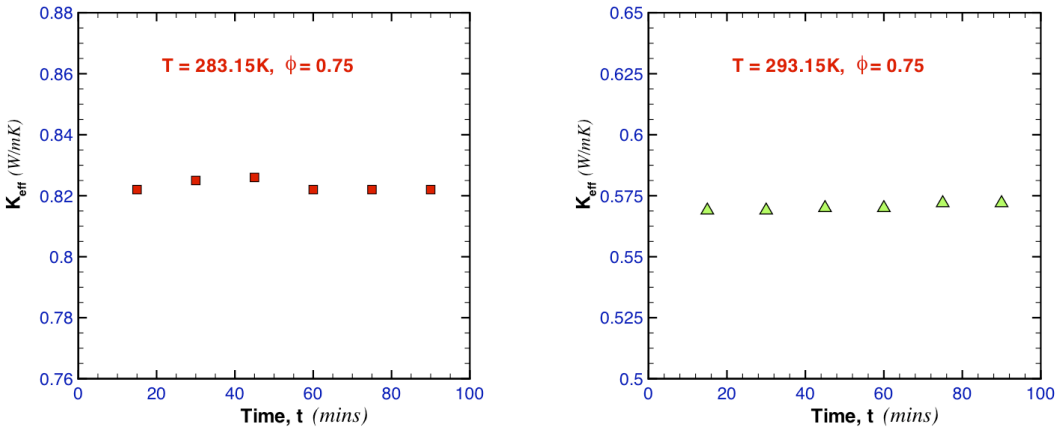

Fig. 55. Thermal conductivity versus time (t = 90 min, ϕ = 0.75) at 283.15K & 293.15K

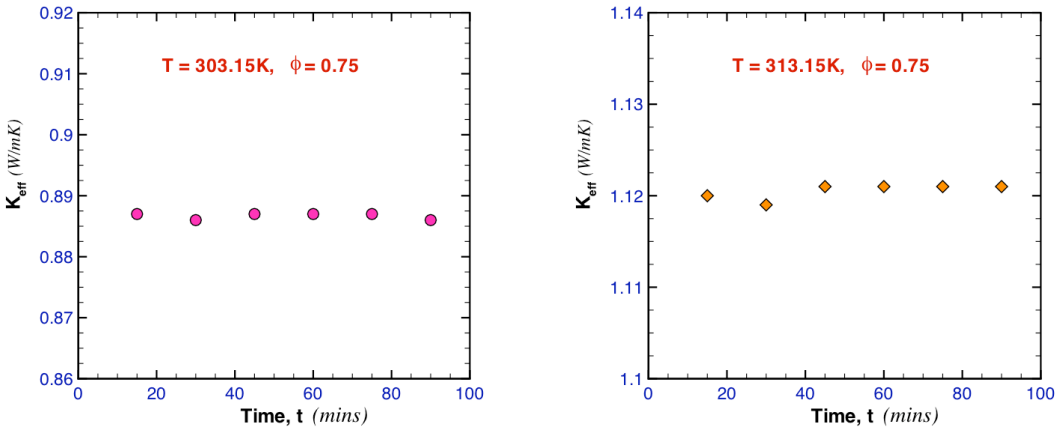

Fig. 56. Thermal conductivity versus time (t = 90 min, ϕ = 0.75) at 303.15K & 313.15K

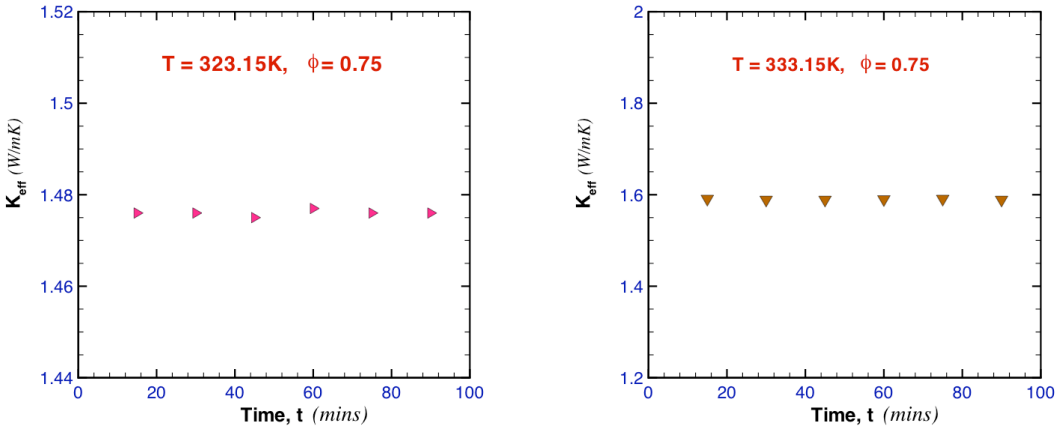

Fig. 57. Thermal conductivity versus time (t = 90 min, ϕ = 0.75) at 323.15K & 333.15K

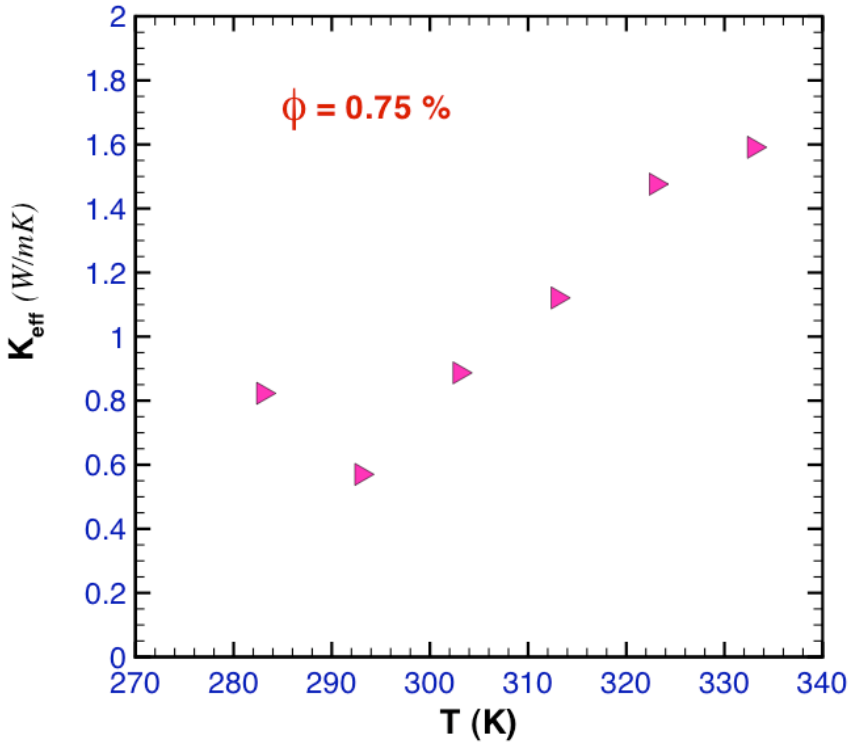

Fig. 58. Variation of thermal conductivity with increase in temperature from 283.15K to 333.15K for ϕ = 0.75%

Measurement of thermal conductivity of CNT-water nanofluids at various temperatures for particle volume fraction, ϕ = 1.0%

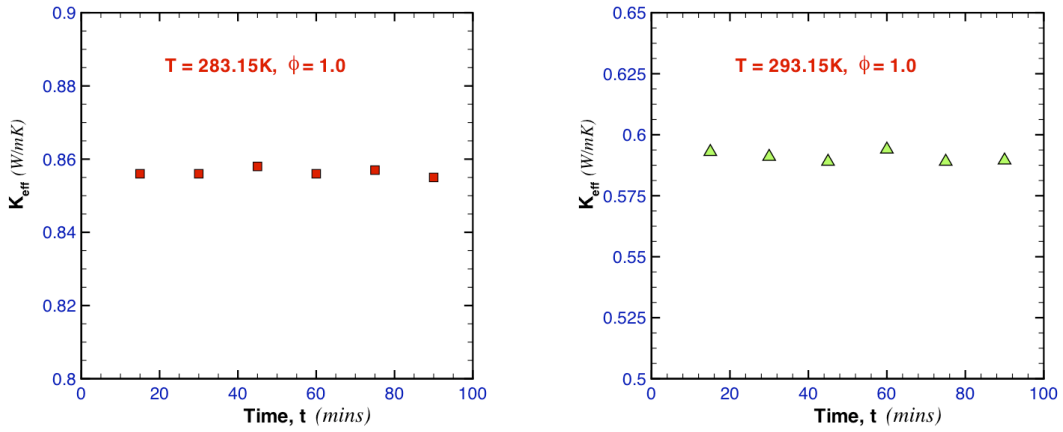

Fig. 59. Thermal conductivity versus time (t = 90 min, ϕ = 1.0) at 283.15K & 293.15K

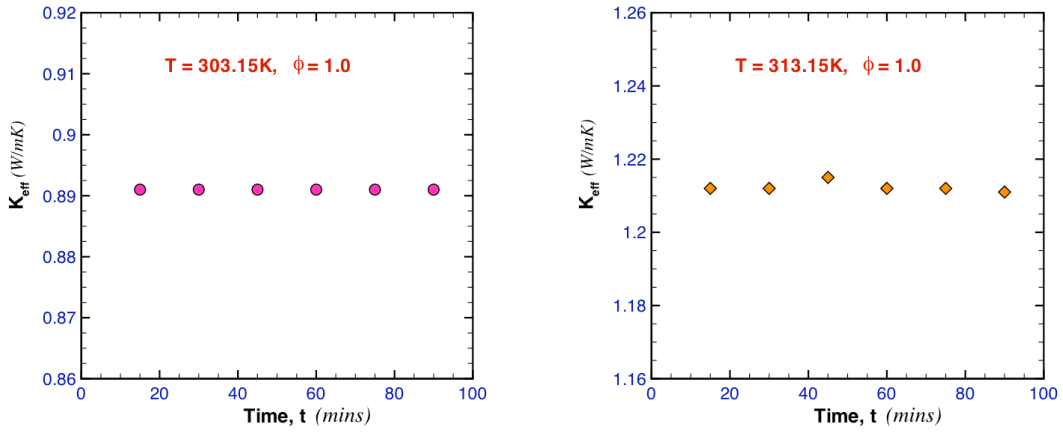

Fig. 60. Thermal conductivity versus time (t = 90 min, ϕ = 1.0) at 303.15K & 313.15K

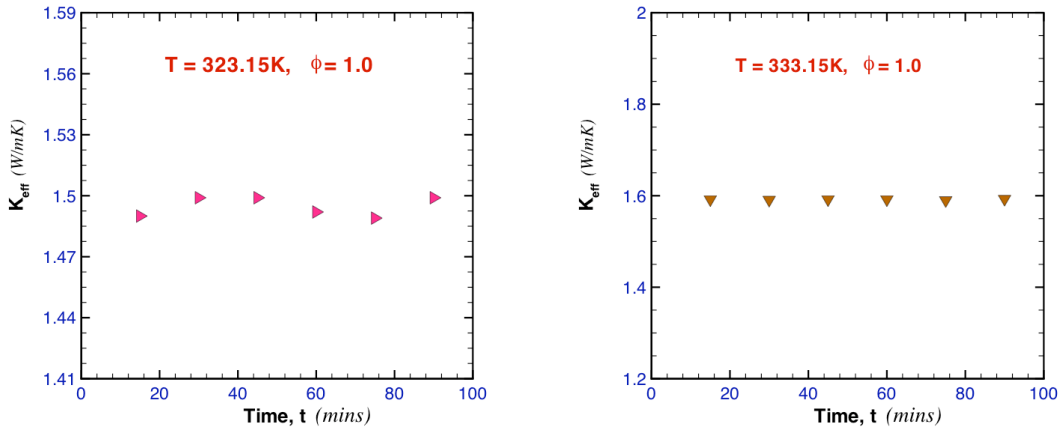

Fig. 61. Thermal conductivity versus time (t = 90 min, ϕ = 1.0) at 323.15K & 333.15K

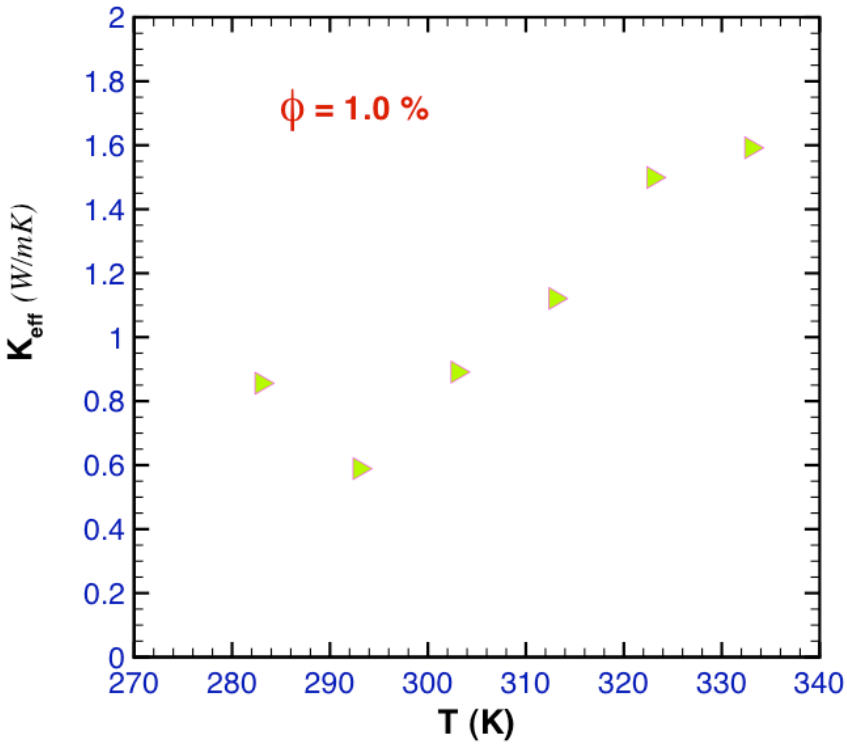

Fig. 62. Variation of thermal conductivity with increase in temperature from 283.15K to 333.15K for ϕ = 1.0%.

Measurement of thermal conductivity of CNT-water nanofluids at various temperatures for particle volume fraction, ϕ = 1.5%

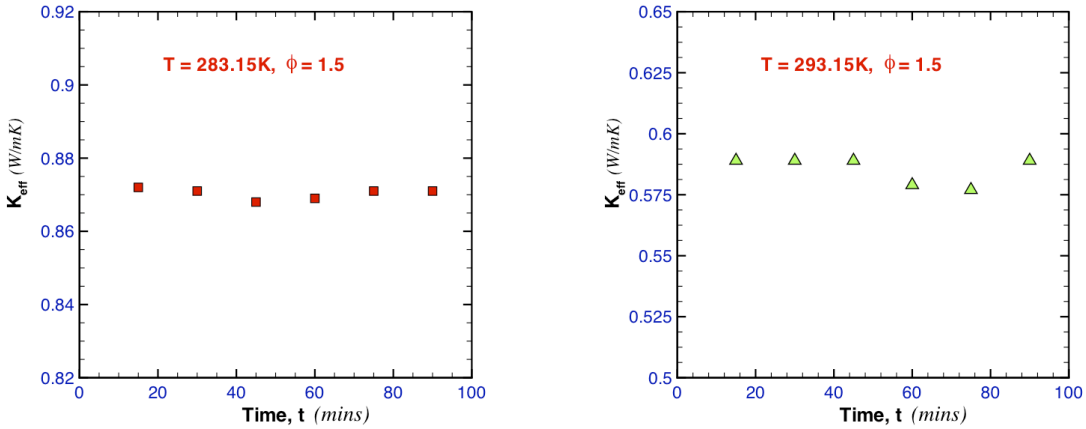

Fig. 63. Thermal conductivity versus time (t = 90 min, ϕ =1.5) at 283.15K & 293.15K

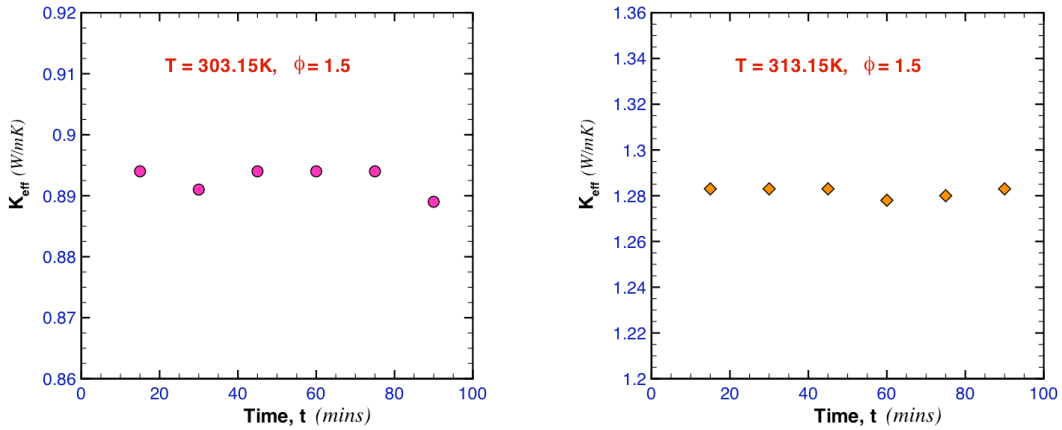

Fig. 64. Thermal conductivity versus time (t = 90 min, ϕ = 1.5) at 303.15K & 313.15K

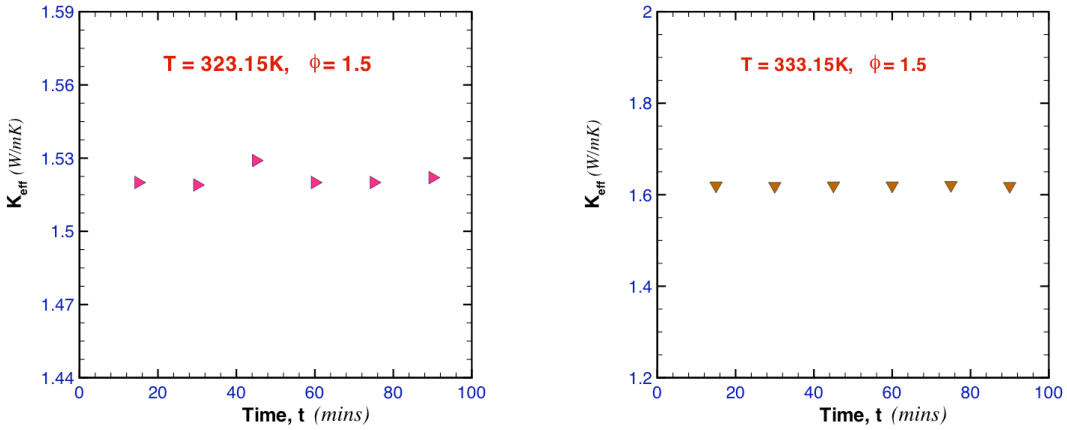

Fig. 65. Thermal conductivity versus time (t = 90 min, ϕ = 1.5) at 323.15K & 333.15K

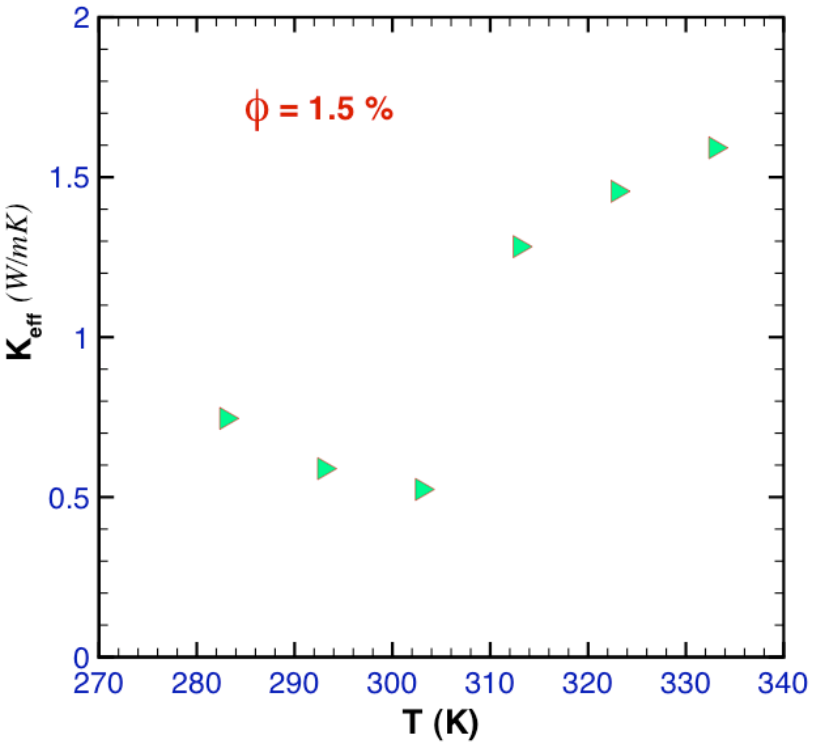

Fig. 66. Variation of thermal conductivity with increase in temperature from 283.15K to 333.15K for ϕ = 1.5%

Measurement of thermal conductivity of CNT-water nanofluids at various temperatures for particle volume fraction, ϕ = 2.0%

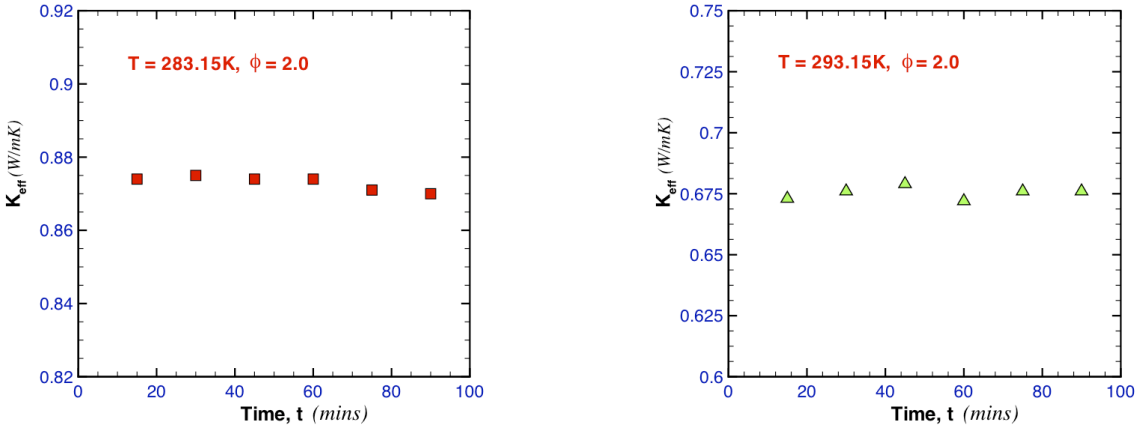

Fig. 67. Thermal conductivity versus time (t = 90 min, ϕ = 2.0) at 283.15K & 293.15K

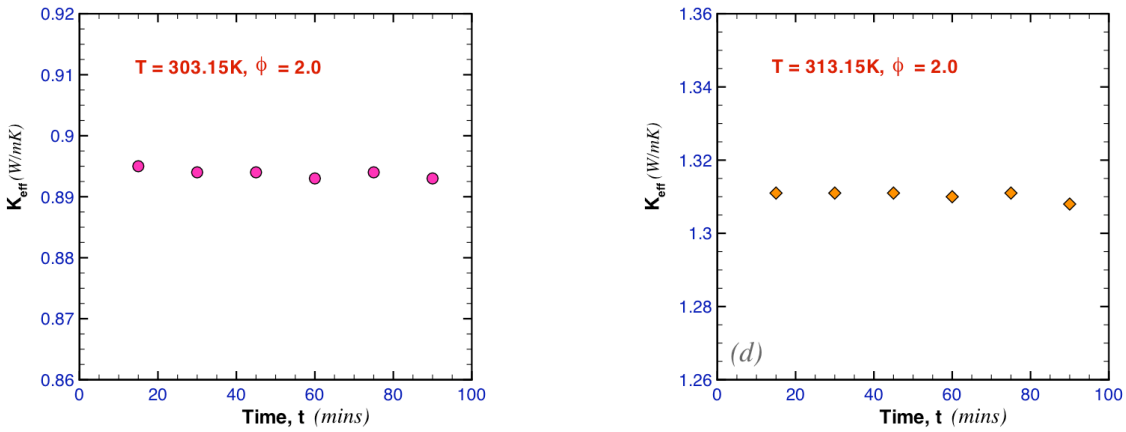

Fig. 68. Thermal conductivity versus time (t = 90 min, ϕ = 2.0) at 303.15K & 313.15K

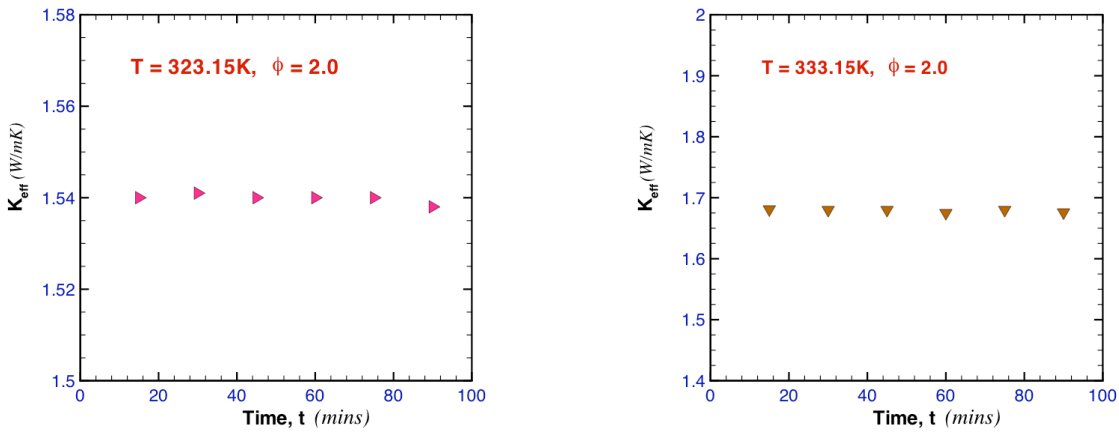

Fig. 69. Thermal conductivity versus time (t = 90 min, ϕ = 2.0) at 323.15K & 333.15K

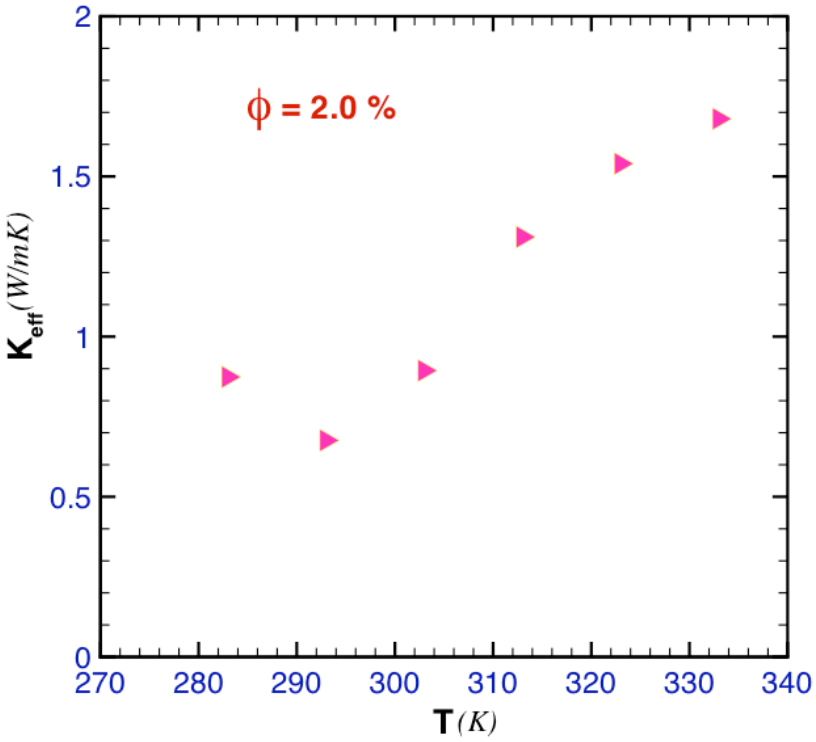

Fig. 70. Variation of thermal conductivity with increase in temperature from 283.15K to 333.15K for ϕ = 2.0%

Measurement of thermal conductivity of CNT-water nanofluids at various temperatures for particle volume fraction, ϕ = 2.5%

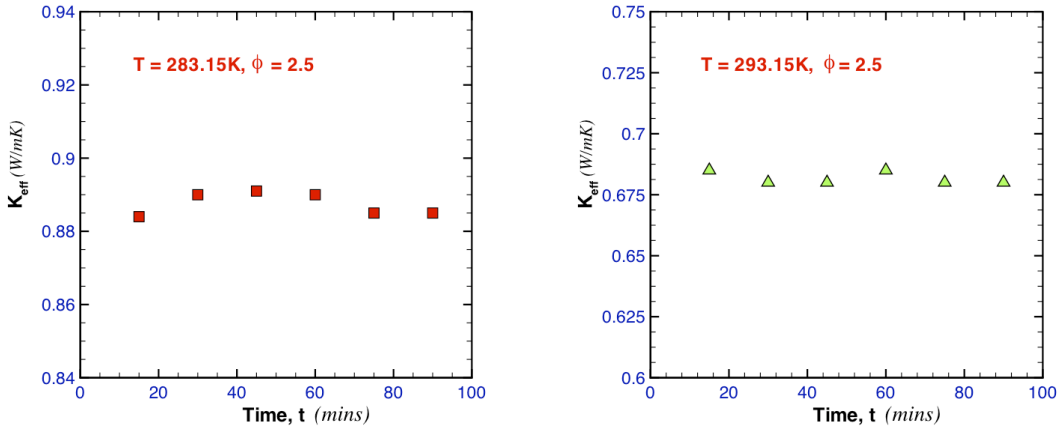

Fig. 71. Thermal conductivity versus time (t = 90 min, ϕ = 2.5) at 283.15K & 293.15K

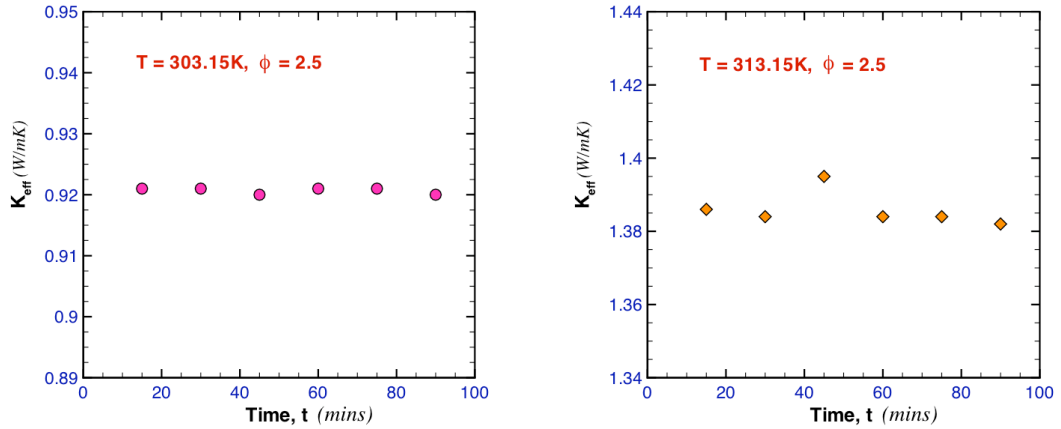

Fig. 72. Thermal conductivity versus time (t = 90 min, ϕ=2.5) at 303.15K & 313.15K

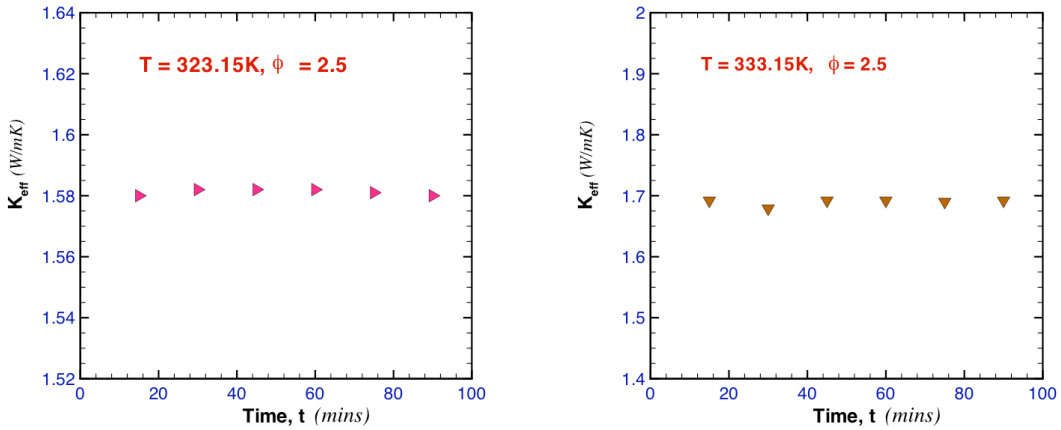

Fig. 73. Thermal conductivity versus time (t = 90 min, ϕ = 2.5) at 323.15K & 333.15K

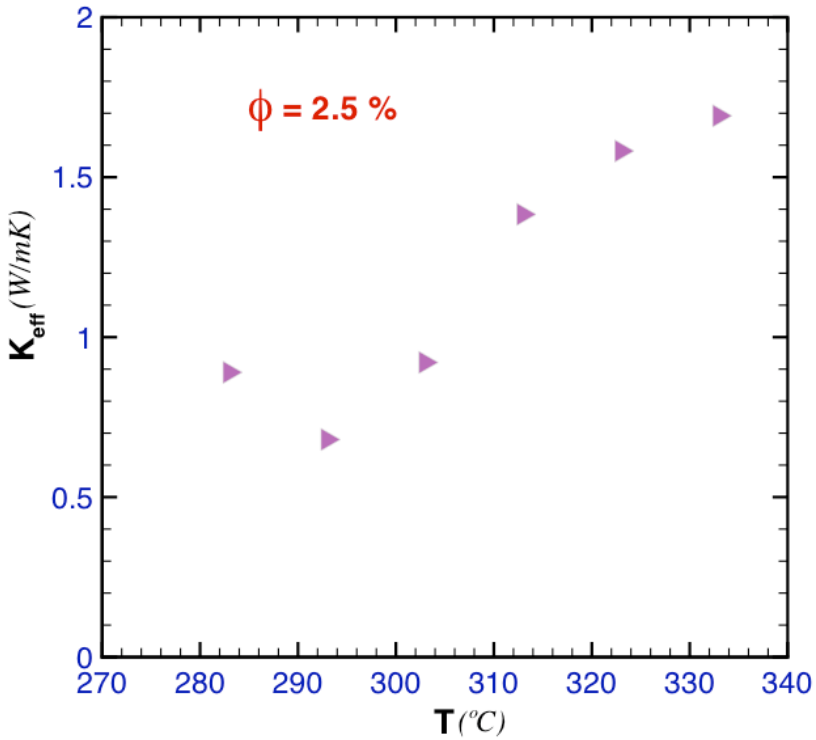

Fig. 74. Variation of thermal conductivity with increase in temperature from 283.15K to 333.15K for ϕ = 2.5%

Viscosity measurement for different volume fractions

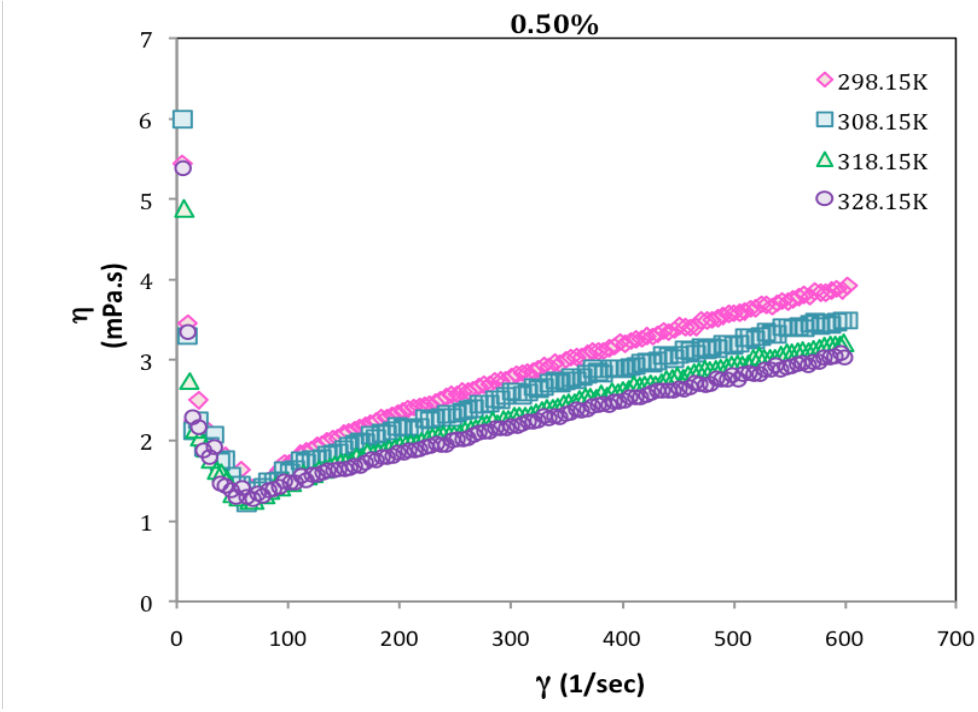

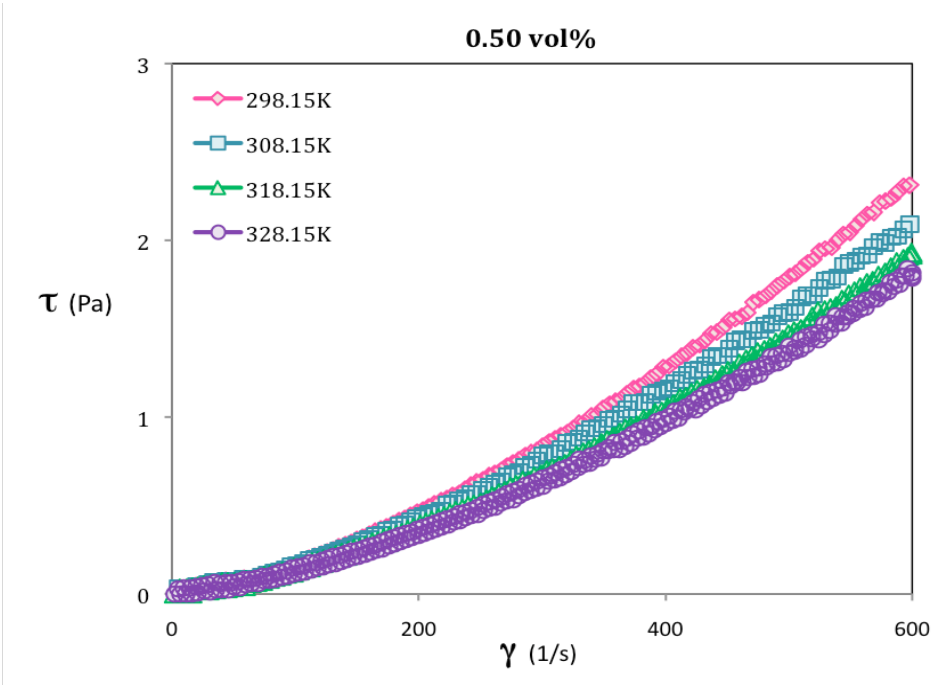

Fig. 75. Viscosity and shear stress for 0.5% at 298.15K, 308.15K, 318.15K,328.15K

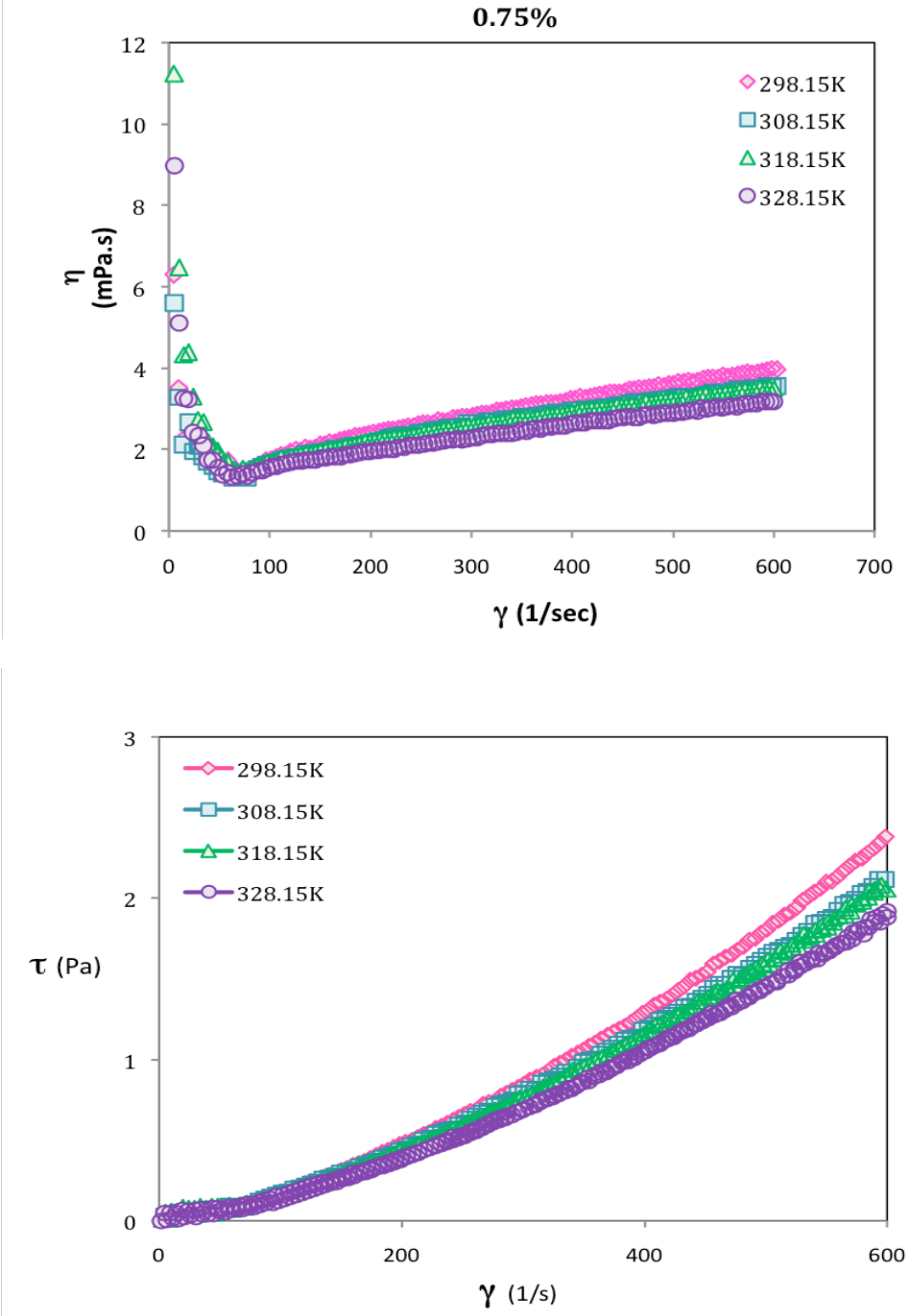

Fig. 76. Viscosity and shear stress for 0.75% at 298.15K, 308.15K, 318.15K,328.15K

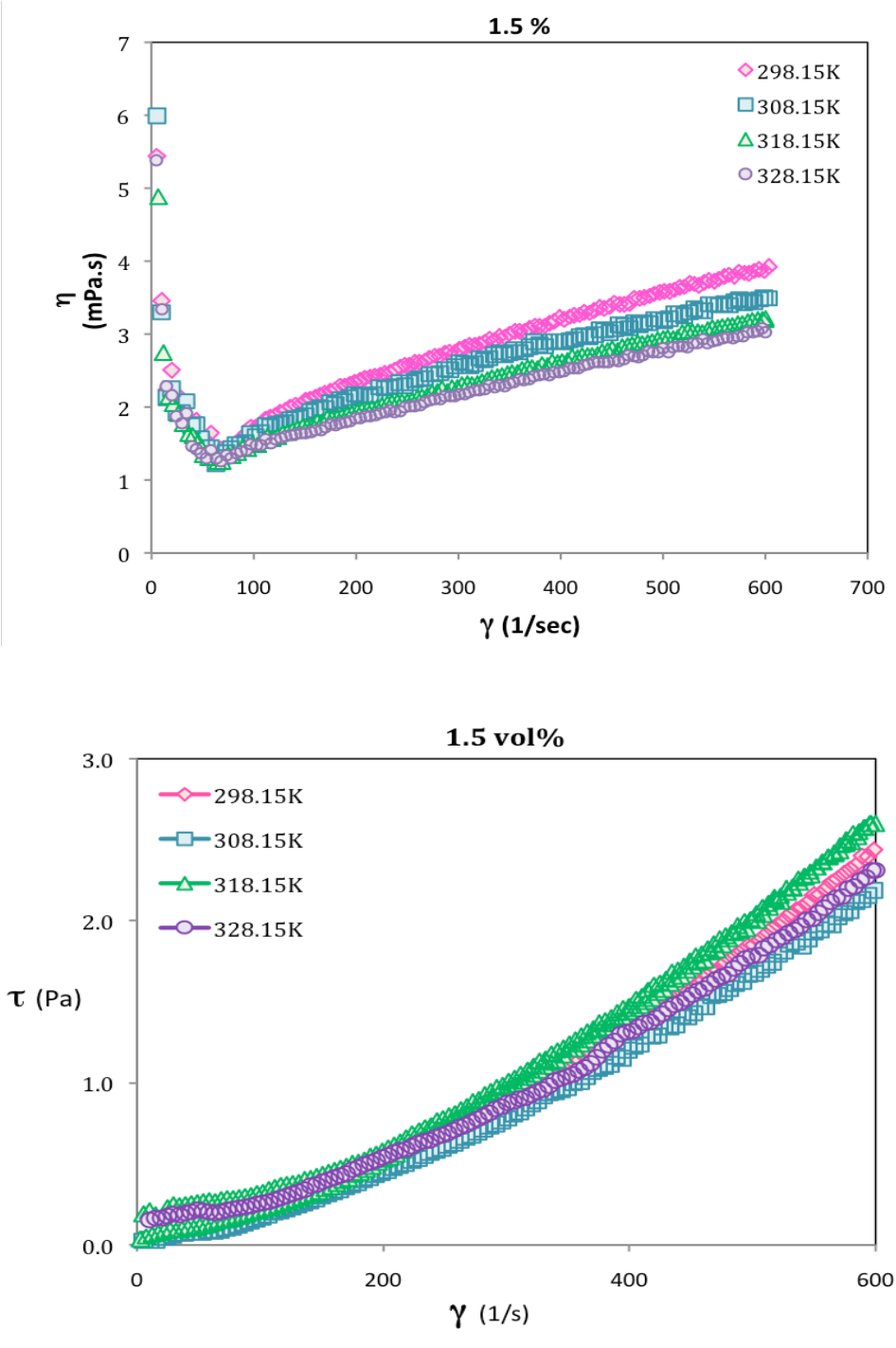

Fig. 77. Viscosity and shear stress for 1.5% at 298.15K, 308.15K, 318.15K,328.15K

.

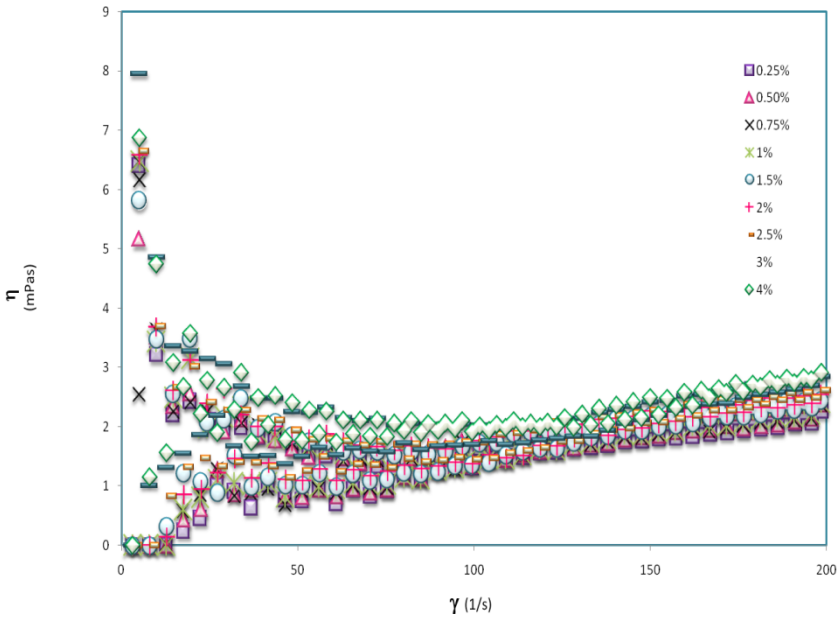

Fig. 78. Viscosity as a function of shear rate for different volume fractions at 298.15K

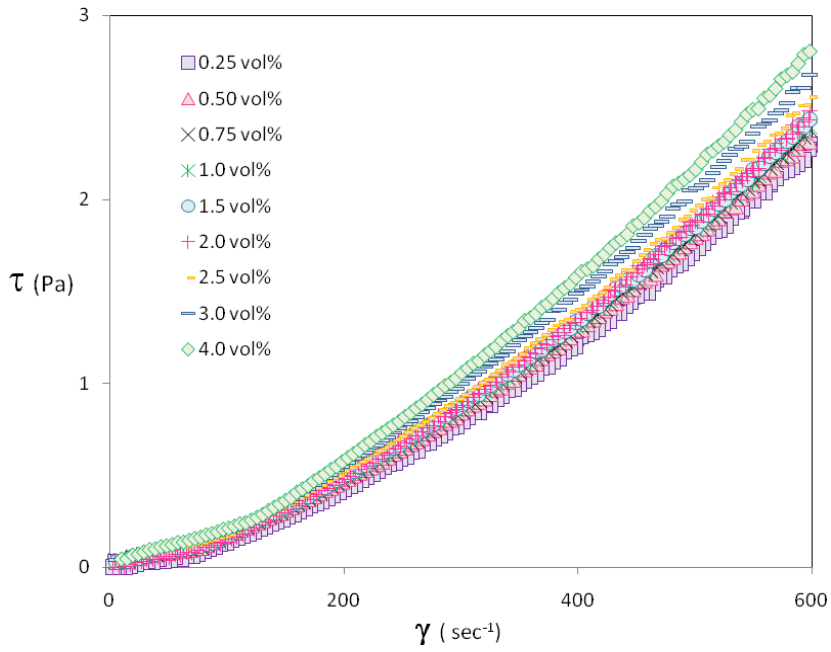

Fig. 79. Shear stress vs shear rate for different volume fractions at 298.15K

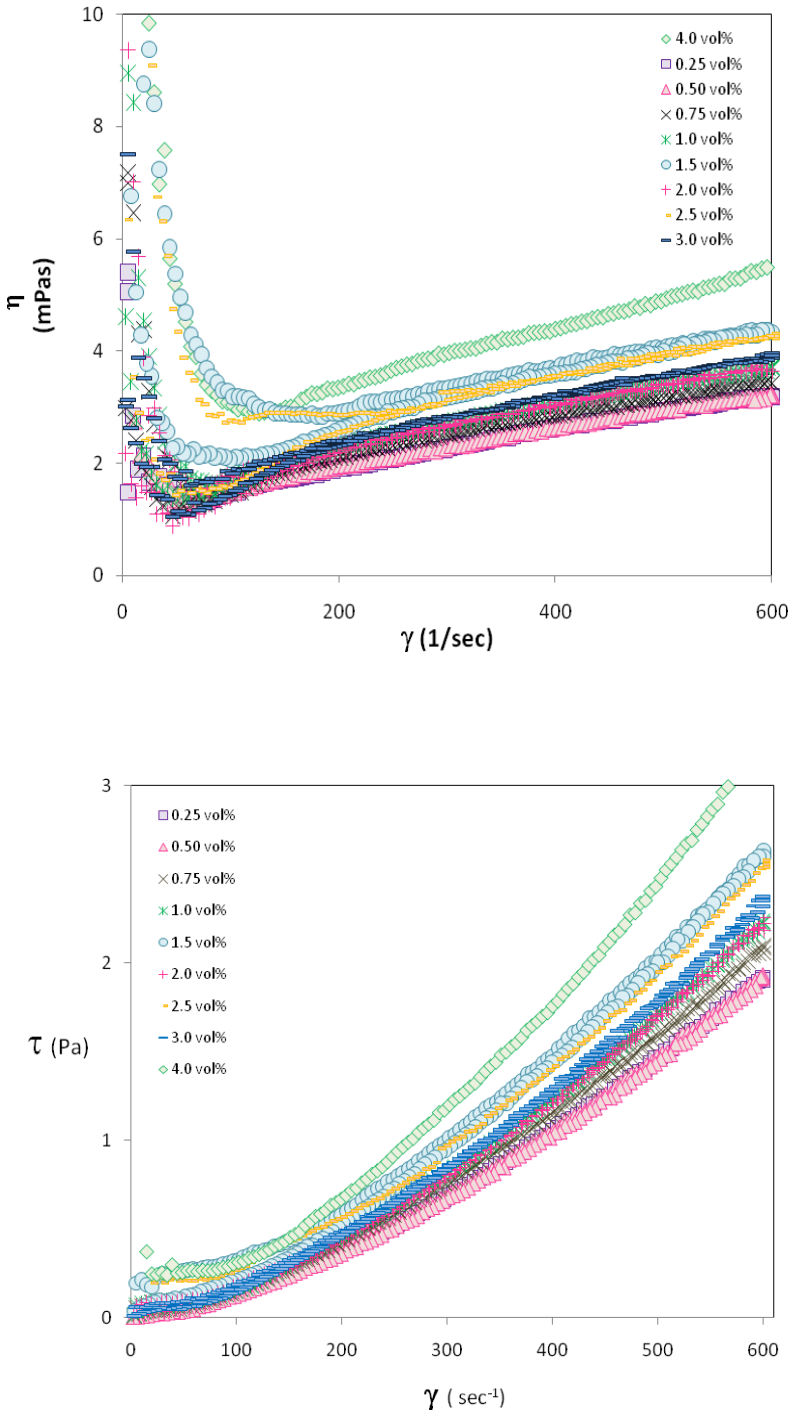

Fig. 80. Viscosity vs shear rate & Shear stress vs shear rate for different volume fractions at 318.15K.

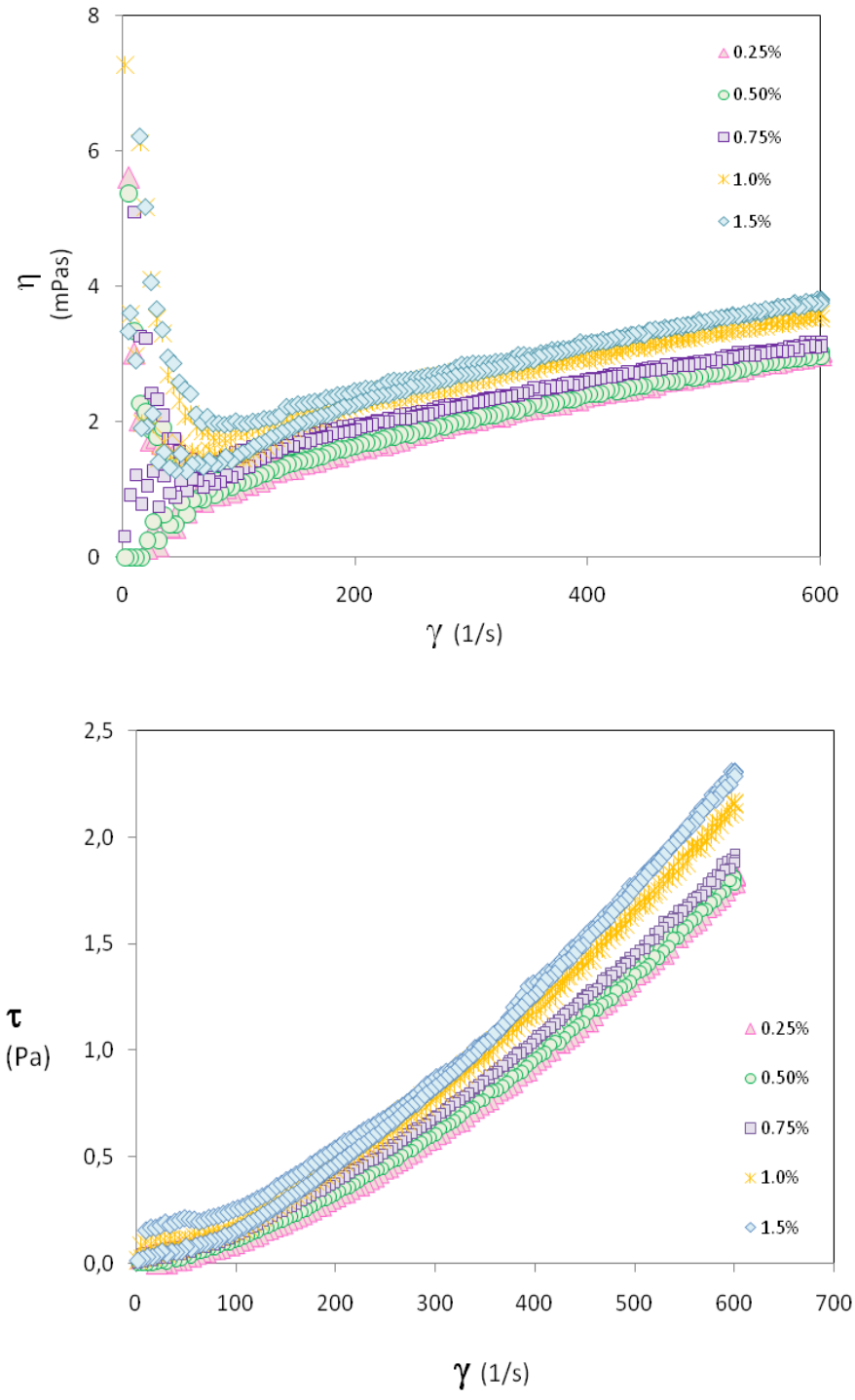

Fig. 81. Viscosity vs shear rate & Shear stress vs shear rate for different volume fractions at 328.15K.

Surface Tension measurement for different volume fractions

Table 19 : Surface tension of CNT-water nanofluid for 0.25 vol% at 298.15K

Sl.No	Time			ST (mN/m)			T (°C)		
1	48	48	49	71.49	71.99	72.00	25.3	25.5	25.6
2	71	71	72	71.51	71.98	71.99	25.3	25.5	25.6
3	94	93	96	71.52	71.99	72.00	25.3	25.6	25.6
4	117	115	119	71.53	71.99	72.00	25.3	25.6	25.6
5	140	137	141	71.54	71.98	72.00	25.3	25.6	25.6
6	164	160	165	71.54	71.99	71.99	25.3	25.6	25.6
7	187	184	188	71.55	71.98	72.01	25.4	25.6	25.6
8	209	207	211	71.55	71.99	72.01	25.4	25.6	25.6
9	232	229	234	71.56	71.98	72.01	25.4	25.6	25.6
10	254	252	257	71.56	71.99	72.01	25.4	25.6	25.6
Total		_		71.53	71.98	72.00		_	
					71.84				

Table 20 **:** Surface tension of CNT-water nanofluid for 0.75 vol% at 298.15K

Sl.No	Time			ST (mN/m)			T (°C)		
1	49	48	49	68,93	69,40	70,73	25,1	25,4	25,4
2	71	71	71	68,83	69,39	70,66	25,1	25,4	25,4
3	93	94	94	68,81	69,40	70,65	25,2	25,4	25,4
4	115	116	117	68,81	69,40	70,64	25,2	25,4	25,4
5	136	137	138	68,81	69,40	70,64	25,2	25,4	25,4
6	159	158	162	68,81	69,42	70,64	25,2	25,4	25,4
7	182	181	184	68,81	69,42	70,63	25,2	25,4	25,4
8	206	203	206	68,82	69,42	70,63	25,2	25,4	25,4
9	229	226	229	68,82	69,44	70,64	25,2	25,4	25,4
10	252	249	251	68,83	69,45	70,63	25,3	25,4	25,4
Total		_		68,83	69,42	70,65		_	
					69,63				

Table 21 **:** Surface tension of CNT-water nanofluid for 1.0 vol% at 298.15K

Sl.No	Time			ST (mN/m)			T (°C)		
1	49	49	49	72,49	71,97	72,1	25,1	25,3	25,3
2	71	72	71	72,40	72,03	72,15	25,1	25,3	25,3
3	94	95	95	72,41	72,06	72,16	25,1	25,3	25,3
4	117	117	118	72,42	72,06	72,18	25,1	25,3	25,3
5	140	140	141	72,42	72,08	72,19	25,1	25,3	25,3
6	162	163	163	72,42	72,09	72,19	25,1	25,3	25,3
7	185	186	186	72,42	72,10	72,2	25,1	25,3	25,3
8	210	210	210	72,42	72,10	72,21	25,2	25,3	25,3
9	233	235	233	72,43	72,10	72,22	25,2	25,3	25,3
10	256	258	256	72,42	72,10	72,23	25,2	25,3	25,3
Total		_		72,42	72,07	72,18		_	
					72,22				

Table 22 **:** Surface tension of CNT-water nanofluid for 1.5 vol% at 298.15K

Sl.No	Time		ST (mN/m)		T (°C)	
1	48	48	67.73	69.65	24.9	25.0
2	71	71	67.69	69.56	24.9	25.1
3	92	94	67.67	69.55	25.0	25.1
4	115	116	67.68	69.55	25.0	25.1
5	139	137	67.67	69.55	25.0	25.1
6	162	158	67.67	69.54	25.0	25.1
7	185	181	67.68	69.54	25.0	25.1
8	207	203	67.69	69.54	25.0	25.1
9	231	226	67.69	69.53	25.0	25.1
10	253	249	67.69	69.53	25.0	25.1
Total		_	67.69	69.55	_	
			68.62			

Table 23 **:** Surface tension of CNT-water nanofluid for 2.0 vol% at 298.15K

Sl.No	Time			ST (mN/m)			T (°C)		
1	50	47	48	71.49	72.06	72.1	24.9	25.2	25.2
2	73	69	73	71.55	72.06	72.14	25.0	25.2	25.2
3	97	93	96	71.57	72.06	72.15	25.0	25.2	25.2
4	120	116	118	71.58	72.06	72.15	25.0	25.2	25.2
5	142	139	142	71.59	72.06	72.15	25.0	25.2	25.2
6	166	162	166	71.60	72.06	72.16	25.0	25.2	25.2
7	188	185	189	71.60	72.07	72.16	25.0	25.2	25.2
8	211	209	212	71.60	72.08	72.17	25.0	25.2	25.2
9	234	233	235	71.60	72.08	72.17	25.0	25.2	25.2
10	256	254	257	71.60	72.08	72.17	25.1	25.3	25.2
Total		_		71.57	72.07	72.15		_	
					71.93				

Table 24 : Surface tension of CNT-water nanofluid for 2.5 vol% at 298.15K

Sl.No	Time				ST (mN/m)		T (°C)		
1	38	38	39	71.08	71.38	71.98	24.9	25.1	25.1
2	59	58	59	71.14	71.43	72.00	24.9	25.1	25.1
3	79	78	79	71.14	71.46	72.00	24.9	25.1	25.2
4	99	99	99	71.15	71.48	72.00	24.9	25.1	25.2
5	119	117	117	71.17	71.49	72.00	25.0	25.1	25.2
6	140	137	138	71.17	71.50	72.00	25.0	25.1	25.2
7	159	158	159	71.19	71.51	72.00	25.0	25.1	25.1
8	180	180	179	71.19	71.52	72.02	25.0	25.1	25.1
9	201	200	199	71.21	71.52	72.02	25.0	25.1	25.1
10	222	221	217	71.21	71.53	72.02	25.0	25.1	25.1
Total		_		71.17	72.49	72.01		_	
					71.89				

Table 25 : Surface tension of CNT-water nanofluid for 3.0 vol% at 298.15K

Sl.No	Time			ST (mN/m)			T (°C)		
1	38	38	34	70.66	70.80	70.62	25.0	25.3	25.3
2	57	58	56	70.62	70.84	70.67	25.0	25.3	25.4
3	76	79	76	70.6	70.86	70.70	25.0	25.3	25.4
4	98	101	97	70.62	70.89	70.71	25.1	25.3	25.4
5	116	120	118	70.62	70.92	70.74	25.1	25.3	25.4
6	136	138	139	70.62	70.93	70.74	25.1	25.3	25.4
7	156	157	160	70.63	70.93	70.76	25.1	25.3	25.4
8	176	178	181	70.63	70.94	70.77	25.1	25.3	25.4
9	194	198	202	70.63	70.94	70.79	25.1	25.3	25.4
10	215	218	223	70.64	70.95	70.80	25.2	25.3	25.4
11	235	237	244	70.65	70.96	70.82	25.2	25.3	25.4
Total		_		70.63	70.90	70.74		_	
					70.76				

Table 26 : Surface tension of CNT-water nanofluid for 4.0 vol% at 298.15K

Sl.No	Time			ST (mN/m)			T (°C)		
1	39	34	37	71,86	71,56	72,52	25,0	25,2	25,4
2	58	55	57	71,94	71,63	72,54	25,0	25,3	25,4
3	79	75	75	71,99	71,66	72,53	25,0	25,3	25,4
4	99	97	97	72,00	71,68	72,55	25,0	25,3	25,4
5	120	114	117	72,03	71,68	72,56	25,1	25,3	25,4
6	140	135	138	72,03	71,69	72,59	25,1	25,3	25,4
7	161	156	159	72,05	71,71	72,59	25,1	25,3	25,4
8	180	177	181	72,06	71,72	72,61	25,1	25,3	25,4
9	201	196	201	72,08	71,72	72,61	25,1	25,3	25,4
10	223	217	221	72,08	71,72	72,61	25,2	25,3	25,4
11	242	236	242	72,09	71,73	72,63	25,2	25,4	25,4
Total		_		72,02	71,68	72,58		_	
					72,09				